



COLLÈGE
DE FRANCE
—1530—



FLATIRON
INSTITUTE

Center for Computational
Quantum Physics

Dynamical Mean-Field Theory: An Introduction

Antoine Georges

TRIQS Summer School 2023 – Port Royal



TRIQS

OUTLINE

- Materials with Strong Electronic Correlations: An Introduction
- The Dynamical Mean Field Theory concept
- The Mott Transition from a DMFT Perspective
- `Appendix': A brief introduction to the Anderson impurity model

Materials with Strong Electron Correlations do “BIG THINGS”

- Because of the strong interdependence of electrons, collective phenomena take place
- Such as: *metal-insulator transitions, magnetism, superconductivity, etc.*
- → Interesting functionalities
- → Fundamental questions in physics and chemistry

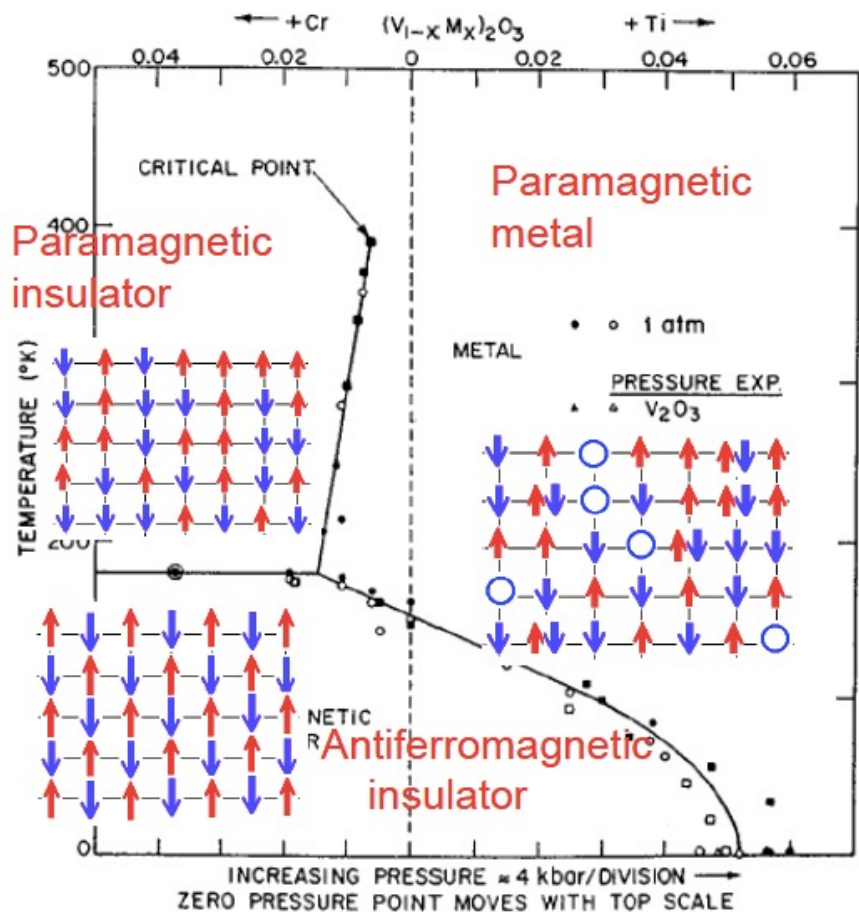
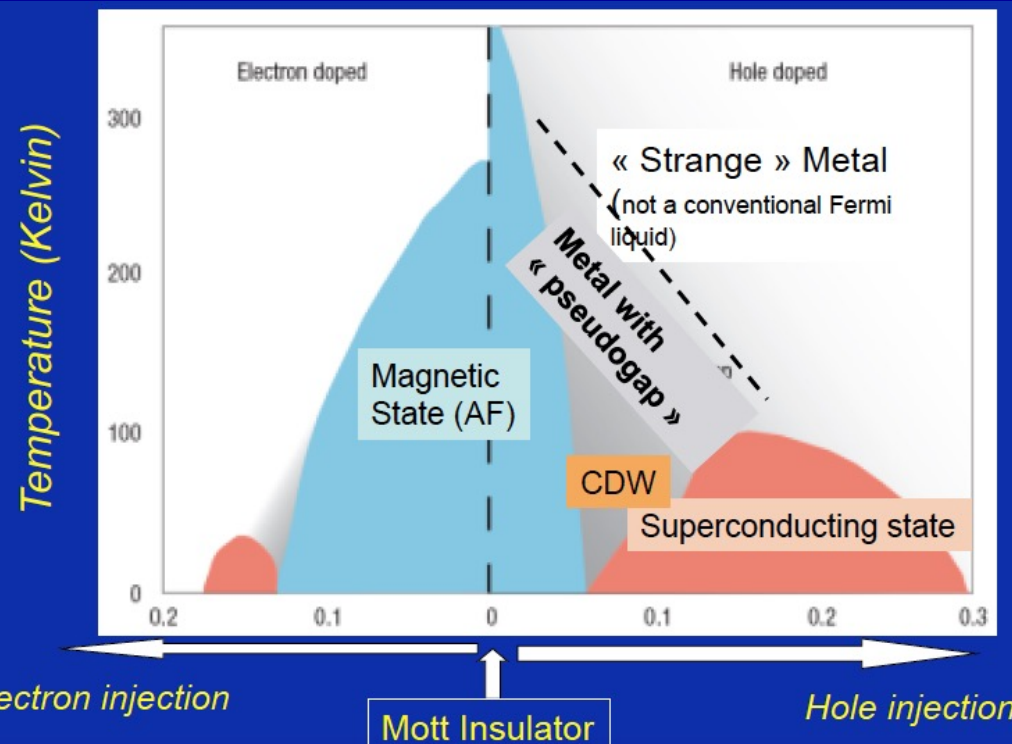
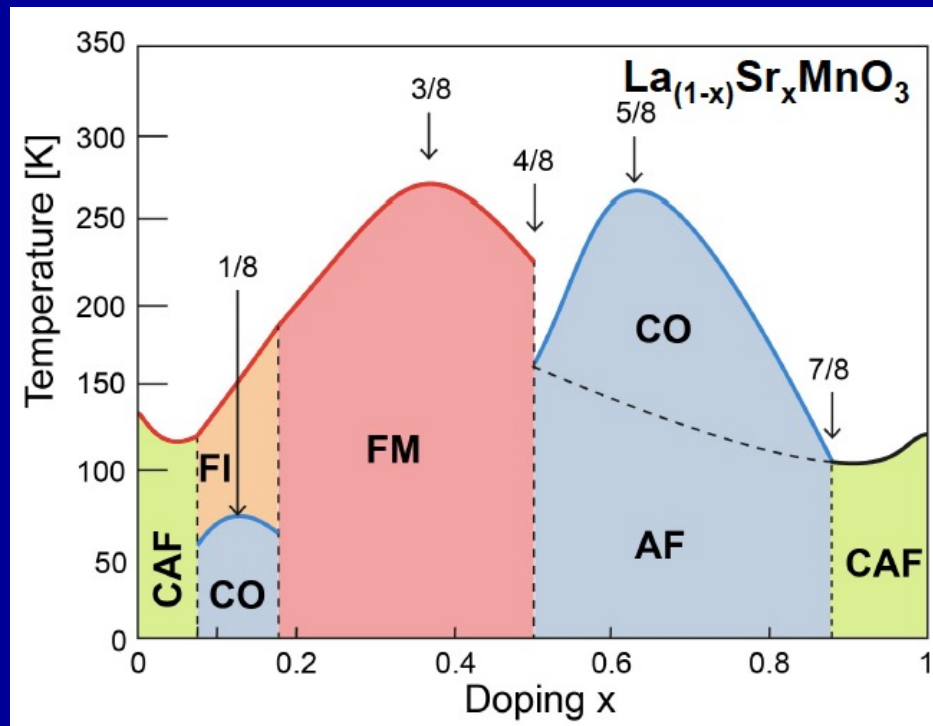


FIG. 70. Phase diagram for doped V_2O_3 systems, $(V_{1-x}Cr_x)_2O_3$ and $(V_{1-x}Ti_x)_2O_3$. From McWhan *et al.*, 1971, 1973.

Remarkable Properties
Complex Phase Diagrams
Competing Phases



Electron injection

Mott Insulator

Hole injection

**Which Materials display
'Strong Electronic Correlations' ?**

Periodic Table of the Elements

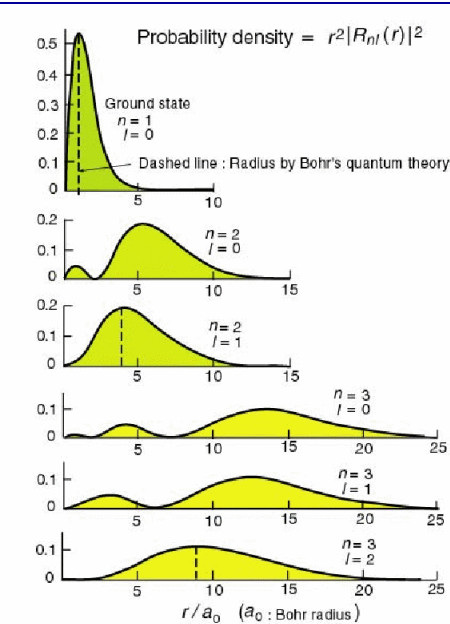
Transition Metals

- 3d transition metals
- 4d transition metals
- 5d transition metals

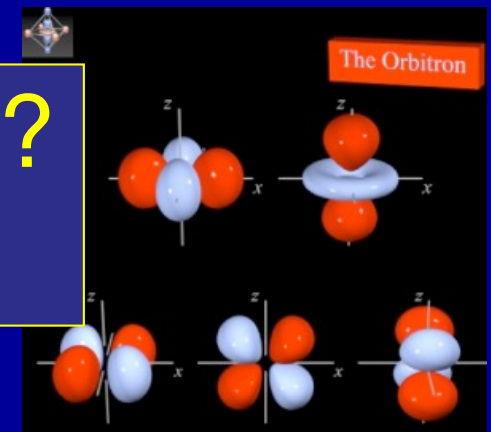
1A 1 H hydrogen 1.008	2A 4 Be beryllium 9.012											3A 5 B boron 10.81	4A 6 C carbon 12.01	5A 7 N nitrogen 14.01	6A 8 O oxygen 16.00	7A 9 F fluorine 19.00	8A 2 He helium 4.003																																				
3 Li lithium 6.941	11 Na sodium 22.99	12 Mg magnesium 24.31	19 K potassium 39.10	20 Ca calcium 40.08	21 Sc scandium 44.96	22 Ti titanium 47.88	23 V vanadium 50.94	24 Cr chromium 52.00	25 Mn manganese 54.94	26 Fe iron 55.85	27 Co cobalt 58.93	28 Ni nickel 58.69	29 Cu copper 63.55	30 Zn zinc 65.39	37 Rb rubidium 85.47	38 Sr strontium 87.62	39 Y yttrium 88.91	40 Zr zirconium 91.22	41 Nb niobium 92.91	42 Mo molybdenum 95.94	43 Tc technetium (98)	44 Ru ruthenium 101.1	45 Rh rhodium 102.9	46 Pd palladium 106.4	47 Ag silver 107.9	48 Cd cadmium 112.4	55 Cs cesium 132.9	56 Ba barium 137.3	57 La* lanthanum 138.9	72 Hf hafnium 178.5	73 Ta tantalum 180.9	74 W tungsten 183.9	75 Re rhenium 186.2	76 Os osmium 190.2	77 Ir iridium 192.2	78 Pt platinum 195.1	79 Au gold 197.0	80 Hg mercury 200.5	87 Fr francium (223)	88 Ra radium (226)	89 Ac~ actinium (227)	104 Rf rutherfordium (257)	105 Db dubnium (260)	106 Sg seaborgium (263)	107 Bh bohrium (262)	108 Hs hassium (265)	109 Mt meitnerium (266)	110 Ds darmstadtium (271)	111 Uuu (272)	112 Uub (277)	114 Uuq (296)	116 Uuh (298)	118 Uuo (?)

Lanthanide Series*	58 Ce cerium 140.1	59 Pr praseodymium 140.9	60 Nd neodymium 144.2	61 Pm promethium (147)	62 Sm samarium (150.4)	63 Eu europium 152.0	64 Gd gadolinium 157.3	65 Tb terbium 158.9	66 Dy dysprosium 162.5	67 Ho holmium 164.9	68 Er erbium 167.3	69 Tm thulium 168.9	70 Yb ytterbium 173.0	
Actinide Series	90 Th thorium 232.0	91 Pa protactinium (231)	92 U uranium (238)	93 Np neptunium (237)	94 Pu plutonium (242)	95 Am americium (243)	96 Cm curium (247)	97 Bk berkelium (247)	98 Cf californium (249)	99 Es einsteinium (254)	100 Fm fermium (253)	101 Md mendelevium (256)	102 Nc nobelium (254)	103 Lr lawrencium (257)

Rare Earths Actinides



Who are the suspects ? Localized orbitals !



d- or f- orbitals are quite close to ions nuclei
(particularly 3d and 4f, for orthogonality reasons)

They do not behave as regular band-forming orbitals
(e.g sp-bonding) and retain atomic-like aspects

→ Electrons “hesitate” between
localized and itinerant behaviour !

Materials: transition-metals and their oxides,
rare-earth/actinides and their compounds, but
also some organic materials

Molecular Materials

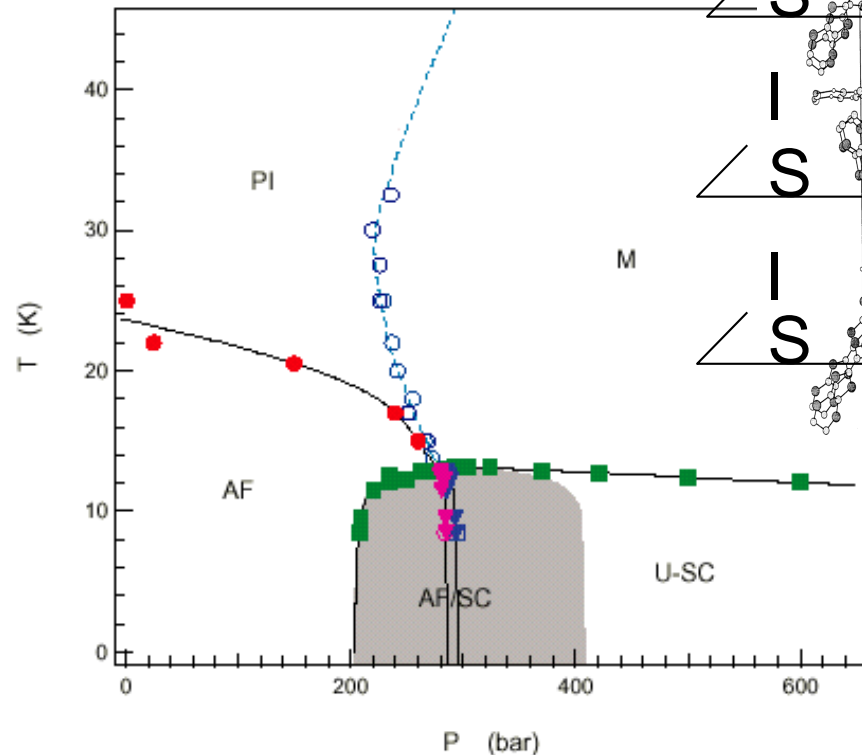
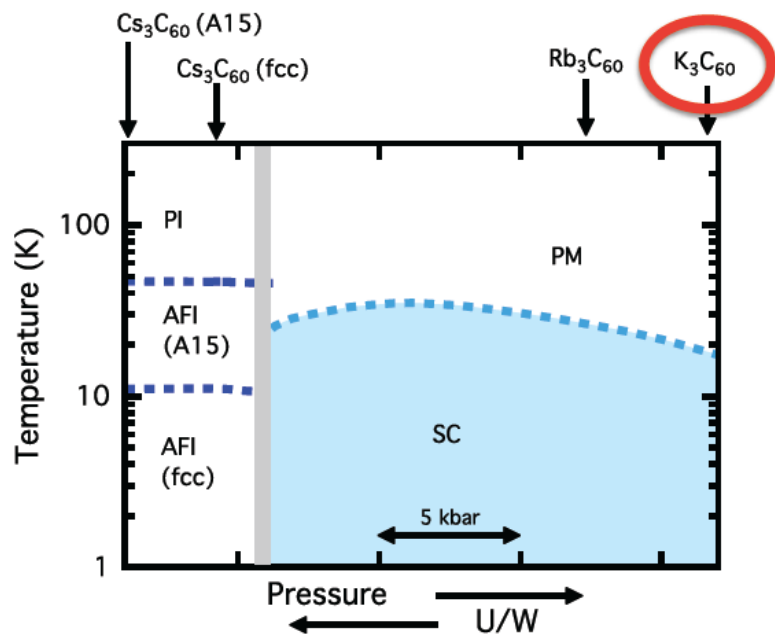
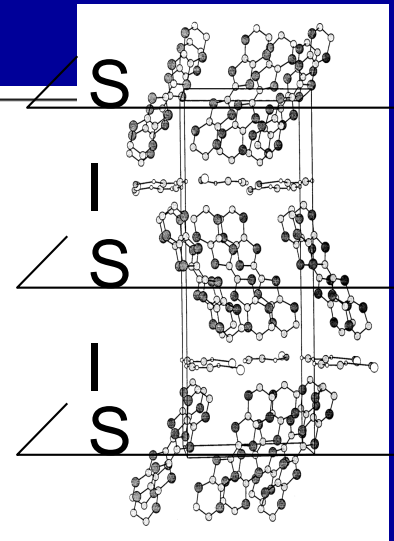
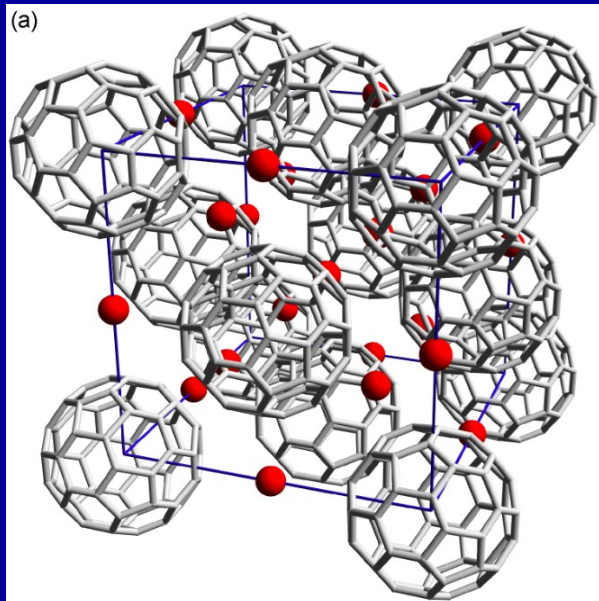


FIG. 1. Temperature *vs* pressure phase diagram of κ -Cl. The antiferromagnetic (AF) critical line $T_N(P)$ (dark circles) was determined from NMR relaxation rate while $T_c(P)$ for unconventional superconductivity (U-SC: squares) and the metal-insulator $T_{MI}(P)$ (MI: open circles) lines were obtained from the AC susceptibility. The AF-SC boundary (double dashed line) is determined from the inflexion point of $\chi'(P)$ and, for 8.5K, from sublattice magnetization. This boundary line separates two regions of inhomogeneous phase coexistence (shaded area).

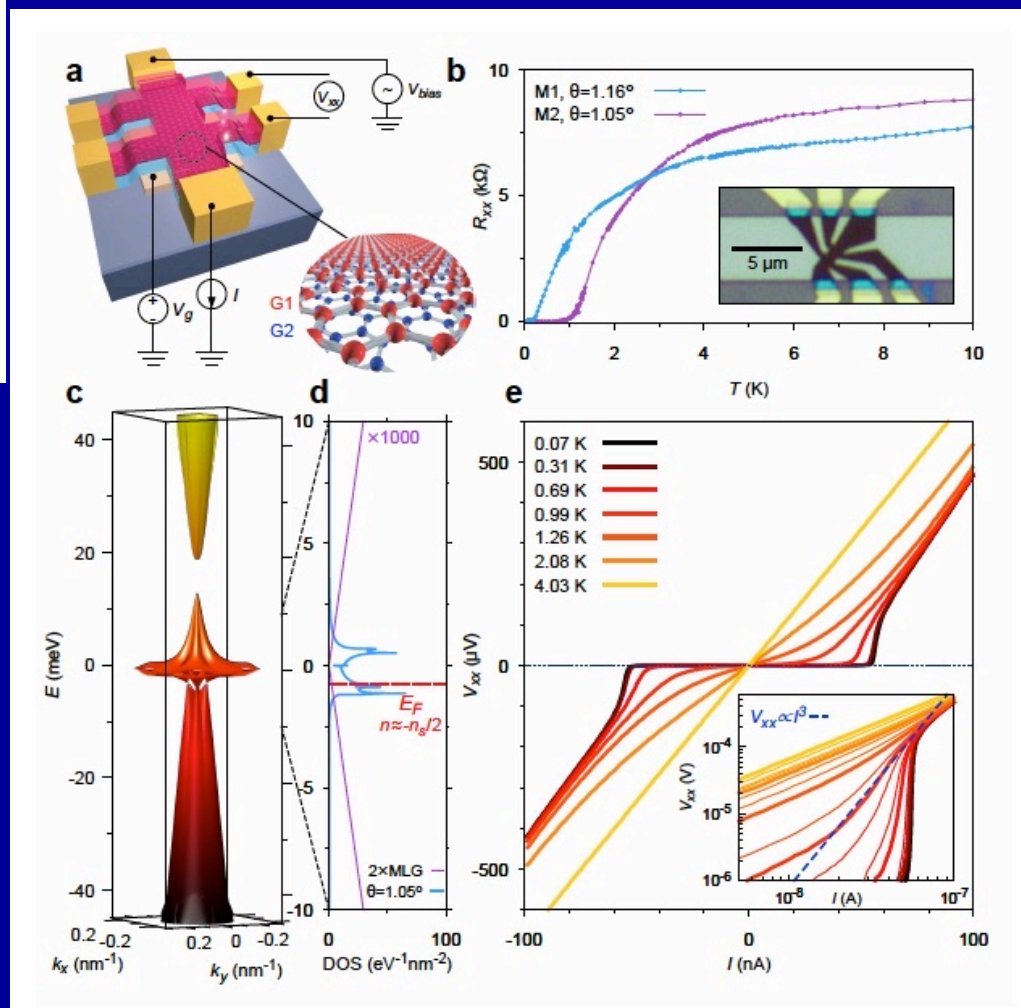
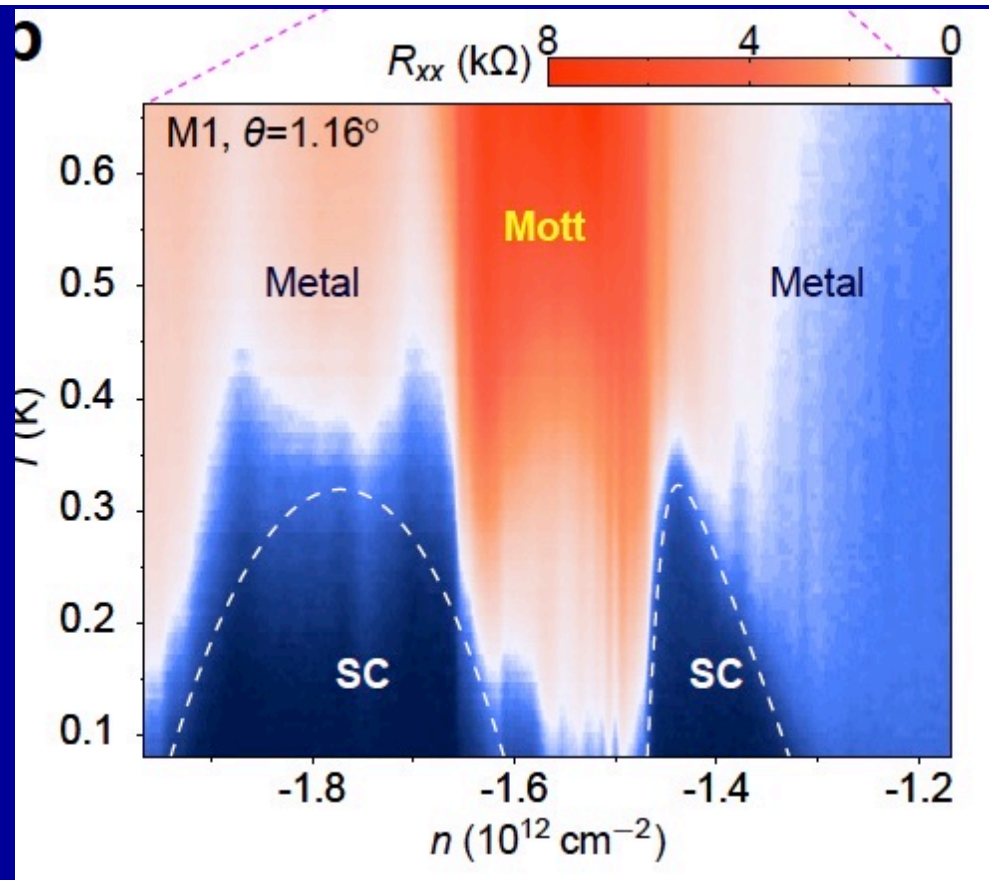


New Kid on the Block: Twisted Bilayer Graphene

Pablo Jarillo-Herrero's group at MIT - 2018

More broadly:
Moiré materials

Two-Dimensional Materials
(van der Waals-bound layers)
Transition-Metal Dichalcogenides



Cao et al.
Nature 556 (2018)
pages 43 and 80

Materials Discovery

(A never-ending story that keeps our field alive and busy)

1930-1950

1980's

1986

2002

2005

2007

2008

2015

2018

2019

- Classic correlated materials: TMs, Oxides/TMOs
- Organic conductors (1D, 2D)
- Heavy fermions
- Cuprates
- Renewal of interest in TMOs: Sr_2RuO_4 , RNiO_3 , Manganites, Iridates, and many many others...
- Mott to superfluid transition of cold atomic gases in optical lattices
- Topological Insulators
- Oxide heterostructures, SC in LAO/STO
- Fe-based superconductors
 - 'Hund metals' (New route to strong correlations)
- SC in pressurized H_2S 155GPa → other hydrides
- SC in twisted bilayer graphene
- Twisted TMDCs
 - Interplay of correlations and topology/Flat bands
 - Strong coupling to light, excitonic physics
- SC in infinite-layer RNiO_2
- Low density metals (STO), kagome metals

AND
SO
ON...

Experiments

Pushing the limits
New Instrumentation
New Techniques

Theory

Simple concepts
and basic mechanisms
Quantitative methods

The Magic Square

Materials Science and Chemistry

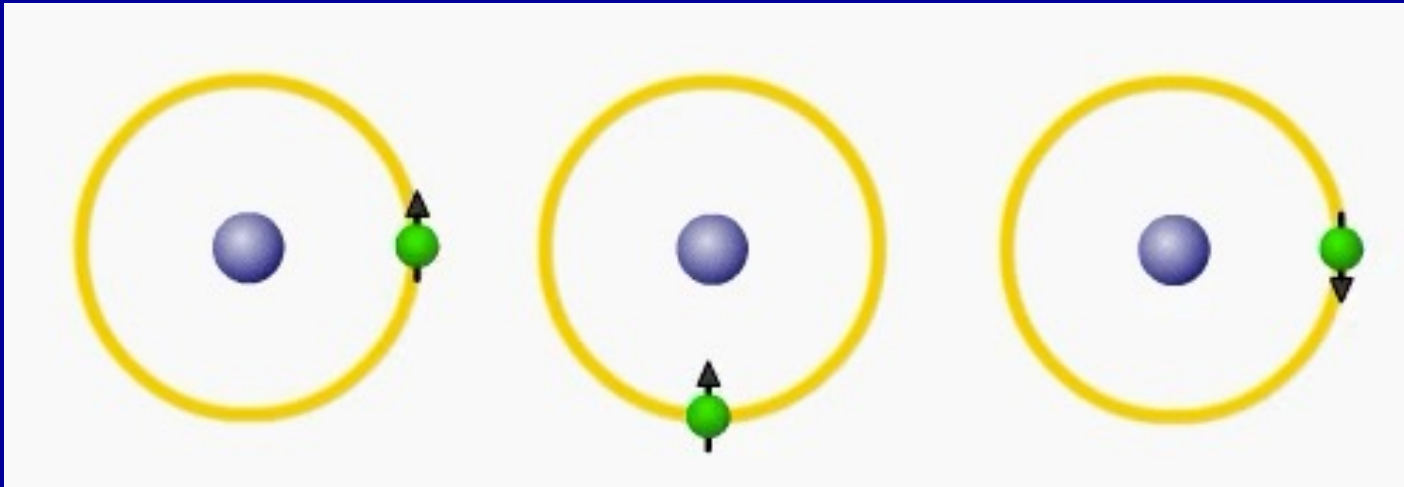
New materials, bulk or `artificial`
High quality samples
New elaboration methods

Devices and Control

Nanoscale devices
e.g gating
Atomic-scale synthesis
e.g. oxide MBE
`Synthetic materials`
e.g. TBLG/Twisted TMOs
Control by light:
Laser control, Cavities,...

In materials with strong
correlations
LOCAL ATOMIC PHYSICS
is crucial

Electrons “hesitate”
between being localized
on short-time-scales
and itinerant on long time-scales

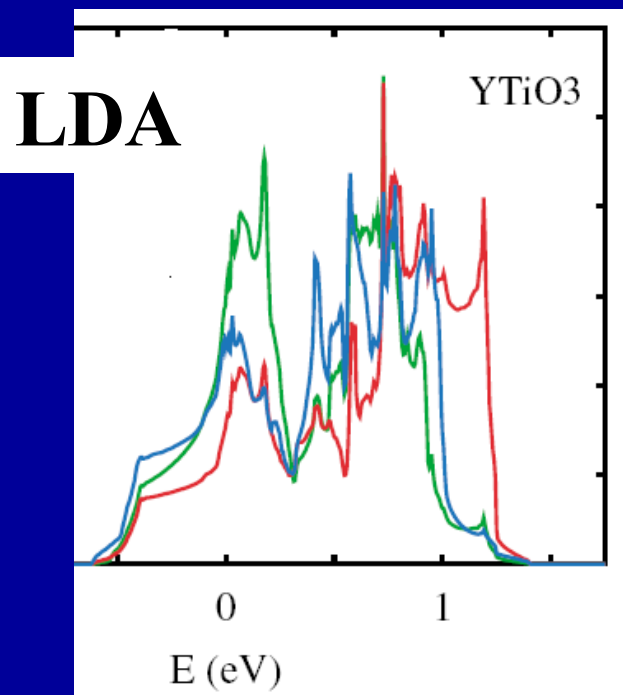


We see this from spectroscopy...

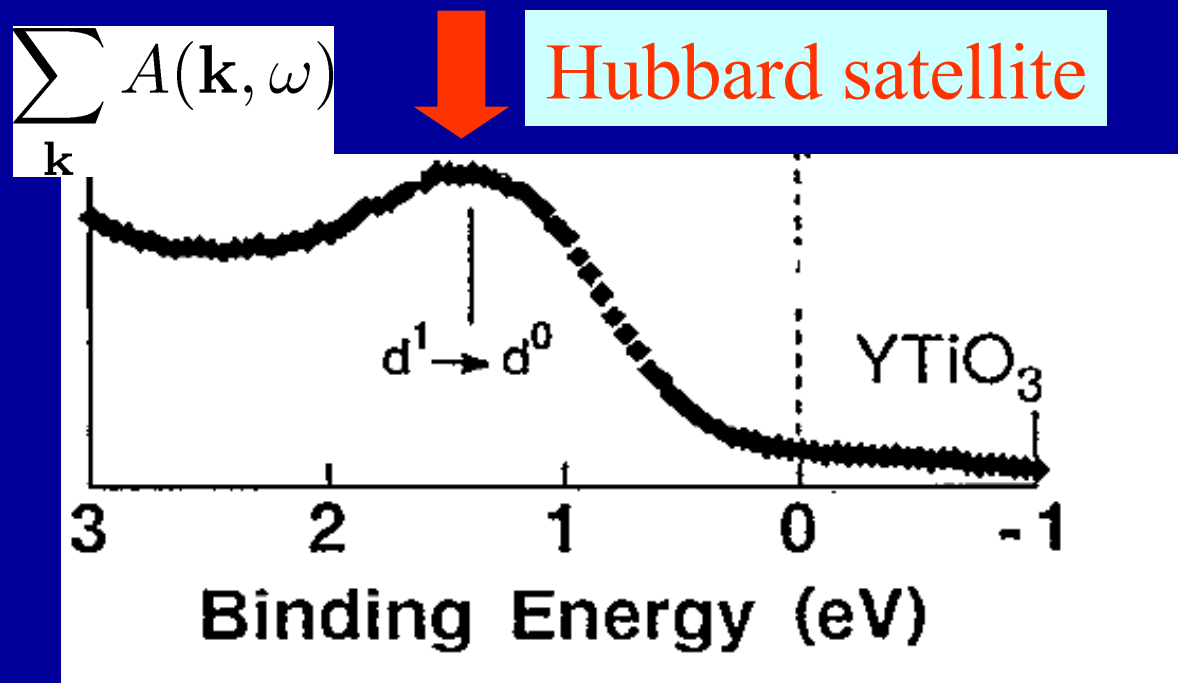
Mott insulators :

Their excitation spectra contain atomic-like excitations

Band structure calculations (interpreting Kohn-Sham spectra as excitations) is in serious trouble for correlated materials !



Metallic (Kohn-Sham) spectrum in DFT-LDA !

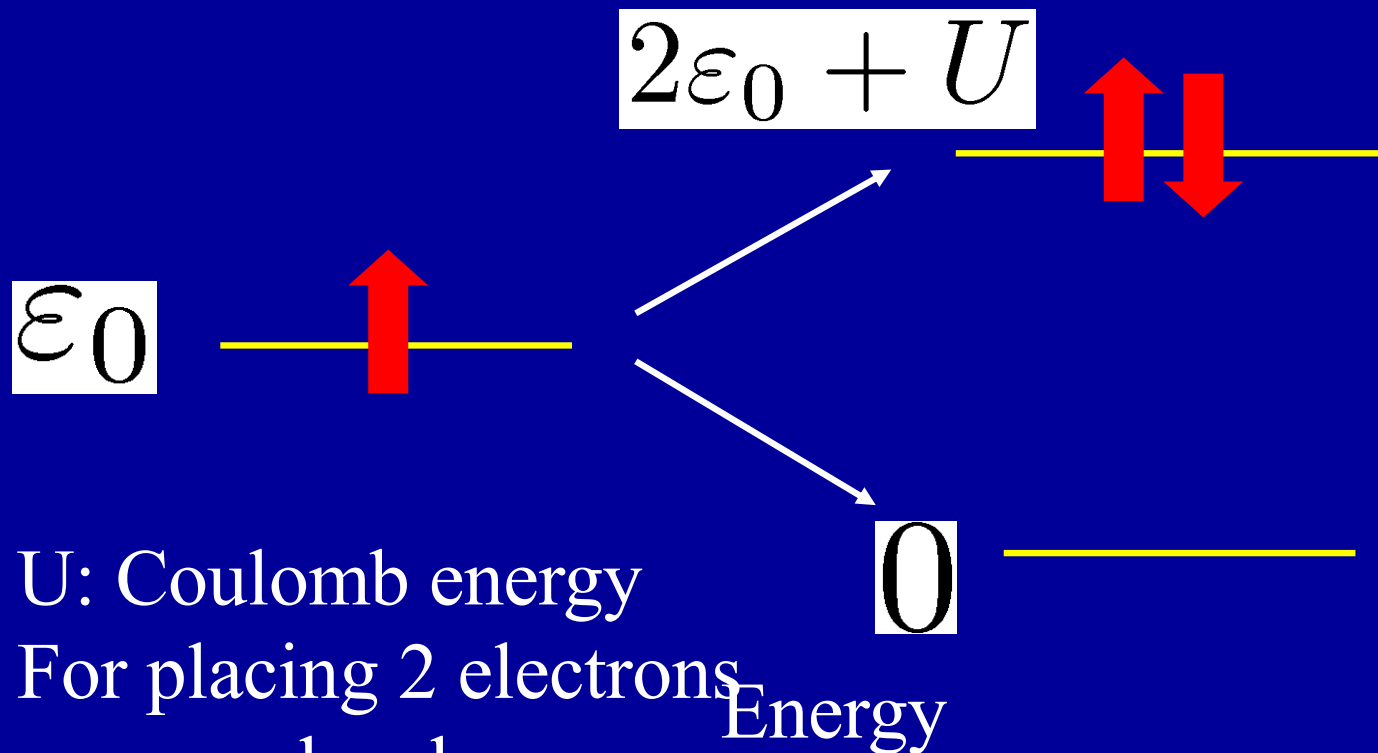


Photoemission: Fujimori et al., PRL 1992

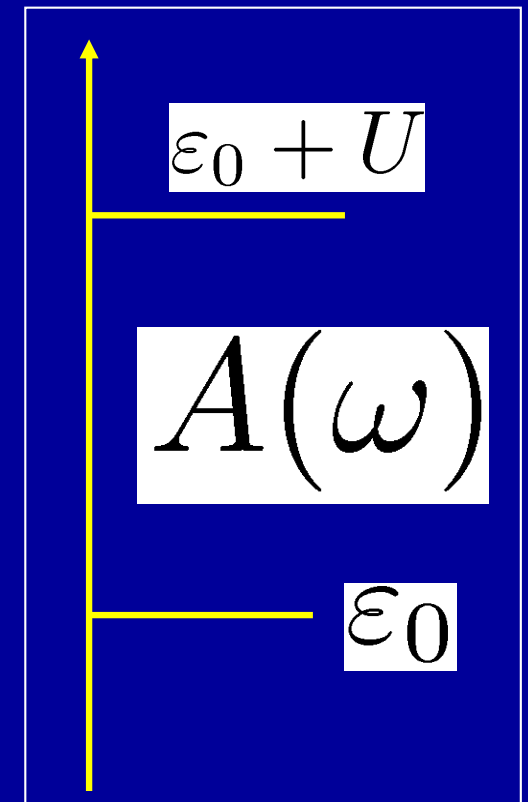
A "Hubbard satellite" is nothing but *an atomic transition*

(broadened by the solid-state environment)

Imagine a simplified atom with a single atomic level



U: Coulomb energy
For placing 2 electrons
on same level



Note: Energetics of the Mott gap
requires an accurate description
of the many-body eigenstates
of individual atoms

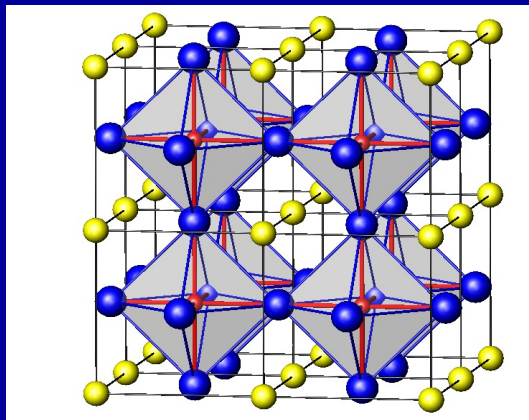
`Multiplets'

Multiple Interactions: $U, J_{\text{Hund}}, \dots$

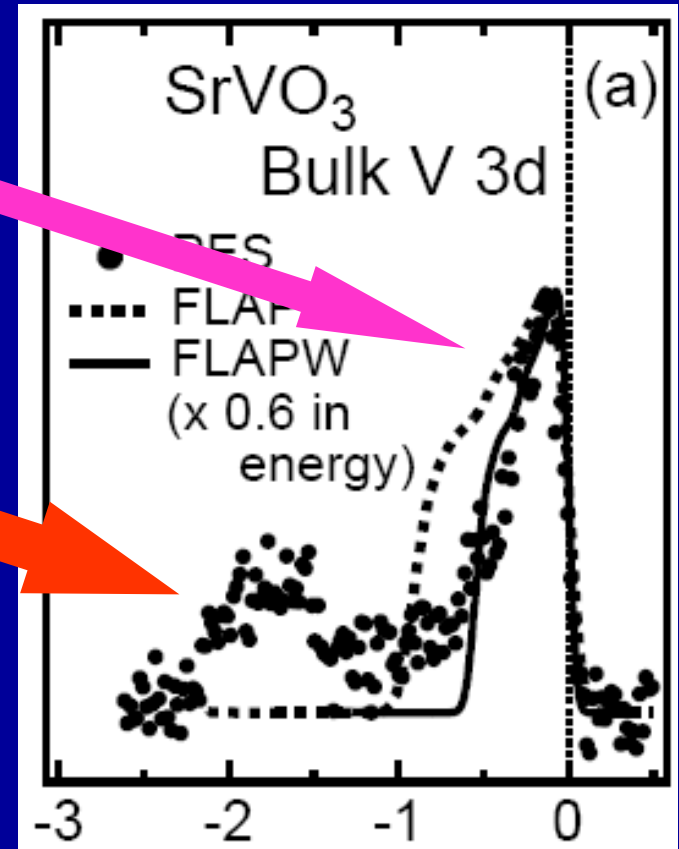
I'll come back to this later on

Correlated metals: atomic-like excitations at high energy, quasiparticles at low energy

- **Narrowing of quasiparticle bands** due to correlations (the Brinkman-Rice phenomenon)
- **Hubbard satellites** (i.e. extension to the solid of atomic-like transitions)



Dashed line:
Spectrum obtained from
Conventional
band-structure methods (DFT-LDA)

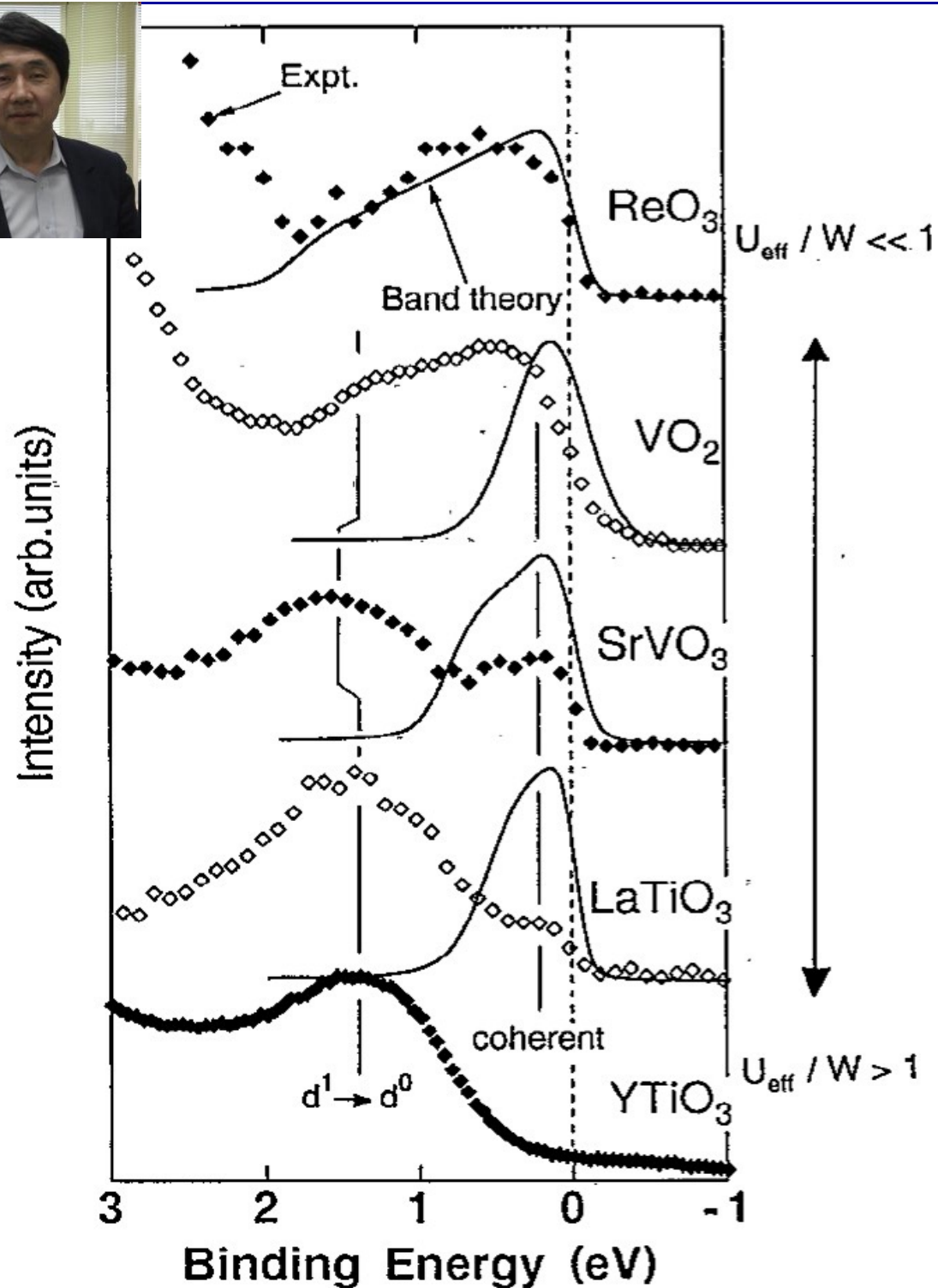
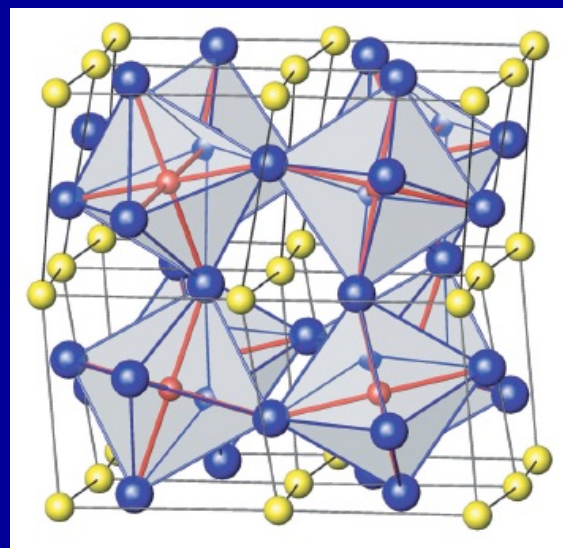


Sekiyama et al., PRL 2004

From weak to strong correlations in d^1 oxides
[Fujimori et al. PRL 69, 1796 (1992)]



Puzzle:
Why is $SrVO_3$
a metal
and $LaTiO_3$, $YTiO_3$
Mott insulators ?



Green's function, Spectral function

$$G_{ij,\sigma}(\tau - \tau') = -\langle T d_{i\sigma}(\tau) d_{j\sigma}^+(\tau') \rangle$$

$$A(\mathbf{k}, \omega) = \frac{1}{Z} \sum_{AB} \delta(\omega + E'_A - E'_B) |\langle A | c_{\mathbf{k}\sigma} | B \rangle|^2 \left[e^{-\beta E'_A} + e^{-\beta E'_B} \right]$$

T=0:

$$\omega < 0 : A(\mathbf{k}, \omega) = \sum_A \delta(\omega + E_A + \mu - E_0) |\langle A | c_{\mathbf{k}\sigma} | \Psi_0 \rangle|^2$$

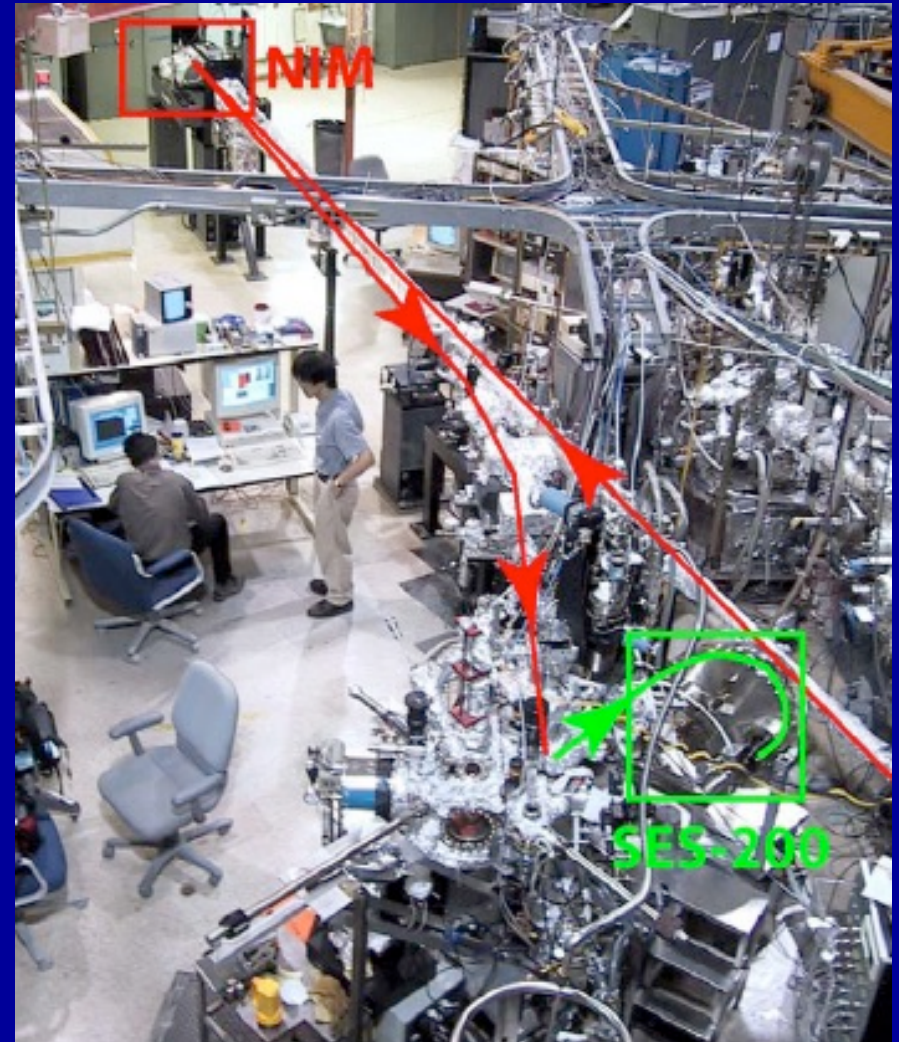
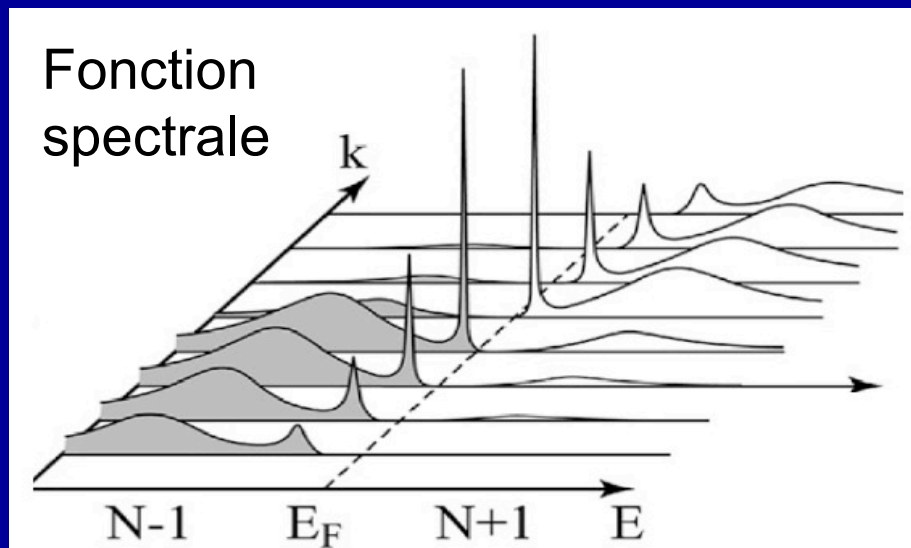
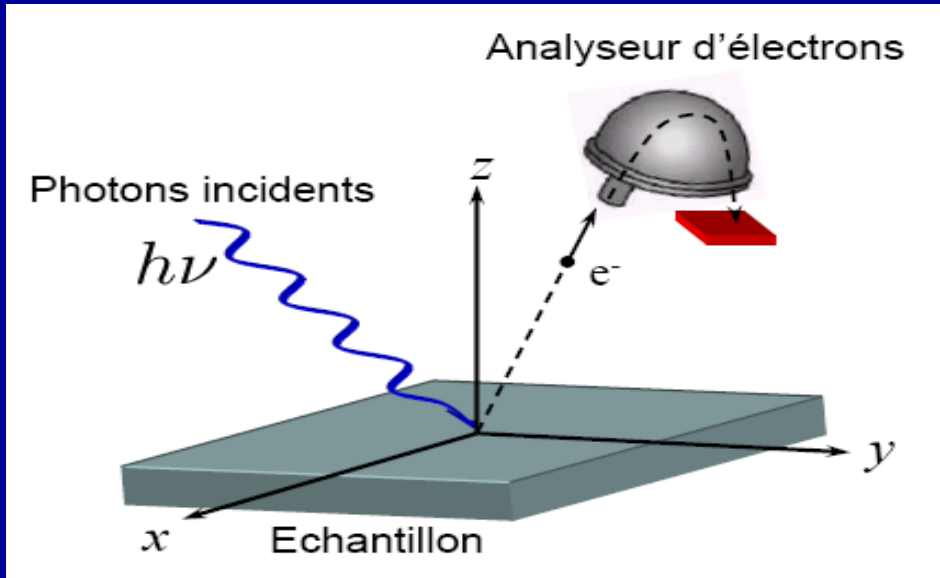
$$\omega > 0 : A(\mathbf{k}, \omega) = \sum_B \delta(\omega + E_0 - E_B + \mu) |\langle B | c_{\mathbf{k}\sigma}^+ | \Psi_0 \rangle|^2$$

$$G(\mathbf{k}, i\omega_n) = \int d\omega \frac{A(\mathbf{k}, \omega)}{i\omega_n - \omega} , \quad A(\mathbf{k}, \omega) = -\frac{1}{\pi} \text{Im} G(\mathbf{k}, \omega + i0^+)$$

$$A^0(\mathbf{k}, \omega) = \delta(\omega + \mu - \varepsilon_{\mathbf{k}}) , \quad G^0(\mathbf{k}, i\omega_n) = \frac{1}{i\omega_n + \mu - \varepsilon_{\mathbf{k}}}$$

Angle Resolved Photoemission Spectroscopy

cf. APS Buckley Prize 2011
Campuzano, Johnson, Shen



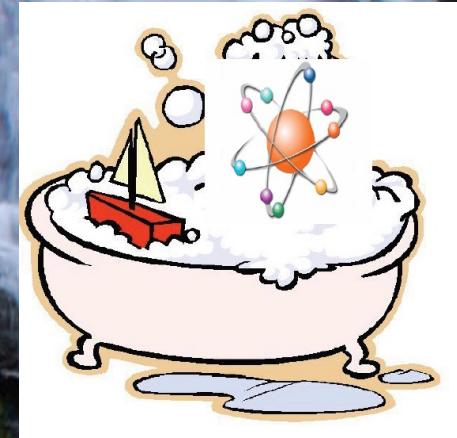
From Particles to Waves...

- High-energy excitations are best described as *localized particle-like atomic transitions*.
(cf. Mott insulators - 'Hubbard bands')
- In metals coherent *wave-like excitations* emerge at low energy: *quasiparticles*
- DMFT starts from atoms (each atom is a small many-body problem) and describes how quasiparticles emerge as one follows the flow from high-energy to low-energy

High energy
High temperature
Short time scales
Short distances
Large lattice spacing
LOCAL
INCOHERENT

Atomic configurations/Multiplets
Intra-shell interactions+crystal fields

Environment Lifts degeneracies...



Collective ground-state
Low-energy excitations
Effective low-energy theory

Low energy
Low temperature
Long time scales
Long distances
Small lattice spacing
NON-LOCAL
COHERENT

A theoretical description of the
solid-state based on ATOMS
rather than on an electron-gas picture:
« ***Dynamical Mean-Field Theory*** »

Dynamical Mean-Field Theory:
A.G. & G.Kotliar, PRB 45, 6479 (1992)
Correlated electrons in large dimensions:
W.Metzner & D.Vollhardt, PRL 62, 324 (1989)

*Important intermediate steps by: Müller-Hartmann,
Schweitzer and Czycholl, Brandt and Mielsch, V.Janis*

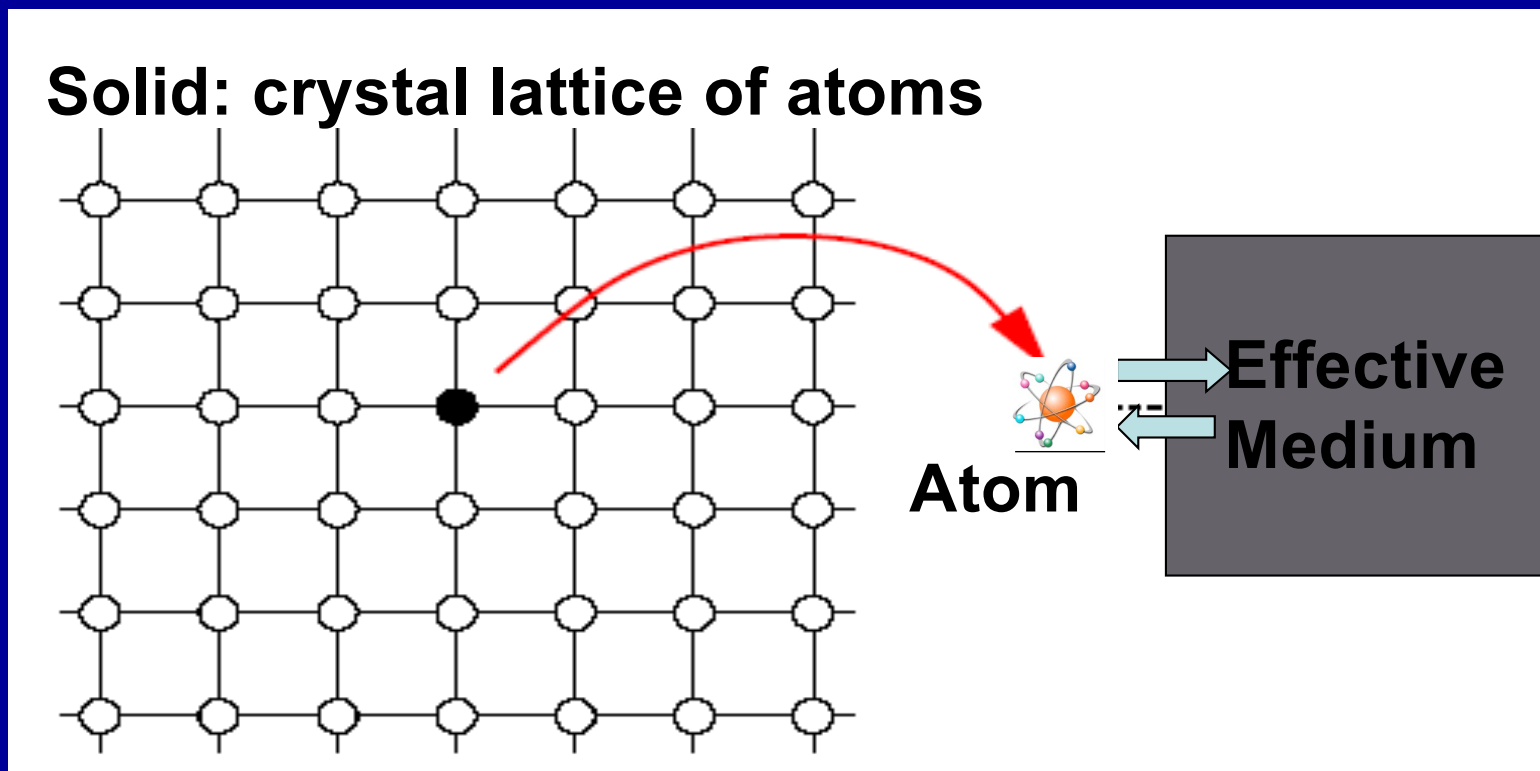
Early review: Georges et al. Rev Mod Phys 68, 13 (1996)

Dynamical Mean Field Theory

- *A theoretical and computational method to approach the many-body quantum problem.* The method becomes exact in limiting cases and can be systematically improved in a controlled way.
- *A conceptual framework to think about materials with strong electron correlations and understand their physics*

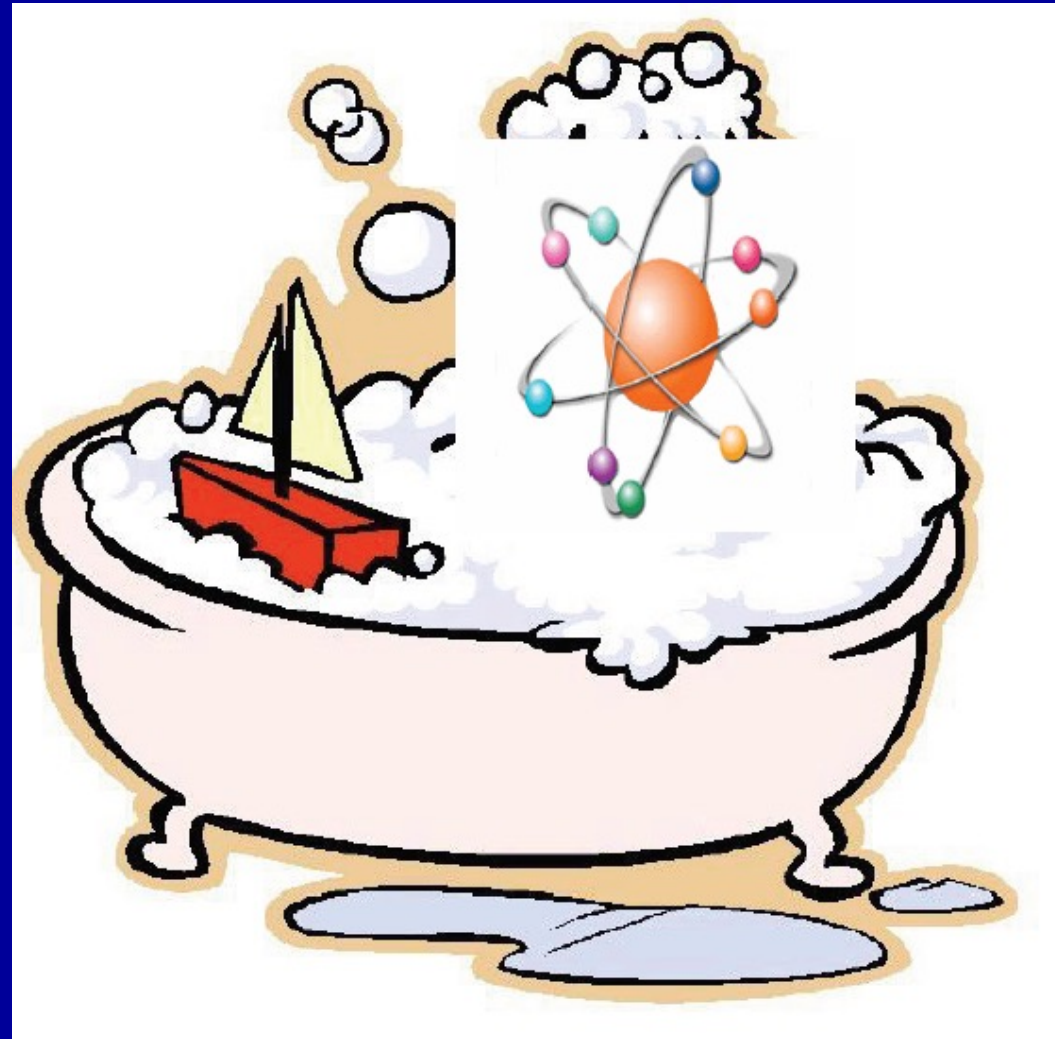
Dynamical Mean-Field Theory:

Viewing a material as an (ensemble of) **atoms** coupled to a **self-consistent effective medium**



Correlated electrons in infinite dimensions W.Metzner & D.Vollhardt, 1989
Dynamical Mean-Field Theory A.G. & G.Kotliar, 1992

'Atom in a Bath'



The Two Components of the DMFT Formalism:

- (1) *A representative system* for the local Green's function (= observable central to the theory): 'atom in a bath/ embedding'
- (2) *A self-consistency condition* relating the bath to the entire system
- (1) is exact – at least in the model context (for solids extension to G and W is required to make it exact)
- (2) is an approximation, which can be systematically improved

Weiss mean-field theory
 Density-functional theory
 Dynamical mean-field theory

Share a similar
 conceptual basis

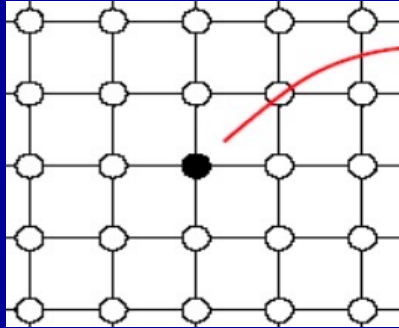
TABLE 2. Comparison of theories based on functionals of a local observable

Theory	MFT	DFT	DMFT
Quantity	Local magnetization m_i	Local density $n(x)$	Local GF $G_{ii}(\omega)$
Equivalent system	Spin in effective field	Electrons in effective potential	Quantum impurity model
Generalised Weiss field	Effective local field	Kohn-Sham potential	Effective hybridisation

$$\Delta(\omega)$$

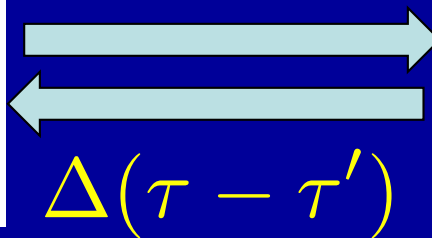
Total Energy Functional: $E[G]$ or $E[\Sigma]$

The Embedding Concept



Observable: Local Green's function

$$G_{ii}(\tau - \tau') = -\langle T d_i(\tau) d_i^\dagger(\tau') \rangle \equiv G_{loc}$$



Effective Medium
(`Bath')

$\Delta(\tau - \tau')$: Dynamical Mean-Field

Quantum generalization of Weiss field

Chosen such as to reproduce the local G:

$$G_{loc} = G_{imp}[\Delta]$$

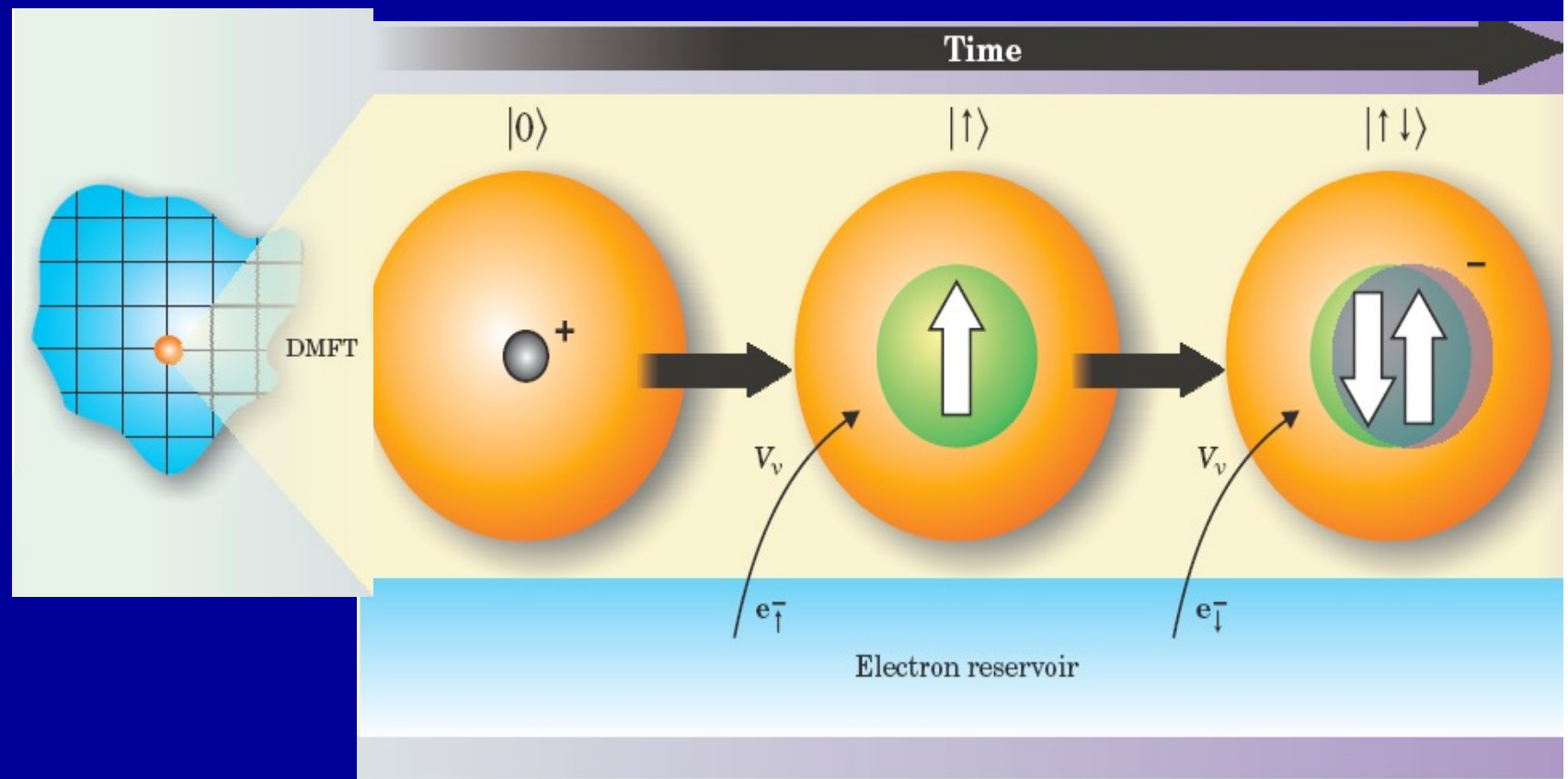
Example: DMFT for the Hubbard model (a model of coupled atoms)

$$\hat{H} = - \sum_{ij} \sum_{\sigma=\uparrow,\downarrow} t_{ij} d_{i\sigma}^+ d_{j\sigma} + \sum_i \hat{H}_{\text{atom}}^{(i)}$$
$$\hat{H}_{\text{atom}} = U \hat{n}_{\uparrow} \hat{n}_{\downarrow} + \varepsilon_d (\hat{n}_{\uparrow} + \hat{n}_{\downarrow})$$

Focus on a given lattice site:

“Atom” can be in 4 possible configurations: $|0\rangle, |\uparrow\rangle, |\downarrow\rangle, |\uparrow\downarrow\rangle$

Describe “history” of quantum jumps between those configurations:



Atom in a bath: Anderson impurity model

$$H_c = \sum_{l\sigma} E_l a_{l\sigma}^\dagger a_{l\sigma}$$

$$H = H_c + H_{\text{at}} + H_{\text{hyb}}$$

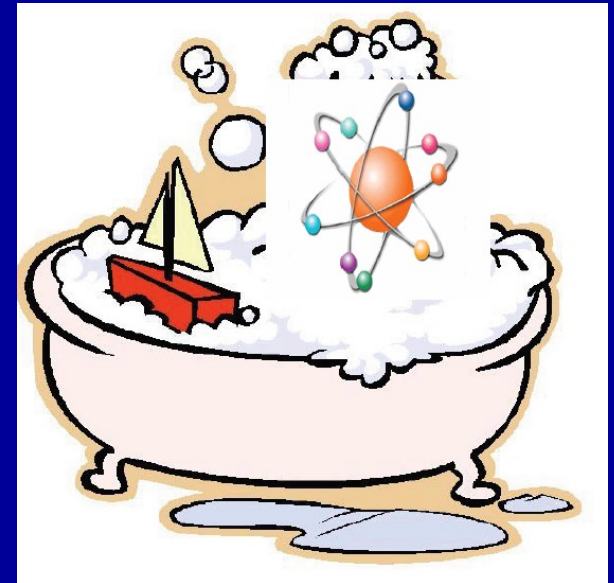
Electrons in the (non-interacting) bath

$$H_{\text{at}} = \varepsilon_d \sum_{\sigma} d_{\sigma}^\dagger d_{\sigma} + U n_{\uparrow}^d n_{\downarrow}^d$$

Single-level "atom"

$$H_{\text{hyb}} = \sum_{l\sigma} [V_l a_{l\sigma}^\dagger d_{\sigma} + \text{h.c.}]$$

Transfers electrons between bath and atom – Hybridization



$$\Delta_{AIM}(i\omega_n) = \sum_l \frac{|V_l|^2}{i\omega_n - E_l}$$

A bit of linear algebra...

$$\hat{G}_0 = \begin{bmatrix} i\omega - \varepsilon_d & -V_1 & \dots & -V_N \\ -V_1^* & i\omega - E_1 & 0 \dots & \dots 0 \\ -V_2^* & 0 & i\omega - E_2 & \dots 0 \\ \dots & \dots & \dots & \dots \\ -V_N^* & 0 \dots & \dots 0 & i\omega - E_N \end{bmatrix}^{-1}$$

$$\Rightarrow \mathcal{G}_0 = \left[\hat{G}_0 \right]_{dd} = \frac{1}{i\omega - \varepsilon_d - \sum_l \frac{|V_l|^2}{i\omega - E_l}}$$

Hint: Look for an inverse of the form: $\hat{G}_0 = \begin{bmatrix} \mathcal{G}_0 & a_1 & \dots & a_N \\ -a_1^* & g_1 & 0 \dots & \dots 0 \\ -a_2^* & 0 & g_2 & \dots 0 \\ \dots & \dots & \dots & \dots \\ -a_N^* & 0 \dots & \dots 0 & g_N \end{bmatrix}$

Hybridization Function

= Dynamical Mean-Field
= Quantum Generalization
of the Weiss field

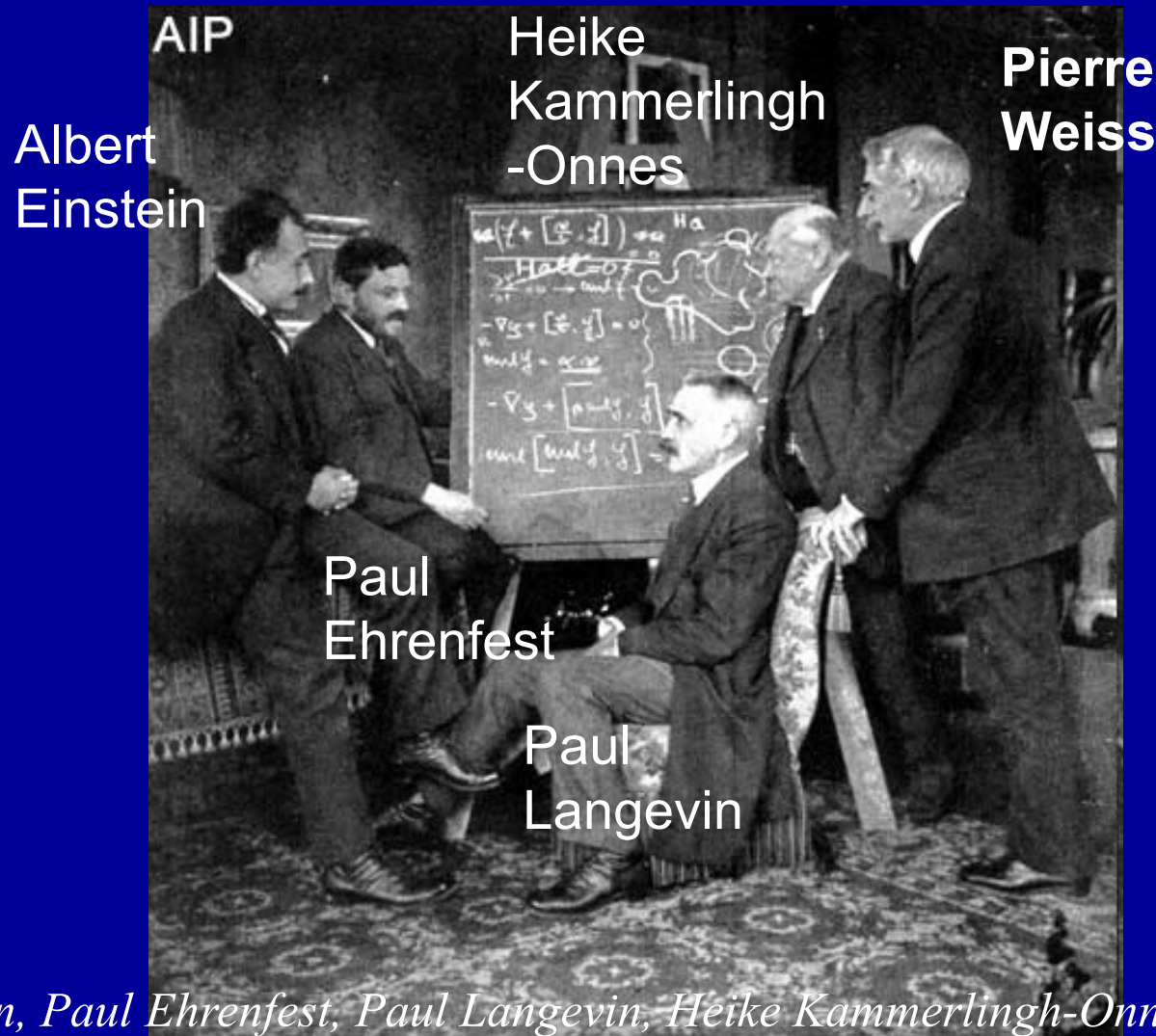
The dynamics of quantum jumps in the embedded atoms is entirely determined by:

(i) U

(ii) ε_d

(iii)
$$\Delta(i\omega) = - \int d\epsilon \frac{-\text{Im}\Delta(\epsilon + i0^+)/\pi}{i\omega - \epsilon}$$

$\Delta(\omega)$: generalizing the Weiss field to the quantum world



Pierre Weiss
1865-1940
« *Théorie du
Champ
Moléculaire* »
(1907)

Einstein, Paul Ehrenfest, Paul Langevin, Heike Kammerlingh-Onnes, and Pierre Weiss at Ehrenfest's home, Leyden, the Netherlands. From Einstein, His Life and Times, by Philipp Frank (New York: A.A. Knopf, 1947). Photo courtesy AIP Emilio Segrè Visual Archives.

Weiss mean-field theory
 Density-functional theory
 Dynamical mean-field theory

Share a similar
 conceptual basis

TABLE 2. Comparison of theories based on functionals of a local observable

Theory	MFT	DFT	DMFT
Quantity	Local magnetization m_i	Local density $n(x)$	Local GF $G_{ii}(\omega)$
Equivalent system	Spin in effective field	Electrons in effective potential	Quantum impurity model
Generalised Weiss field	Effective local field	Kohn-Sham potential	Effective hybridisation

$$\Delta(\omega)$$

Total Energy Functional: $E[G]$ or $E[\Sigma]$

Imaginary-time effective action describing the histories of quantum jumps / valence changes

$$S = S_{at} + S_{hyb}$$

$$S_{at} = \int_0^\beta d\tau \sum_{\sigma} d_{\sigma}^{\dagger}(\tau) \left(\frac{\partial}{\partial \tau} + \varepsilon_d \right) d_{\sigma}(\tau) + U \int_0^\beta d\tau n_{\uparrow}(\tau) n_{\downarrow}(\tau)$$

$$S_{hyb} = \int_0^\beta d\tau \int_0^\beta d\tau' \sum_{\sigma} d_{\sigma}^{\dagger}(\tau) \Delta(\tau - \tau') d_{\sigma}(\tau')$$

The amplitude $\Delta(\tau)$ for hopping in and out of the selected site is self-consistently determined: it is the quantum-mechanical Generalization of the Weiss effective field.

$$\mathcal{G}_0^{-1}(i\omega) = i\omega + \mu - \Delta(i\omega) \quad \text{Effective 'bare propagator'}$$

Organizing Principle: Locality

The single-site DMFT approximation (1 band): local self-energy

$$\Sigma_{\text{lattice}}(\mathbf{k}, \omega) \simeq \Sigma(\omega) \Leftrightarrow \Sigma_{ij}(\omega) \simeq \Sigma(\omega) \delta_{ij}$$

With $\Sigma(\omega)$ the self-energy of the embedded atom ('impurity')

A good approximation when correlation lengths are SMALL (e.g. high temperature, high doping, frustration, several competing fluctuations, etc.)

Can be improved in a systematic and controlled way by enlarging the size of the embedded fragment:
Cluster Extensions of DMFT, Generalized Embedding Methods...

The Dyson equation then leads to a self-consistency condition:

$$G_{loc}(\omega) \equiv \int d\mathbf{k} [\omega + \mu - H_{\mathbf{k}}^0 - \Sigma(\mathbf{k}, \omega)]^{-1}$$

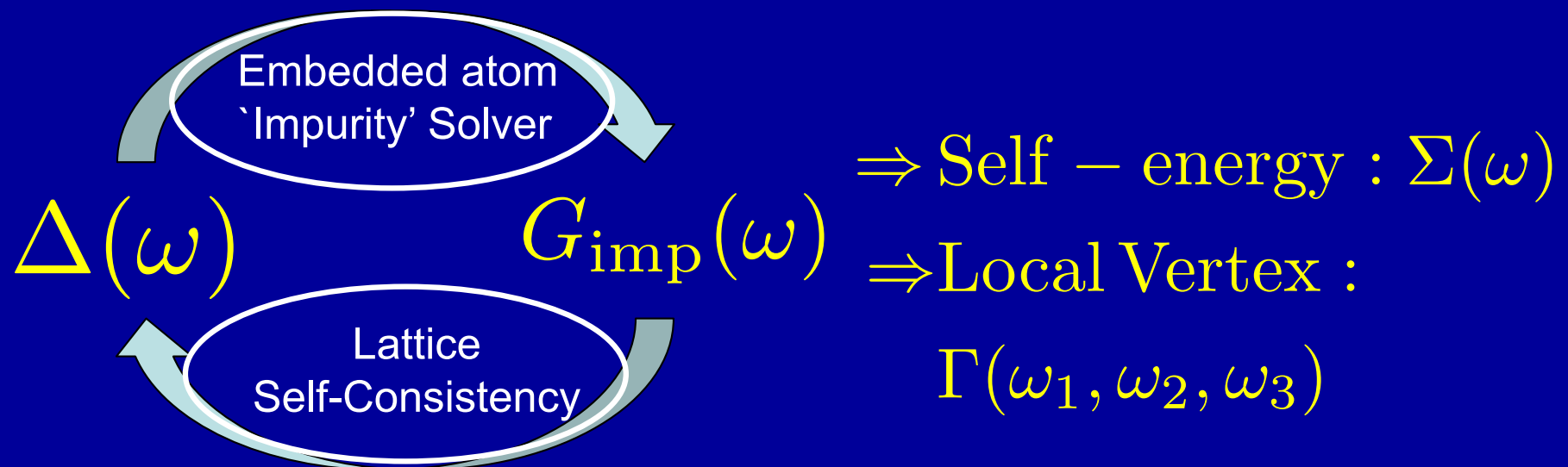
$$G_{loc} = G_{imp}$$

$$G_{imp}^{-1} = \mathcal{G}_0^{-1} - \Sigma_{imp} = \omega + \mu - \Delta(\omega) - \Sigma_{imp}$$

$$\Sigma(\mathbf{k}, \omega) \simeq \Sigma_{imp}(\omega)$$

$$\Rightarrow G_{loc}(\omega) \equiv \int d\mathbf{k} [G^{-1}(\omega) + \Delta(\omega) - H_{\mathbf{k}}^0]^{-1}$$

The DMFT Self-Consistency Loop



Gives access to the lattice momentum-dependent Green's function and response functions:

$$G(\mathbf{k}, \omega) = [\omega + \mu - H_{\mathbf{k}} - \Sigma(\omega)]^{-1}$$

$$\chi(\mathbf{q}, \omega) \sim \chi_0 + \chi_0 \star \Gamma \star \chi$$

The single-site DMFT construction is EXACT:

- For the non-interacting system

$U = 0 \rightarrow \Sigma = 0$ - hence k-independent!

- For the isolated atom

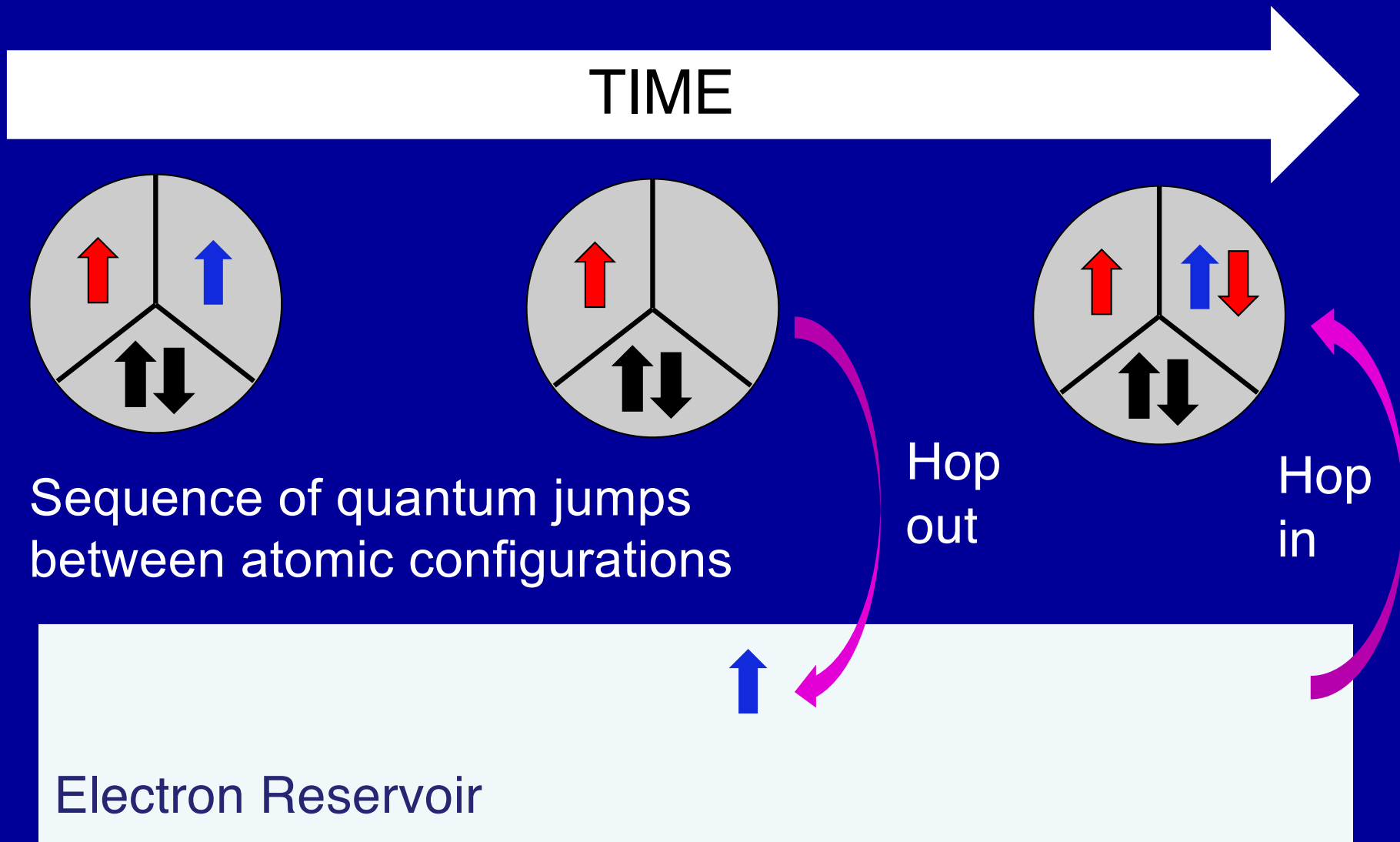
`Atomic' limit $t=0 \rightarrow \Sigma = \Sigma_{\text{atom}}(\omega)$

Hence provides an interpolation
from weak to strong coupling

- In the formal limit of infinite dimensionality (infinite lattice coordination) [introduced by Metzner and Vollhardt, PRL 62 (1989) 324]

And, more relevant to physics:
it is a good approximation
when spatial correlations are not too long-range

Generalization to an atomic shell with several orbitals (m)



Effective action describing these sequences: Generalized Anderson impurity model

$$S = S_{at} + S_{hyb}$$

$$S_{at} = \int_0^\beta d\tau \sum_{m\sigma} d_{m\sigma}^+(\tau) \frac{\partial}{\partial \tau} d_{m\sigma}(\tau) + \int_0^\beta d\tau H_{at}[d, d^+]$$

$$S_{hyb} = \int_0^\beta d\tau \int_0^\beta d\tau' \sum_{\sigma} d_{m\sigma}^+(\tau) \Delta_{mm'}(\tau - \tau') d_{m'\sigma}(\tau')$$

The amplitude $\Delta(\tau)$ for hopping in and out of the selected site is self-consistently determined: it is the quantum-mechanical Generalization of the Weiss effective field.

$$\mathcal{G}_0^{-1}(i\omega) = i\omega + \mu - \Delta(i\omega) : \text{Effective 'bare propagator'}$$

Self-Energy: The DMFT *ansatz*

For a multi-band/multi-orbital material

$|\chi_m^{\mathbf{k}}\rangle$: A set of localized orbitals with many-body interactions $U_{m_1 m_2 m_3 m_4}$ are added: correlated Hilbert space

$|\psi_\nu^{\mathbf{k}}\rangle$: The (usually larger) set of Bloch bands (e.g. Kohn-Sham states) describing the material (larger Hilbert space)

$$\Sigma_{\nu\nu'}(\omega, \mathbf{k}) = \sum_{mm'} \langle \psi_\nu^{\mathbf{k}} | \chi_m^{\mathbf{k}} \rangle \Sigma_{mm'}(\omega) \langle \chi_{m'}^{\mathbf{k}} | \psi_{\nu'}^{\mathbf{k}} \rangle$$

↑
Self-energy
`unfolded' to
the whole system
(k-dependent)

↑
Orbital content
of Bloch states
(k-dep)

↑
Local self-energy
`unfolded' to
the whole system
(k-dependent)

Derivations of the
DMFT Equations
in the large dimensionality/
large lattice connectivity
limit

$$t_{ij} = \frac{t}{\sqrt{z}}$$

Derivation of DMFT equations: The BK functional route

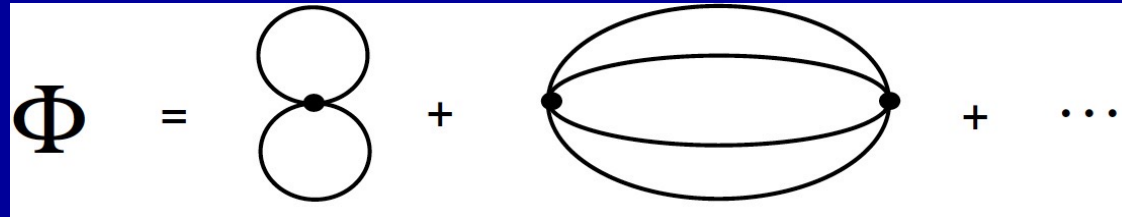
Locality of the Luttinger-Ward functional:

$$\begin{aligned}\Omega_{BK}[G, \Sigma] = & -Tr \ln [(i\omega_n + \mu)\delta_{ij} - t_{ij} - \Sigma_{ij}] - \\ & - Tr [\Sigma \cdot G] + \\ & + \sum_i \phi_{atom}[G_{ii}]\end{aligned}$$

$$\frac{\delta\Omega}{\delta\Sigma} = 0 \rightarrow \hat{G}^{-1} = \hat{G}_0^{-1} - \hat{\Sigma} \quad (\text{Dyson})$$

$$\frac{\delta\Omega}{\delta G_{ij}} = 0 \rightarrow \Sigma_{ij} = \delta_{ij} \Sigma_{atom}[G_{ii}]$$

The Luttinger-Ward Functional

$$\Phi = \text{[Diagram 1]} + \text{[Diagram 2]} + \dots$$


Does it really exist ? 😊

PRL **114**, 156402 (2015)

PHYSICAL REVIEW LETTERS

week ending
17 APRIL 2015

Nonexistence of the Luttinger-Ward Functional and Misleading Convergence of Skeleton Diagrammatic Series for Hubbard-Like Models

Evgeny Kozik,^{1,2,*} Michel Ferrero,² and Antoine Georges^{3,2,4}

IOP Publishing

Journal of Physics A: Mathematical and Theoretical

J. Phys. A: Math. Theor. **48** (2015) 485202 (6pp)

doi:10.1088/1751-8113/48/48/485202

Skeleton series and multivaluedness of the self-energy functional in zero space-time dimensions

Riccardo Rossi¹ and Félix Werner²

Classical StatMech Model in which an infinite series of terms must be summed in $d \rightarrow \infty$: fully frustrated Ising

J. Phys. A: Math. Gen. **23** (1990) 2165–2171. Printed in the UK

The fully frustrated Ising model in infinite dimensions

Jonathan S Yedidia[†] and Antoine Georges[‡]

[†] Department of Physics, Jadwin Hall, Princeton University, Princeton, NJ 08544, USA
[‡] Laboratoire de Physique Théorique, Ecole Normale Supérieure, 24 rue Lhomond, 75231 Paris Cedex 05, France

Received 28 September 1989

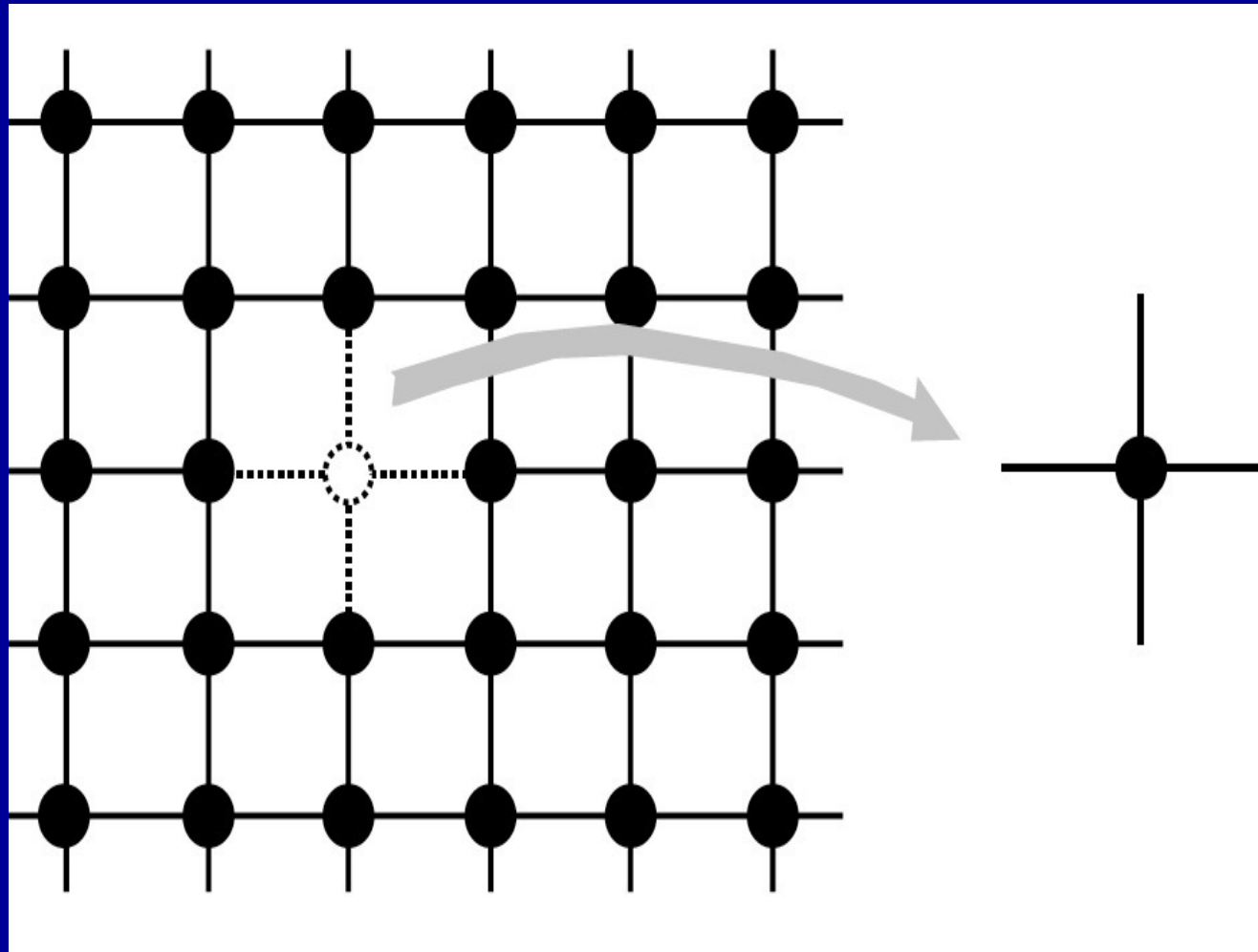
Abstract. We solve, subject to the validity of some reasonable assumptions, the 'fully frustrated' Ising model in the limit of infinite dimensions using an extension of the TAP theory for spin glasses. In contrast to the TAP theory of the infinite-range spin glass, an infinite summation of diagrams is required to recover the Gibbs free energy for this model. The model undergoes a first-order transition. The method used to solve the model should have many applications to other physical problems.

$$\begin{aligned}
 -\beta G &= \bullet + \bullet\text{---}\bullet + \text{---}\circ\text{---} + \text{---}\square\text{---} + \text{---}\hexagon\text{---} + \text{---}\octagon\text{---} + \dots \\
 &= -\sum_i \left(\frac{1+m_i}{2} \right) \ln \left(\frac{1+m_i}{2} \right) + \left(\frac{1-m_i}{2} \right) \ln \left(\frac{1-m_i}{2} \right) \\
 &\quad + \beta \sum_{(ij)} J_{ij} m_i m_j + \frac{\beta^2}{2} \sum_{(ij)} J_{ij}^2 (1-m_i^2)(1-m_j^2) \\
 &\quad + \beta^4 \sum_{(ijkl)} J_{ij} J_{jk} J_{kl} J_{li} (1-m_i^2)(1-m_j^2)(1-m_k^2)(1-m_l^2) + \dots
 \end{aligned}$$

Figure 1. The Gibbs free energy of the 'fully frustrated' Ising model on a hypercubic lattice in the limit of infinite dimensions.

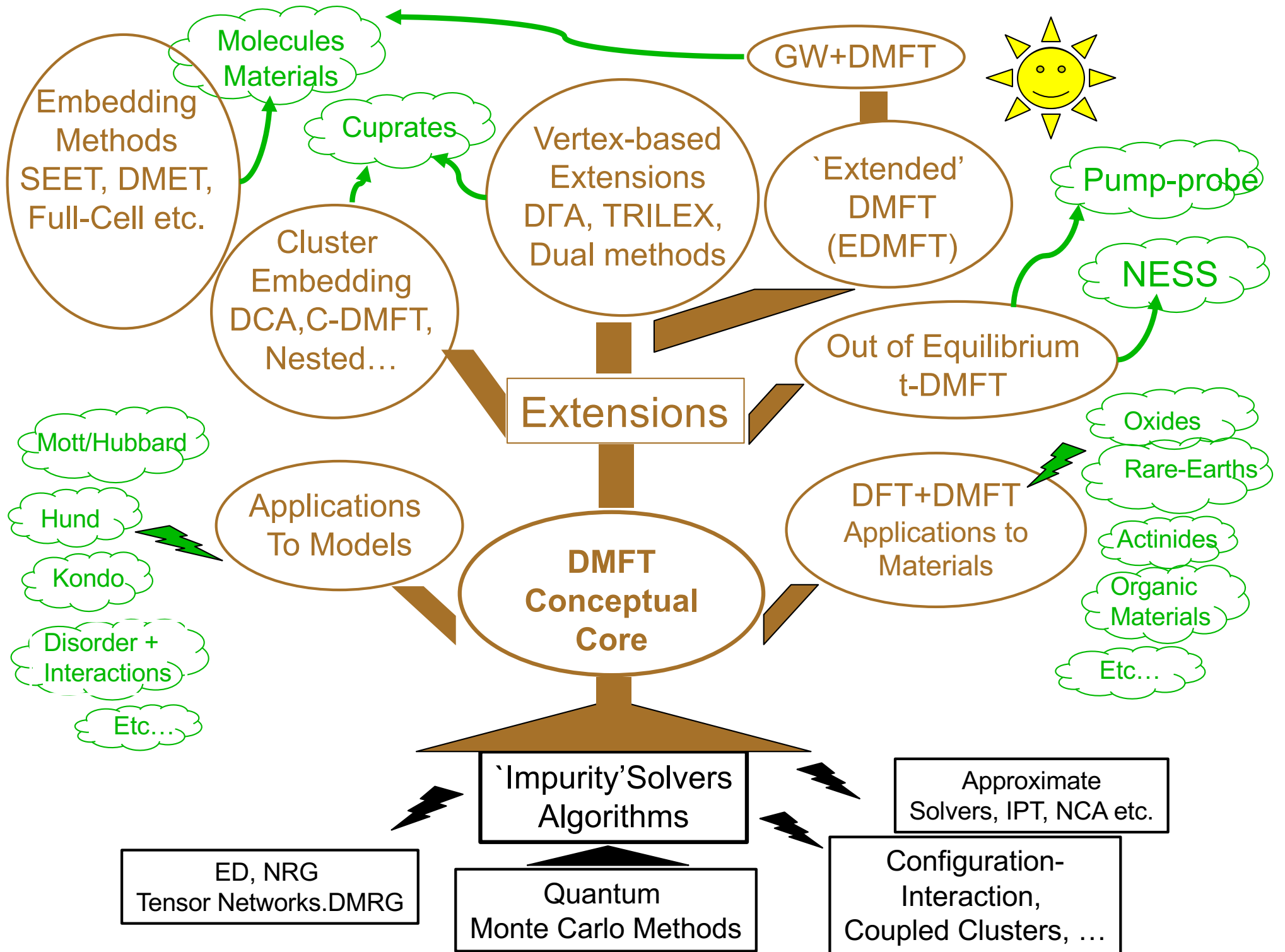
Cavity method

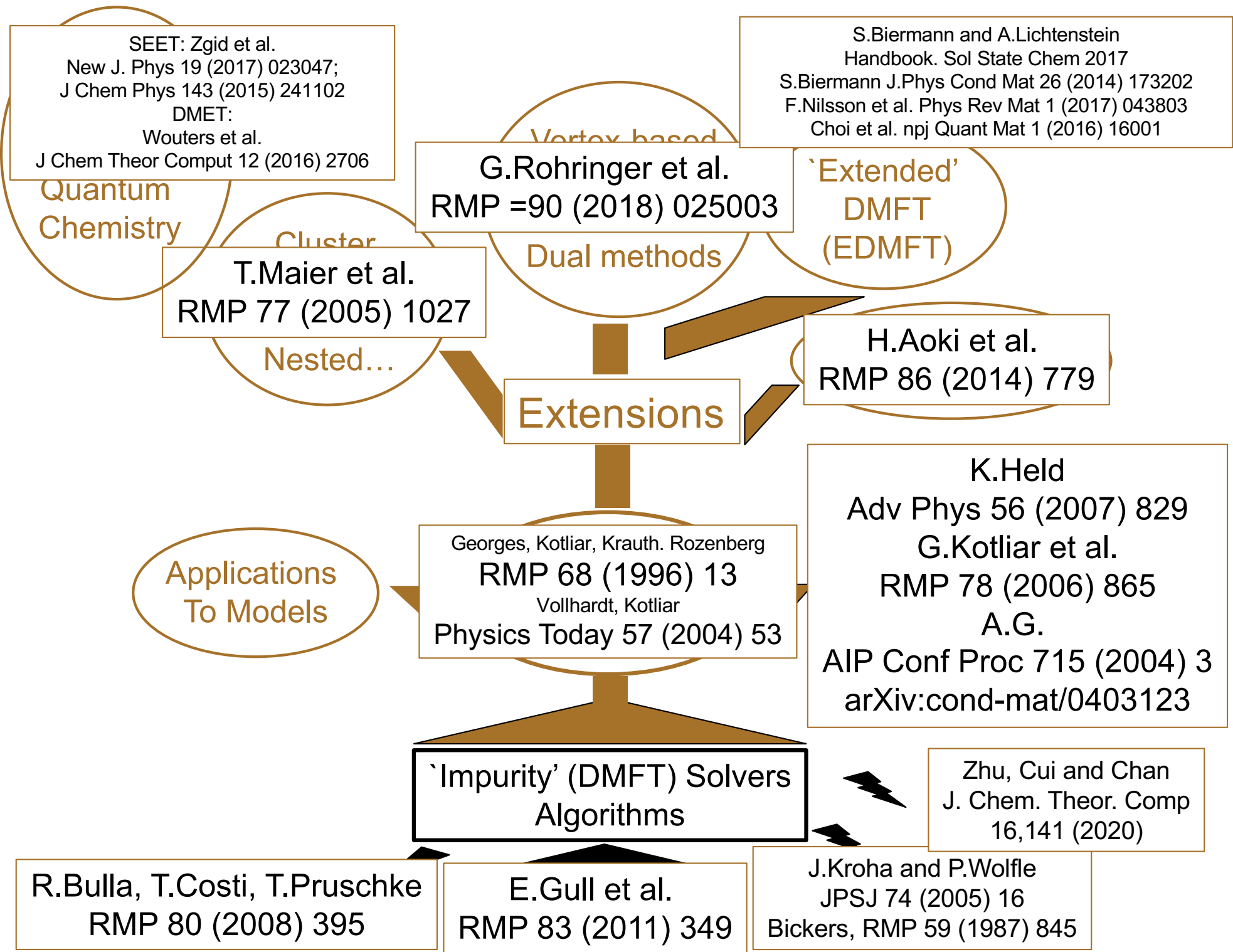
See Rev Mod Phys 1996



DMFT and Quantum Embedding Theories:

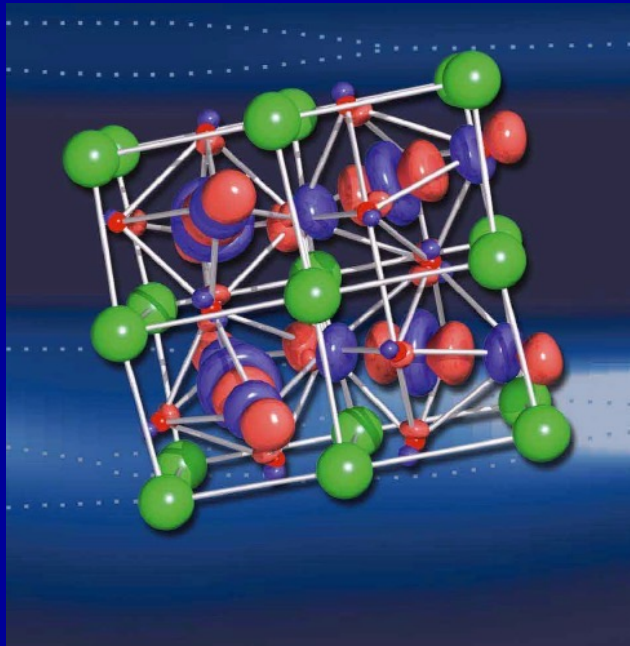
Entering the 4th decade of
development and generalizations



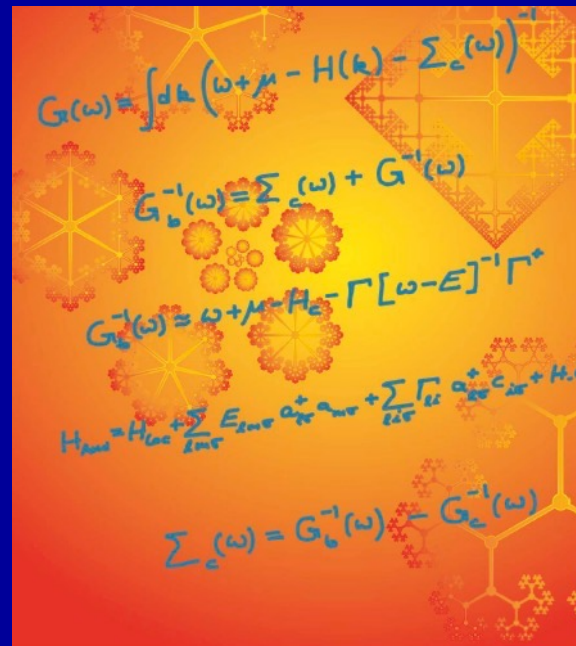


Jülich Autumn School on Correlated Electrons

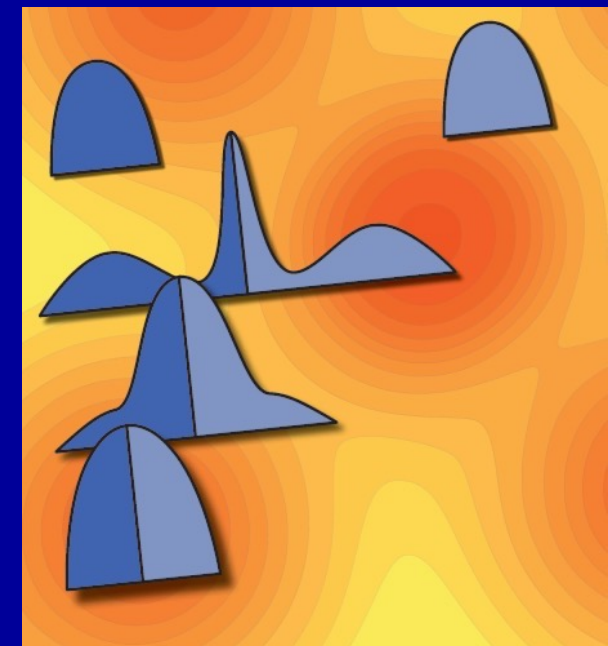
Book series – available as free eBooks



The LDA+DMFT approach to strongly correlated materials
Eva Pavarini, Erik Koch, Dieter Vollhardt, and Alexander Lichtenstein (Eds.)



DMFT at 25: Infinite Dimensions
Eva Pavarini, Erik Koch, Dieter Vollhardt and Alexander Lichtenstein (Eds.)



DMFT: From Infinite Dimensions to Real Materials
Eva Pavarini, Erik Koch, Alexander Lichtenstein, and Dieter Vollhardt (Eds.)



<https://www.cond-mat.de/events/correl.html>

Also: recent book by V. Turkowski (Springer)

Dynamical mean-field theory of strongly correlated fermion systems and the limit of infinite dimensions

Reviews of Modern Physics
68, 13 (1996)

Antoine Georges

Laboratoire de Physique Théorique de l'Ecole Normale Supérieure, 24, rue Lhomond, 75231 Paris Cedex 05, France

Gabriel Kotliar

Serin Physics Laboratory, Rutgers University, Piscataway, New Jersey 08854

Werner Krauth and Marcelo J. Rozenberg

Laboratoire de Physique Statistique de l'Ecole Normale Supérieure, 24, rue Lhomond, 75231 Paris Cedex 05, France

We review the dynamical mean-field theory of strongly correlated electron systems which is based on a mapping of lattice models onto quantum impurity models subject to a self-consistency condition. This mapping is exact for models of correlated electrons in the limit of large lattice coordination (or infinite spatial dimensions). It extends the standard mean-field construction from classical statistical mechanics to quantum problems. We discuss the physical ideas underlying this theory and its mathematical derivation. Various analytic and numerical techniques that have been developed recently in order to analyze and solve the dynamical mean-field equations are reviewed and compared to each other. The method can be used for the determination of phase diagrams (by comparing the stability of various types of long-range order), and the calculation of thermodynamic properties, one-particle Green's functions, and response functions. We review in detail the recent progress in understanding the Hubbard model and the Mott metal-insulator transition within this approach, including some comparison to experiments on three-dimensional transition-metal oxides. We present an overview of the rapidly developing field of applications of this method to other systems. The present limitations of the approach, and possible extensions of the formalism are finally discussed. Computer programs for the numerical implementation of this method are also provided with this article.

Collège de France Lectures Spring 2019 devoted to DMFT (2019)

Website:

<https://www.college-de-france.fr/site/antoine-georges/index.htm>

Lectures (in French) are video recorded
PDF and Audio of lectures also available for all years
PDF for (almost) all seminars

Under the Hood: Development of Efficient 'Impurity Solver' Algorithms is CRUCIAL

- **Solvers working directly with a continuous bath**
Typically: Quantum Monte Carlo (various kinds)
- **Solvers requiring a discretization (Hamiltonian form) of the bath** - Exact Diagonalisation, Wilson Numerical Renormalisation Group, Fork Tensor Product States, Configuration Interaction, Coupled Cluster, etc.
- **Approximation Schemes** e.g. IPT, NCA, OCA, ...

QMC algorithmic breakthroughs

Early days: Hirsch-Fye Algorithm (1986)

First application to DMFT (1992):

Mark Jarrell; Rozenberg and Kotliar; AG and W.Krauth

Continuous-time quantum Monte Carlo (CT-QMC): 2005 → Today

- Interaction expansion(CT-INT) Rubtsov (2005)
 - Hybridization expansion (CT-HYB)
P. Werner, M.Troyer, A.Millis et al 2006; Haule 2007
- Auxiliary field (CT-AUX) E.Gull O.Parcollet 2008

Review: Gull et al. Rev Mod Phys 83, 349 (2011)

- **Inchworm**: Cohen, Gull et al. 2015→
- **Real-time Diagrammatic MC**: Waintal, Parcollet, Messio, Profumo, Bertrand, Dumitrescu et al (2017→)

A Vital Community Endeavor: Efficient and Sustainable Open-Source Software Libraries

The screenshot shows the TRIQS website homepage. The header includes the TRIQS logo and version 3.1.1. A search bar is present. The main content area has a 'Welcome' section with a description of TRIQS as a scientific project for developing tools for interacting quantum systems. It mentions that the toolkit is free software under the GPL license and provides applications for various materials. A 'Python & C++' section is also visible. A GitHub logo is prominently displayed on the right side of the page.

The screenshot shows the GitHub repository page for 'solid_dmft'. The repository description states that it allows for performing DFT+DMFT 'one-shot' and charge self-consistent (CSC) calculations. It lists supported input files and software libraries like VASP and Quantum Espresso. A GitHub logo is also present on the right side of the page.

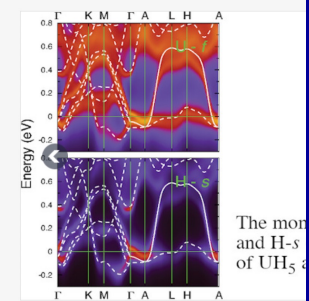
A navigation bar from the GitHub website, featuring the GitHub logo and links for 'Why GitHub?', 'Team', 'Enterprise', and 'Education'.



EDMFTF: DFT+Embedded DMFT Functional
main developer: Kristjan Haule
supported by: Gheorghe L. Pascut
hosted by: Rutgers University

w2dynamics / w2dynamics

AMULET
Advanced Materials simUlation Ekaterinburg's Toolbox



DCore

integrated DMFT software for Correlated electrons

DMFTwDFT: An open-source code combining Dynamical Mean Field Theory with various density functional theory packages ★, ★★

Vijay Singh ^{a, b}, Uthpala Herath ^b, Benny Wah ^a, Xingyu Liao ^a, Aldo H. Romero ^b, Hyowon Park ^a

COMSCOPE

about

software

abinit

User Guide Topics Variables Tutorial FAQ Theory Developers About

Topics

Features
Topic List
Abipy
APPA

DMFT

This page gives hints on how to perform a DMFT calculation with the ABINIT package.

ALPSCore Home GitHub Issues Wiki Doxygen

ALPSCore

Applications and Libraries for Physics Simulations Core libraries

The ALPS Core libraries aim to provide a set of well tested, robust, and standardized components for numerical simulations of condensed matter systems, in particular systems with strongly correlated electrons. They consist of a set of components that are used in state of the art high performance codes. The ALPSCore libraries are a spinoff of the ALPS libraries available from alps.comp-physics.org

Install

Cite

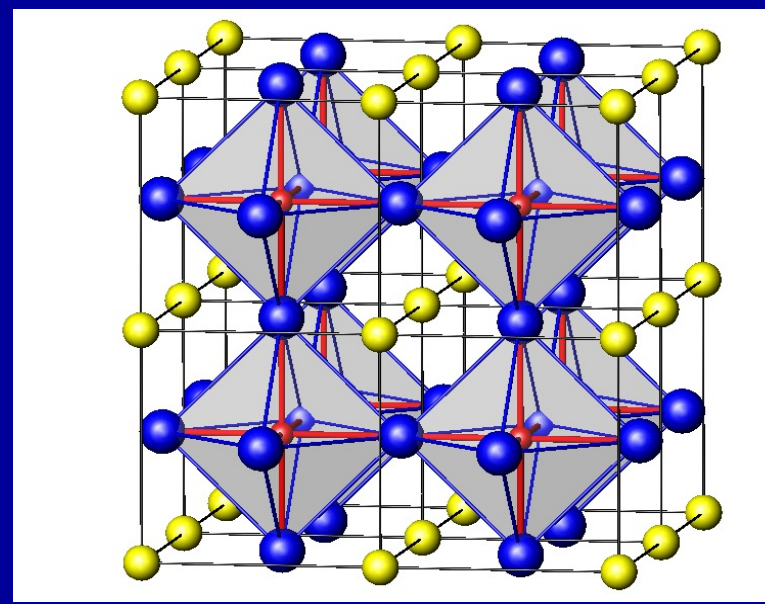
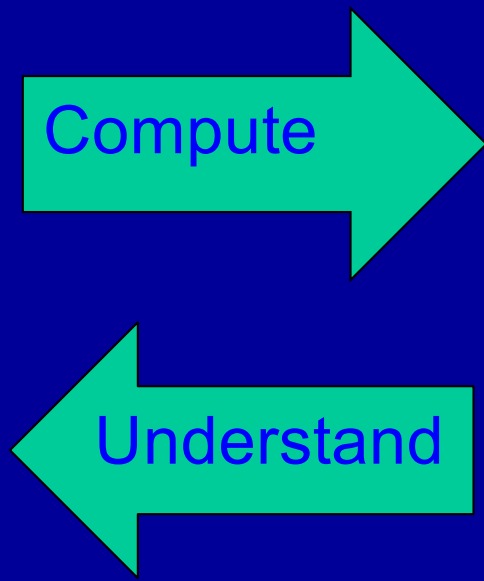
Use

Contribute

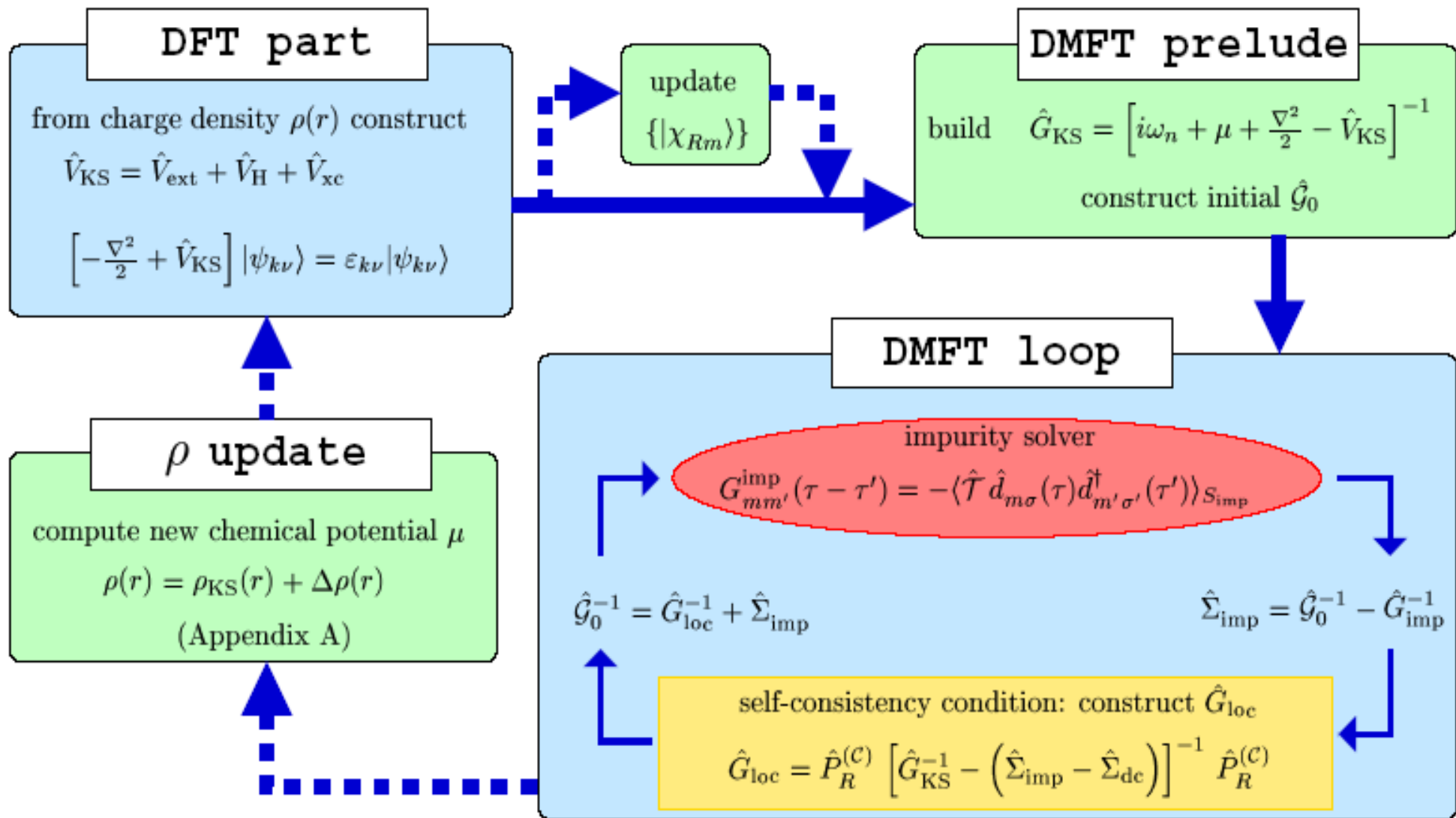
The Happy Marriage of DMFT With Electronic Structure (DFT, GW,...)

An interdisciplinary collective effort started ~ 1996 and still continuing today

Anisimov, Kotliar et al. J.Phys Cond Mat 9, 7359 (1997)
Lichtenstein and Katsnelson Phys Rev B 57, 6884 (1998)

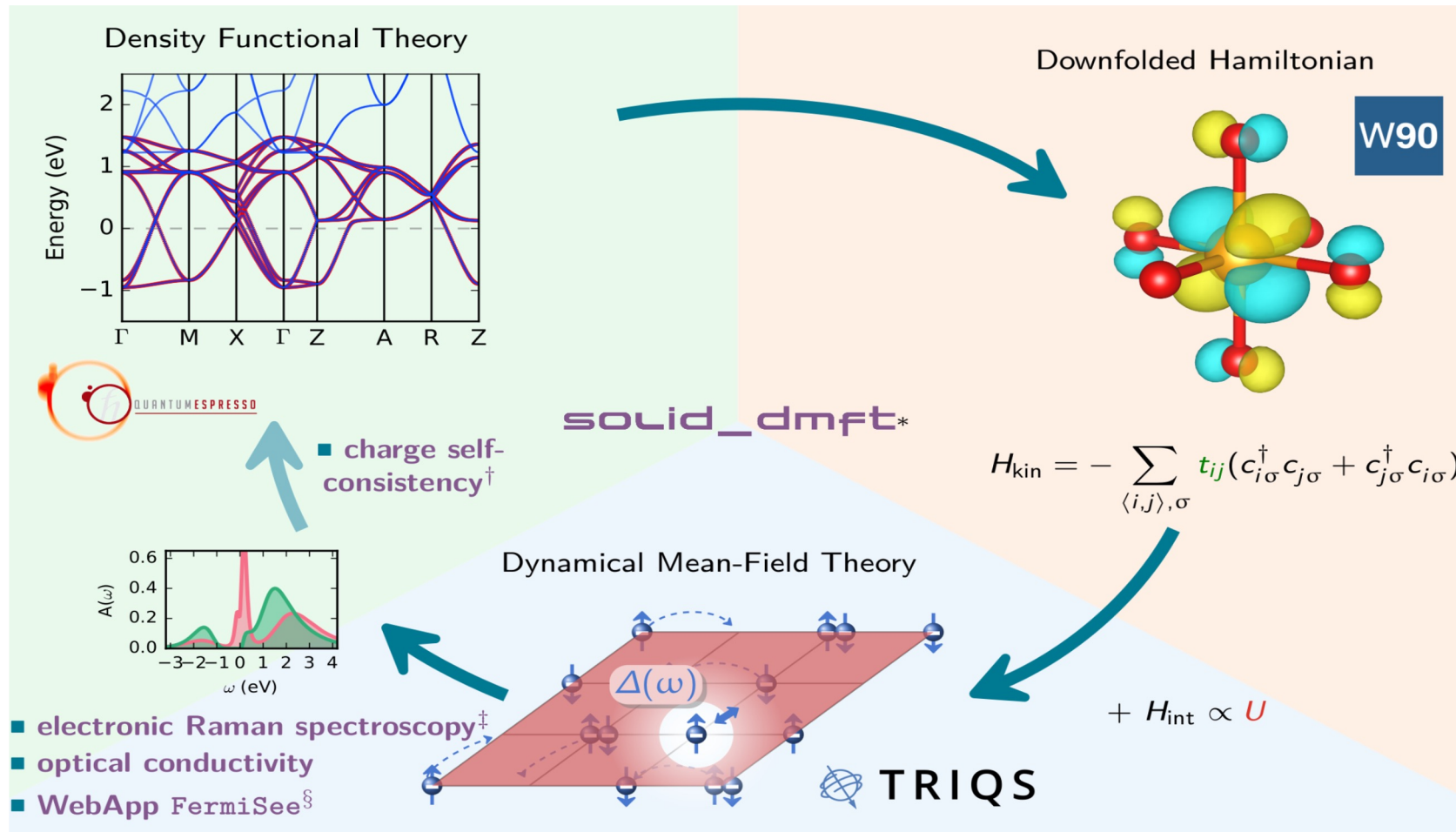


Realistic DMFT, in a nutshell...



Total Energy Functional: $E [\rho(r), G_{mm'}^{\text{loc}}(\omega)]$

Realistic materials modeling using TRIQS



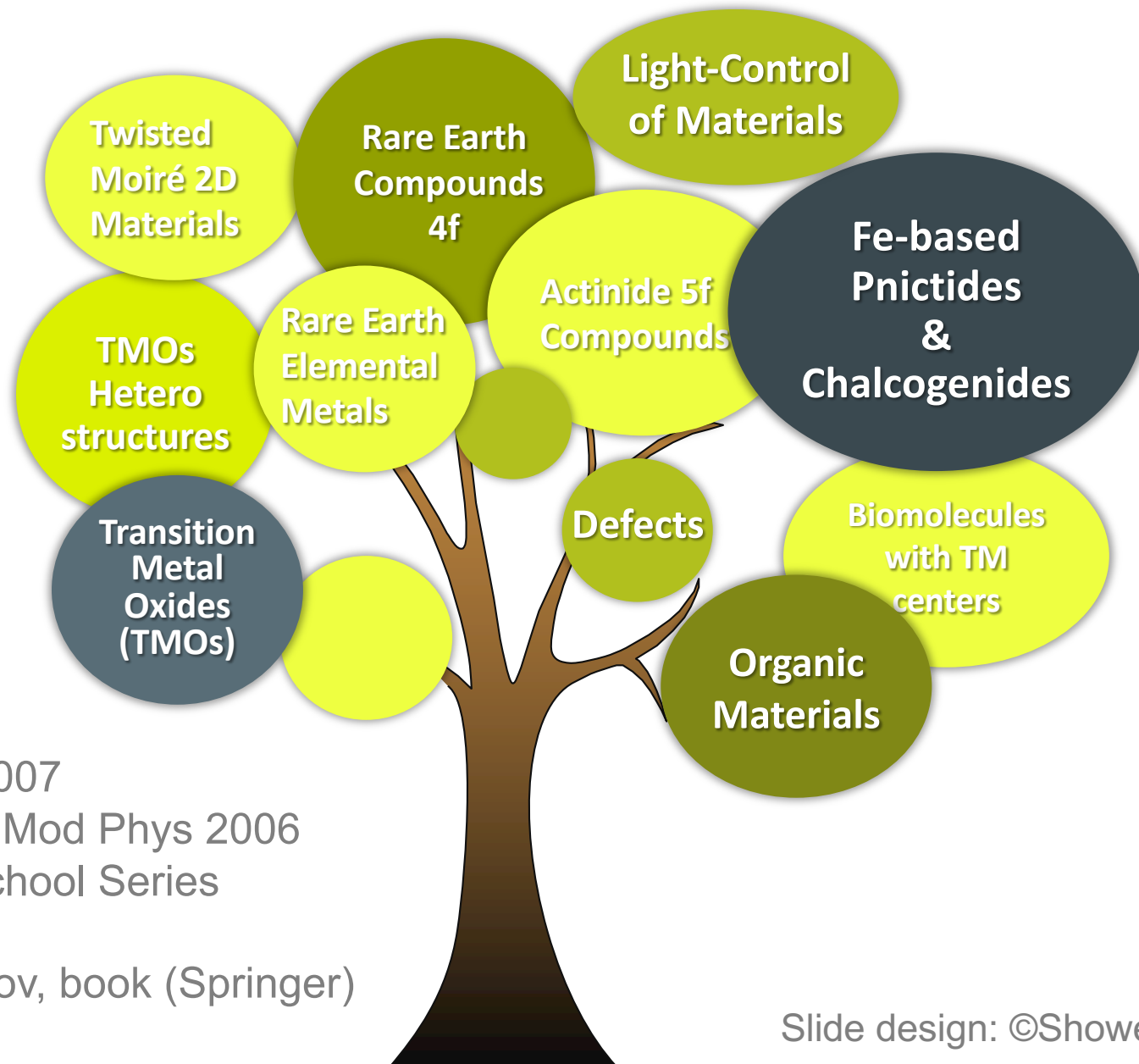
* M. Merkel, A. Carta, S. Beck and A. Hampel, J. Open Source Softw. 7(77), 4623 (2022)

† S. Beck, A. Hampel, O. Parcollet, C. Ederer, and A. Georges, J. Phys.: Condens. Matter 34, 235601 (2022)

‡ G. Blesio, S. Beck, J. Mravlje, and A. Georges, arxiv:2211.12959 (2023)

§ S. Beck, S. Rahim, A. Hampel <https://github.com/TRIQS/FermiSee/>

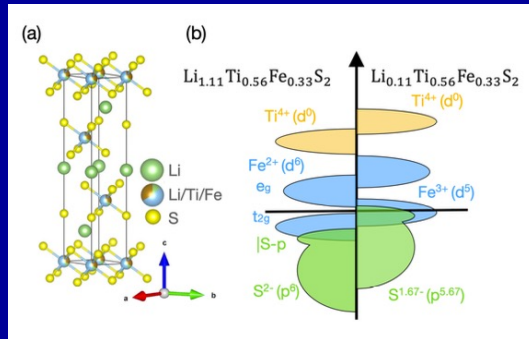
Electronic Structure with DMFT: A Multitude of Materials



Reviews:

- Held Adv Phys 2007
- Kotliar et al. Rev Mod Phys 2006
- Jülich Autumn School Series (Pavarini et al.)
- Anisimov&Izyumov, book (Springer)
- Etc.

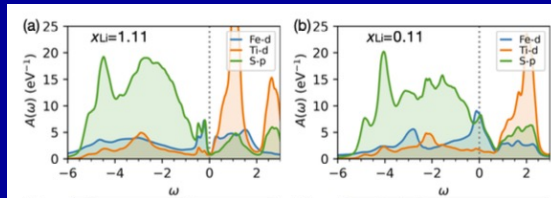
Among many applications of DMFT to materials of recent interest...



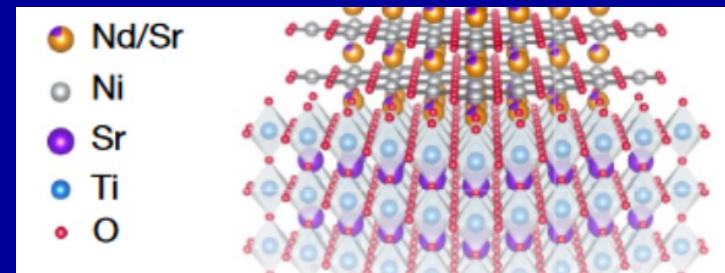
Materials For Batteries

Sim, Sarma, Tarascon and Biermann
arXiv:2305.08526

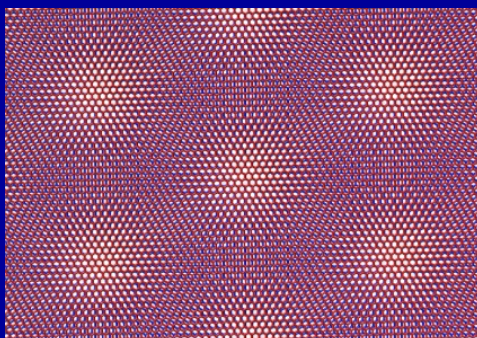
Other sulfide,
 $\text{NiS}_{2-x}\text{Se}_x$
Jang et al.
NatComm2021



Infinite-Layer Nickelates



Many authors and recent papers using DMFT



moiré: TBLG and dichalcogenides

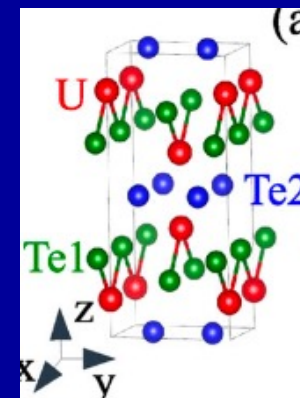
Symmetric Kondo Lattice States in Doped Strained Twisted Bilayer Graphene

H. Hu,¹ G. Rai,² L. Crippa,³ J. Herzog-Arbeitman,⁴ D. Călugăru,⁴ T. Wehling,^{2,5}
G. Sangiovanni,³ R. Valentí,⁶ A. M. Tsvelik,⁷ and B. A. Bernevig^{4,1,8,*}

Dynamical Mean-Field Theory of Moiré Bilayer Transition Metal Dichalcogenides:
Phase Diagram, Resistivity, and Quantum Criticality

J.Zang et al. PRX 12, 021064 (2022)

UTe₂



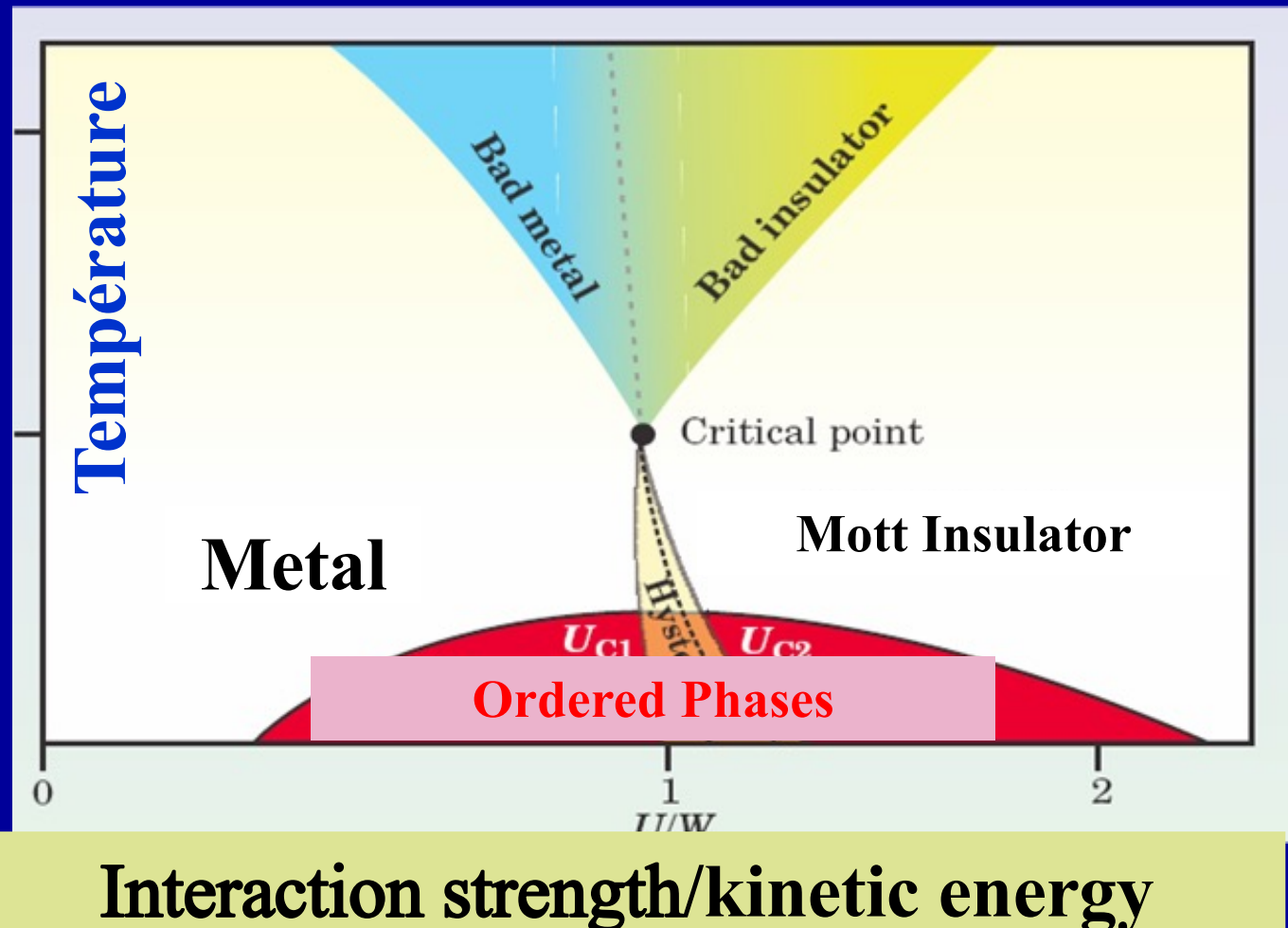
Orbital selective Kondo effect in heavy fermion
superconductor UTe_2

Byungkyun Kang^{1,2,✉}, Sangkook Choi² and Hyunsoo Kim^{3,4}

npj-qm, 2022

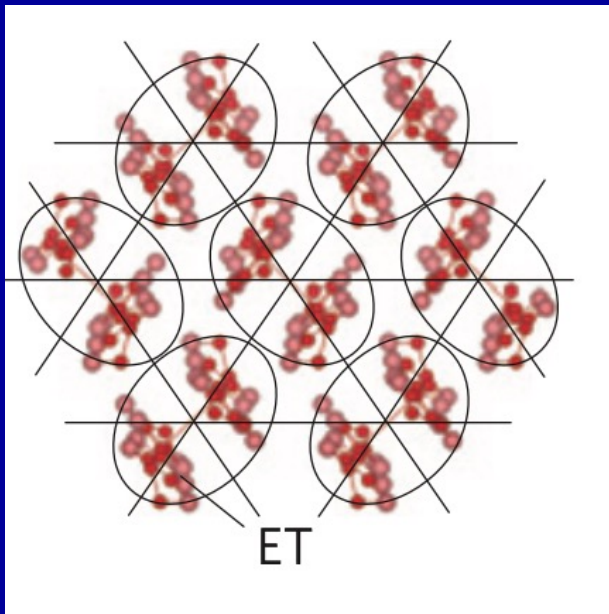
The Mott Transition from a DMFT perspective

Frustrating Magnetic Ordering: Revealing the 'genuine' Mott phenomenon

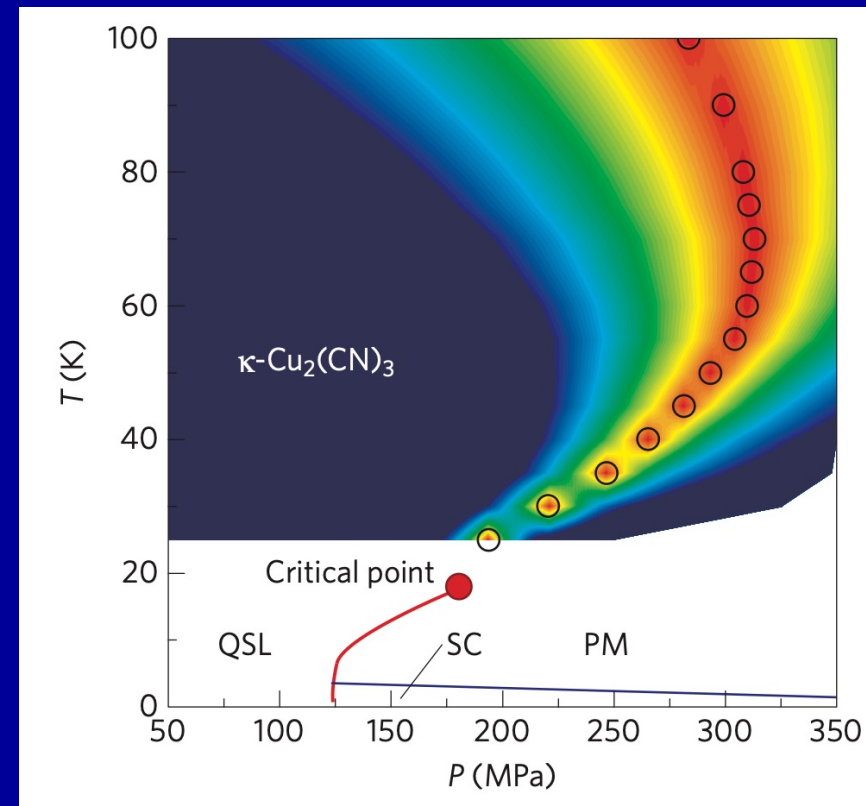


Quantum criticality of Mott transition in organic materials

Tetsuya Furukawa^{1*}, Kazuya Miyagawa¹, Hiromi Taniguchi², Reizo Kato³ and Kazushi Kanoda^{1*}



See also Pustogow, Dressel et al.
Optical measurements



Continuous Mott transition in semiconductor moiré superlattices

<https://doi.org/10.1038/s41586-021-03853-0>

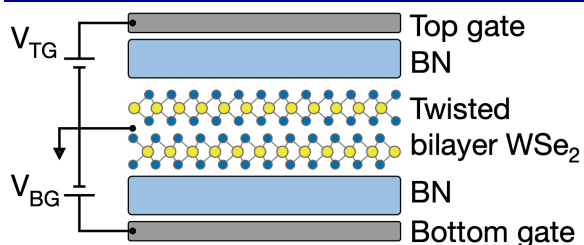
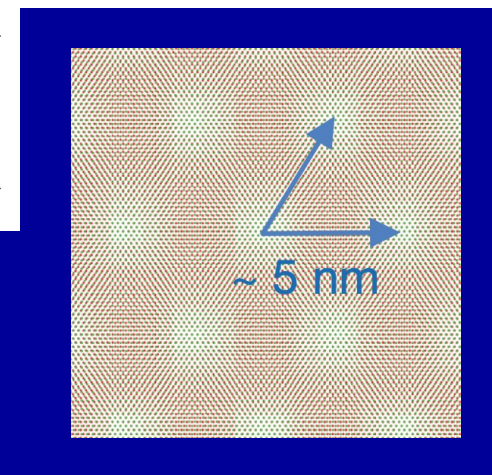
Received: 3 March 2021

Accepted: 22 July 2021

Published online: 15 September 2021

Tingxin Li^{1,6}, Shengwei Jiang^{2,6}, Lizhong Li^{1,6}, Yang Zhang³, Kaifei Kang¹, Jiacheng Zhu¹, Kenji Watanabe⁴, Takashi Taniguchi⁴, Debanjan Chowdhury², Liang Fu³, Jie Shan^{1,2,5} & Kin Fai Mak^{1,2,5}✉

The evolution of a Landau Fermi liquid into a non-magnetic Mott insulator with



Quantum criticality in twisted transition metal dichalcogenides

<https://doi.org/10.1038/s41586-021-03815-6>

Received: 17 March 2021

Accepted: 6 July 2021

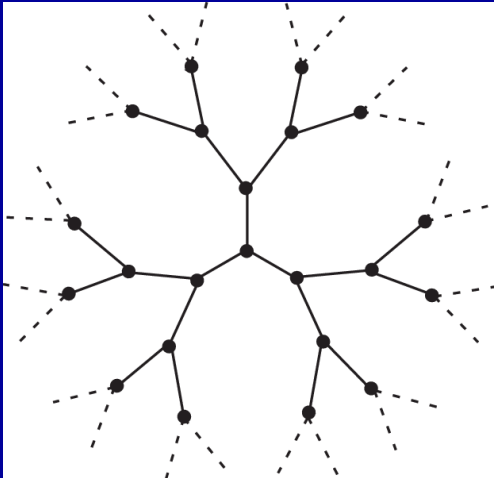
Published online: 15 September 2021

Check for updates

Augusto Ghiotto¹, En-Min Shih¹, Giancarlo S. S. G. Pereira¹, Daniel A. Rhodes², Bumho Kim², Jiawei Zang¹, Andrew J. Millis^{1,3}, Kenji Watanabe⁴, Takashi Taniguchi⁴, James C. Hone², Lei Wang^{1,5}✉, Cory R. Dean¹✉ & Abhay N. Pasupathy^{1,6}✉

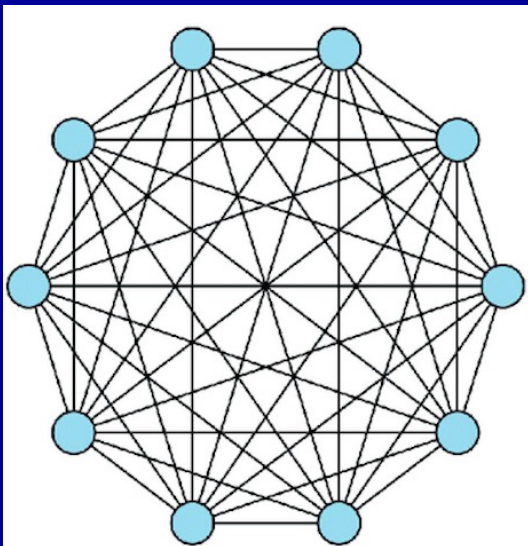
Near the boundary between ordered and disordered quantum phases, several experiments have demonstrated metallic behaviour that defies the Landau Fermi paradigm^{1–5}. In moiré heterostructures, gate-tunable insulating phases driven by electronic correlations have been recently discovered^{6–23}. Here, we use transport measurements to characterize metal–insulator transitions (MITs) in twisted WSe₂ near half filling of the first moiré subband. We find that the MIT as a function of both density and displacement field is continuous. At the metal–insulator boundary, the

A simple form of the self-consistency condition: Fully connected with random hopping and Bethe lattice



$$t_{ij} = \frac{t}{\sqrt{z}} , \quad z \rightarrow \infty$$

$$\Delta(i\omega) = t^2 G(i\omega)$$



Fully connected lattice with random hopping

$$t_{ij} = \frac{\epsilon_{ij}}{\sqrt{N}} , \quad N \rightarrow \infty$$

$$\overline{\epsilon_{ij}} = 0 , \quad \overline{\epsilon_{ij}^2} = 1$$

Non-interacting DOS:
Wigner semi-circle

$$D(\epsilon) = \frac{1}{2\pi t^2} \sqrt{4t^2 - \epsilon^2}$$

Half-bandwidth:
D=2t

Magnetic ordering is FULLY FRUSTRATED

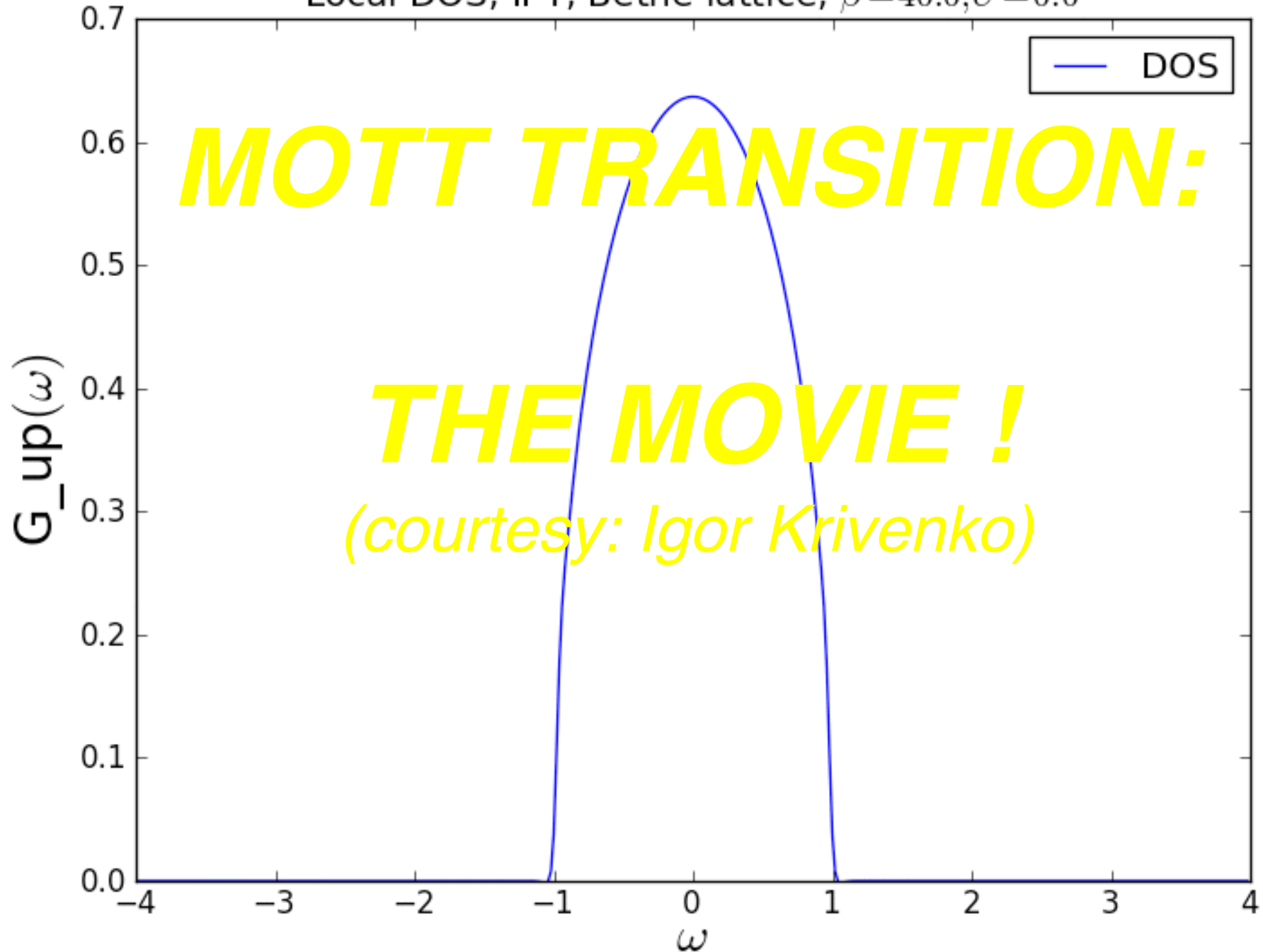
Revealing the 'genuine' Mott phenomenon

- Frustrating magnetic ordering
- The basic equations:

$$G = G_{\text{imp}}[\Delta] , \quad \Delta = t^2 G , \quad (D = 2t)$$

- NB: General lattice: $\Delta[G] = R[G] - 1/G$
- Do these equations have a solution and if so, is it unique ?
- How does the physical nature of this solution change as U/D , T/D is varied ?

Local DOS, IPT, Bethe lattice, $\beta=40.0, U=0.0$



The movie just shown was obtained
with an approximate solver:
Iterated Perturbation Theory (IPT)
- *see hands-on session –*
but is qualitatively consistent
with exact numerical solvers
(QMC, Wilson NRG)

The IPT approximation (G.Kotliar & AG, 1992)

(~ simplest approximate solver)

Motivated by regularity of perturbation theory in U for the AIM

Integral equation easily solved iteratively w/ FFTs

EXACT (at $\frac{1}{2}$ filling for $U=0$ and in the atomic limit !)

IPT approximate solver:

$$\Sigma(\tau) \simeq U^2 \mathcal{G}_0(\tau)^3$$

Iteration scheme: $\mathcal{G}_0 \rightarrow$ $\Sigma(\tau) \simeq U^2 \mathcal{G}_0(\tau)^3$ solver



Dyson

$$G(i\omega_n)^{-1} = \mathcal{G}_0^{-1}(i\omega_n) - \Sigma(i\omega_n)$$



$$\mathcal{G}_{0,\text{new}}^{-1} = i\omega_n - t^2 G(i\omega_n) \quad \text{self-consistency}$$

A first DMFT calculation

The goal of this notebook is to make a first DMFT calculation using the iterated perturbation theory (IPT) to solve the impurity problem. You will proceed in two steps: first you will set up the IPT impurity solver and then you will set up the DMFT loop.

The iterated perturbation theory

The IPT is a cheap way to solve the impurity problem which is restricted to half-filling. It approximates the self-energy by second-order perturbation theory, just like in the last exercise of the notebook on Green's functions:

$$\Sigma(i\omega_n) = \frac{U}{2} + U^2 \int_0^\beta d\tau e^{i\omega_n \tau} G_0(\tau)^3$$

```
[1]: from triqs.gf import *
import numpy as np
from math import pi
class IPTSolver:
    def __init__(self, beta):
        self.beta = beta

        # Matsubara frequency Green's functions
        iw_mesh = MeshImFreq(beta=beta, S='Fermion', n_iw=1001)
        self.G_iw = Gf(mesh=iw_mesh, target_shape=[1,1])
        self.G0_iw = self.G_iw.copy() # self.G0 will be set by the user after initialization
        self.Sigma_iw = self.G_iw.copy()

        # Imaginary time
        tau_mesh = MeshImTime(beta=beta, S='Fermion', n_tau=10001)
        self.G0_tau = Gf(mesh=tau_mesh, target_shape=[1,1])
        self.Sigma_tau = self.G0_tau.copy()

    def solve(self, U):
        self.G0_tau << Fourier(self.G0_iw)
        self.Sigma_tau << (U**2) * self.G0_tau * self.G0_tau * self.G0_tau
        self.Sigma_iw << Fourier(self.Sigma_tau)

        # Dyson
        self.G_iw << inverse(inverse(self.G0_iw) - self.Sigma_iw)
```

```
[2]: from triqs.plot.mpl_interface import *
%matplotlib inline
# change scale of all figures to make them bigger
import matplotlib as mpl
mpl.rcParams['figure.dpi']=100

t = 1.0
U = 5.0
beta = 20
n_loops = 25

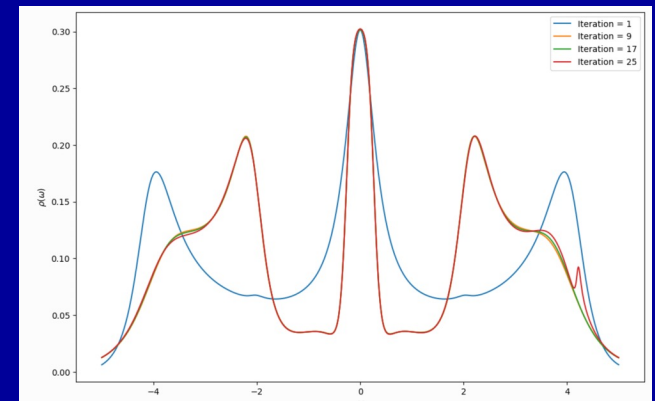
S = IPTSolver(beta = beta)
S.G_iw << SemiCircular(2*t)

fig = plt.figure(figsize=(12,8))

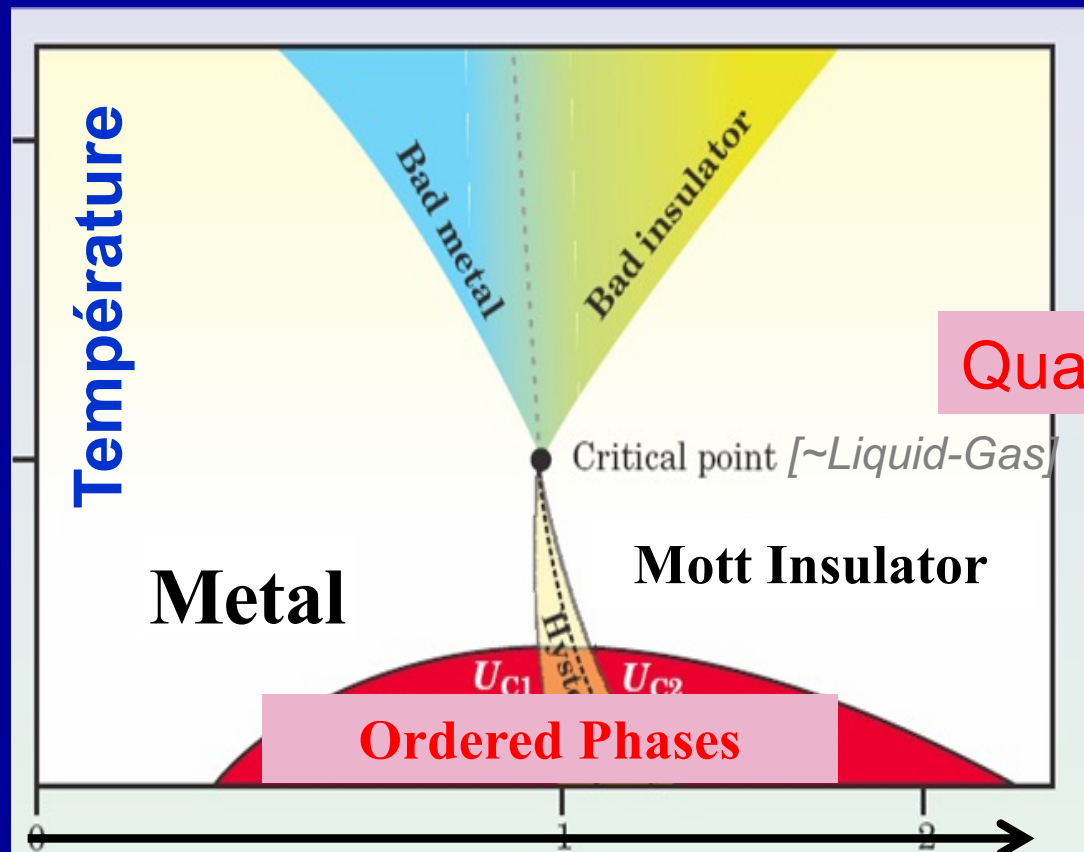
for i in range(n_loops):
    S.G0_iw << inverse( i0mega_n - t**2 * S.G_iw )
    S.solve(U = U)

    # Get real axis function with Pade approximation
    G_w = Gf(mesh=MeshReFreq(window = (-5.0,5.0), n_w=1000), target_shape=[1,1])
    G_w.set_from_pade(S.G_iw, 100, 0.01)

    if i % 8 == 0:
        oplot(-G_w.imag/pi, figure = fig, label = "Iteration = %i" % (i+1), name=r"$\rho$")
```



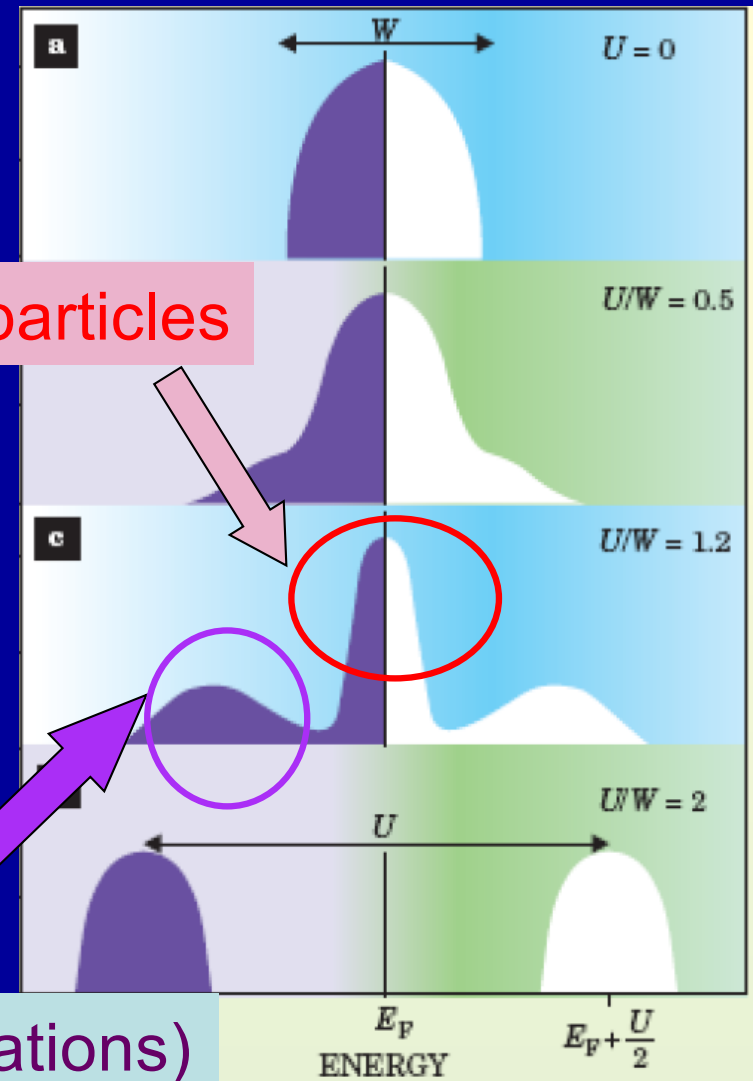
An early success of DMFT (1992-1999) Theory of the Mott transition



Interaction strength/Bandwidth

Hubbard 'bands' (Quasi atomic excitations)

Quasiparticles



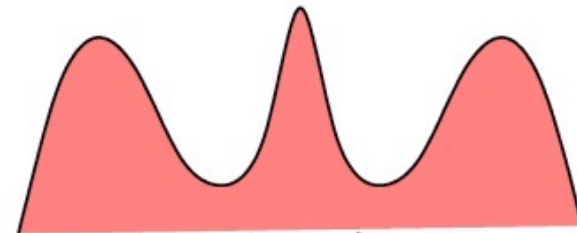
Low-frequency behavior of $\Delta(\omega)$ determines nature of the phase

- $\Delta(\omega \rightarrow 0)$ finite \rightarrow local moment is screened. 'Self-consistent' Kondo effect.
Gapless metallic state.
- $\Delta(\omega)$ gapped \rightarrow no Kondo effect, degenerate ground-state, insulator with local moments

Self-consistent structure of the bath



(usual) impurity model



correlated lattice model

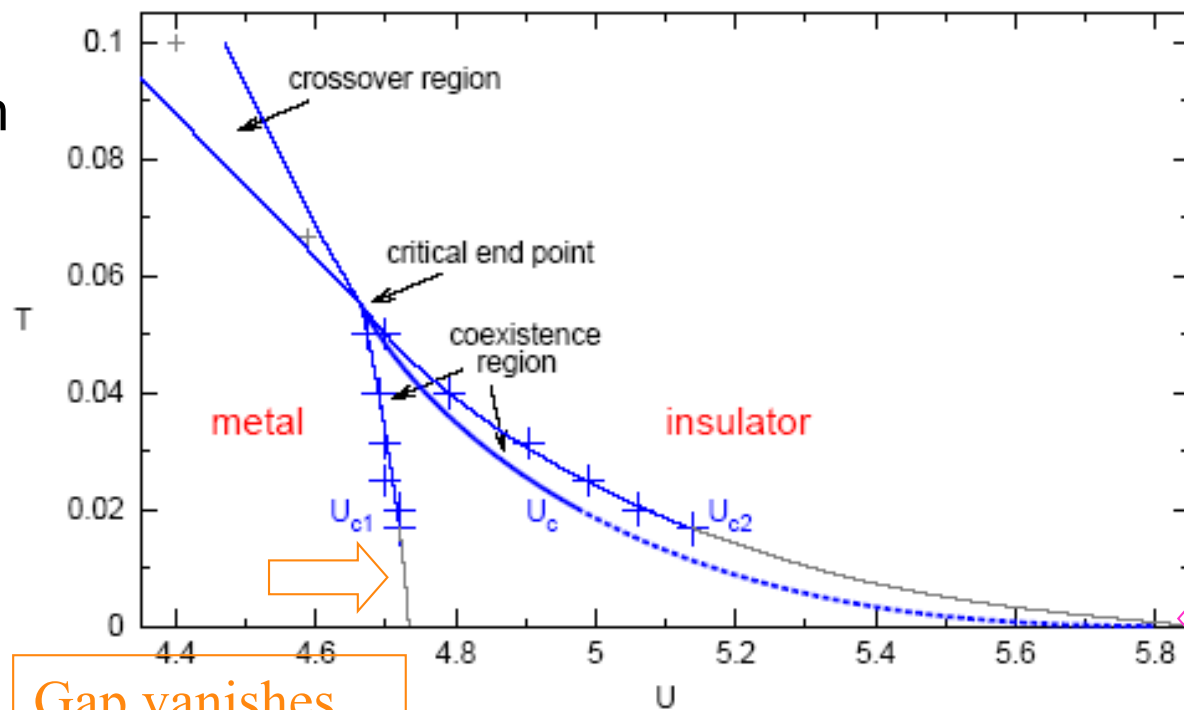
Cartoon from Held, Peters and Toschi PRL 110, 246402 (2013)

Phase diagram : zoom on paramagnetic solutions

Hubbard model, Bethe lattice, homog. phase, $n = 1$, e.g., DMFT(QMC)

[Blümer '02]

Unit:
Bandwidth



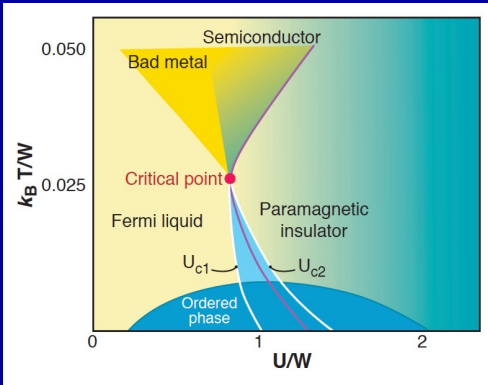
- coexistence region $[U_{c1}; U_{c2}]$, first-order transition
- crossover above critical region

57

Blümer et al. Units here are $4D=2*$ bandwidth

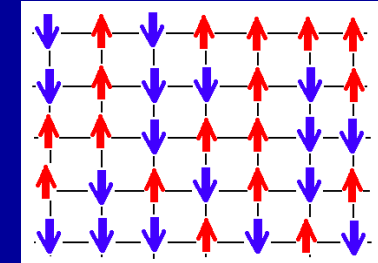
SLIDE IN PROGRESS (optional)

The Mott critical endpoint: a liquid-gas like (Ising) transition



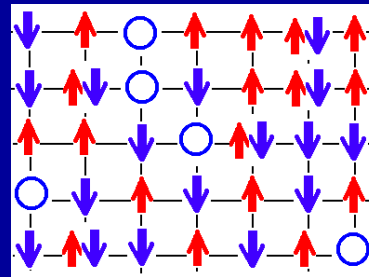
Insulator:

low-density of doubly occupied sites \longrightarrow GAS

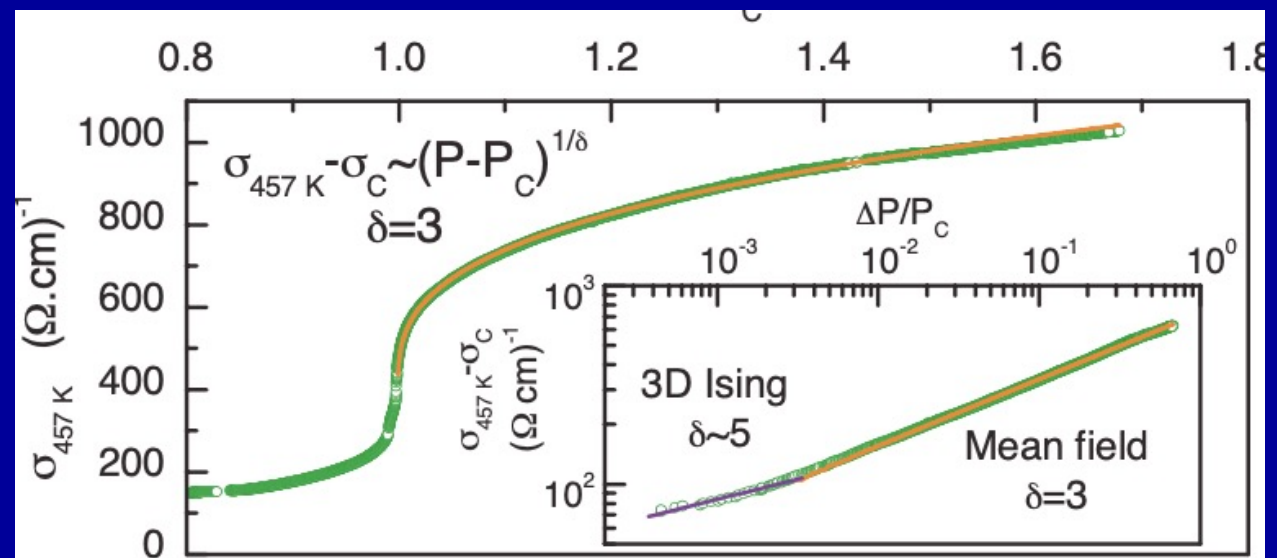


Metal:

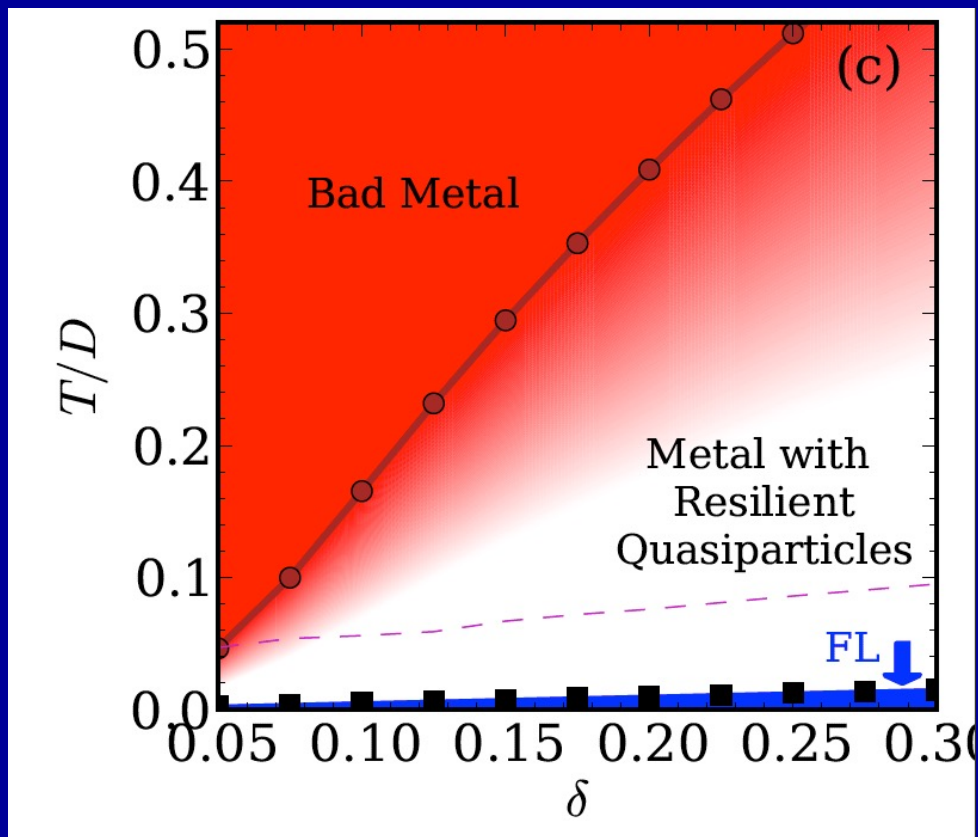
High-density \longrightarrow LIQUID



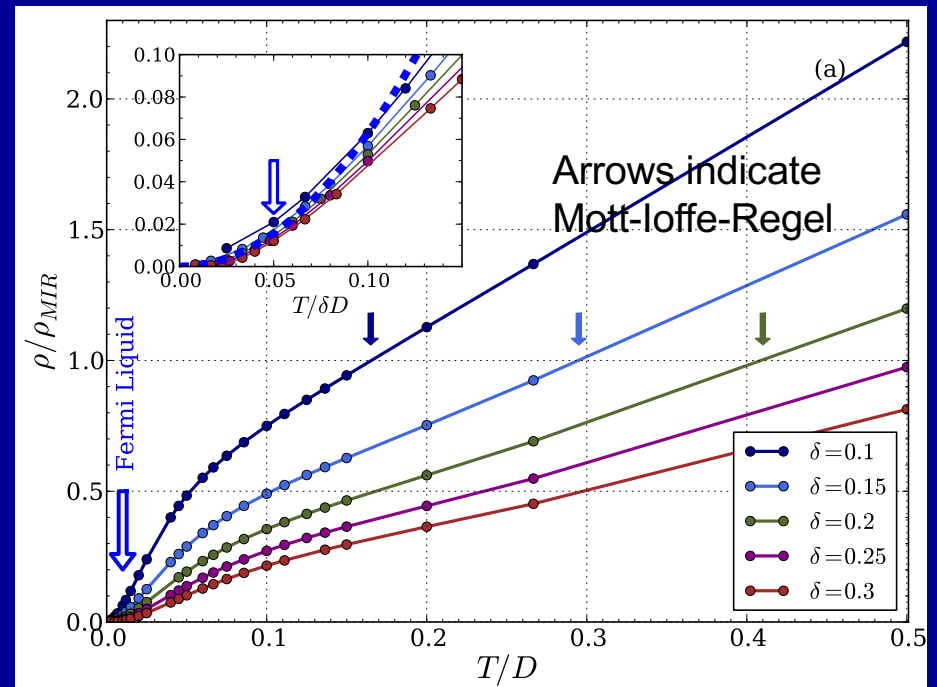
+ cf. early ideas of Castellani et al.
+ DMFT/Landau theory approach:
scalar order Parameter.

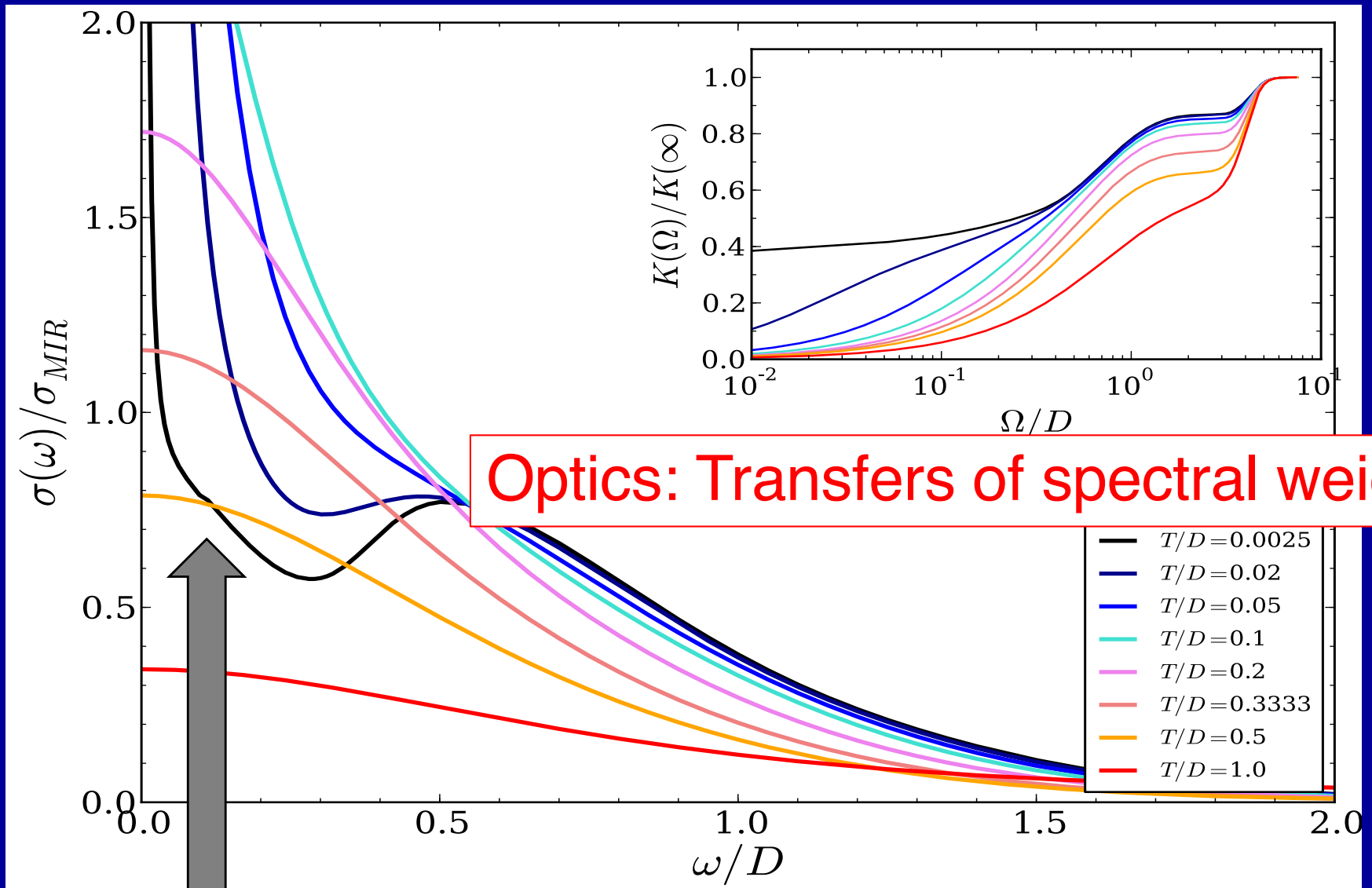


DMFT insight into a long-standing problem: “How bad metals become good” ‘Resilient’ quasiparticles beyond Landau Theory



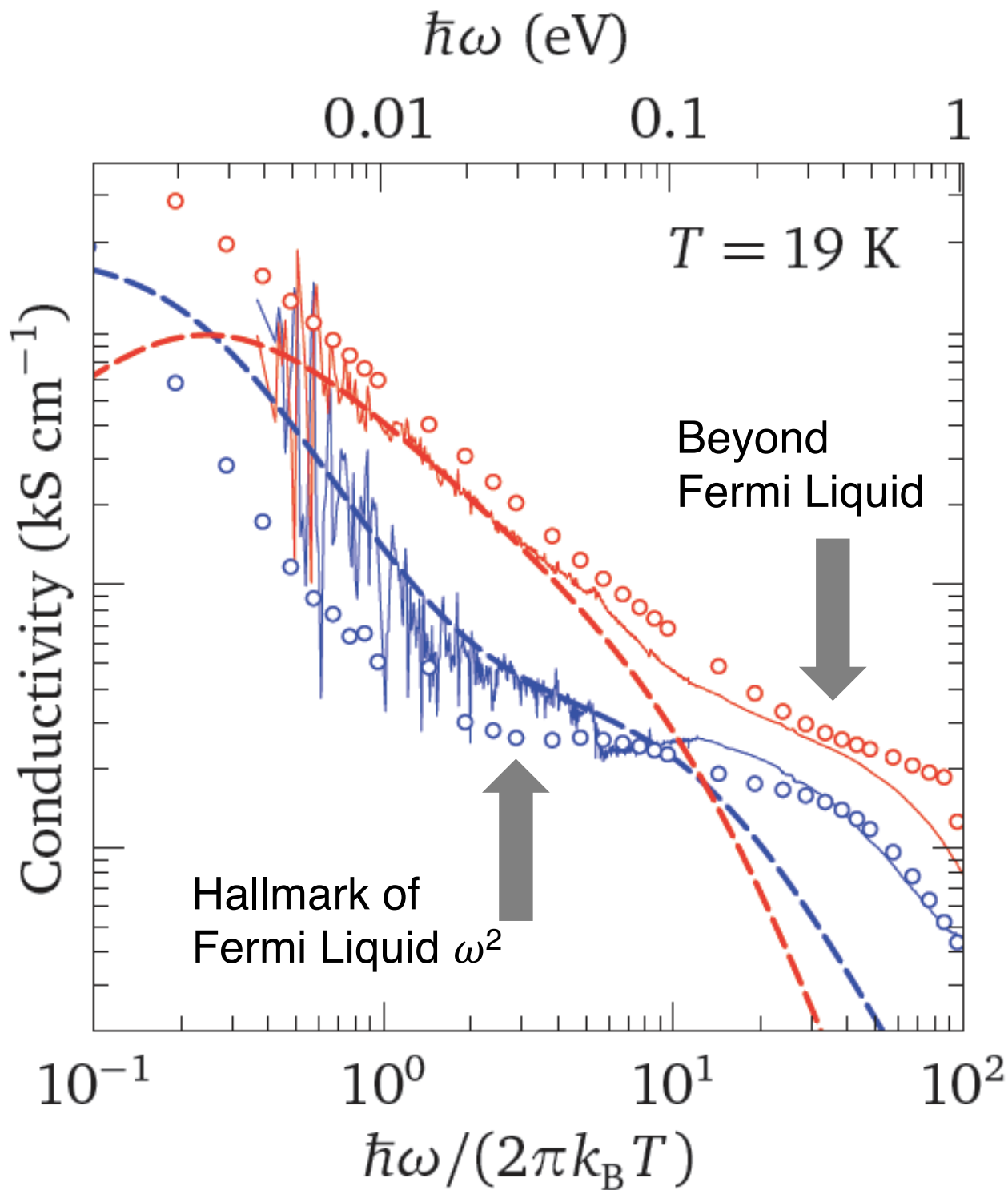
Resistivity: from a Fermi Liquid to a bad metal above Mott-Ioffe-Regel





Optics: Transfers of spectral weight

This non-Drude "foot" is actually the signature of Landau's Fermi liquid (ω^2) in the optical spectrum



Sr_2RuO_4

Re $\sigma(\omega)$

Im $\sigma(\omega)$

Plain Lines:
Experiment

Dashed Line:
Fermi Liquid Theory

Dots:
Theoretical
Calculation
(LDA+DMFT)

D. Stricker et al.
PRL 113, 087404
(2014)

Fermi Liquid nature of the metallic phase

- At (possibly very) low T, ω : a Fermi liquid

$$\text{Re}\Sigma(\omega + i0^+) = U/2 + (1 - 1/Z)\omega + O(\omega^3),$$

$$\text{Im}\Sigma(\omega + i0^+) = -B\omega^2 + O(\omega^4).$$

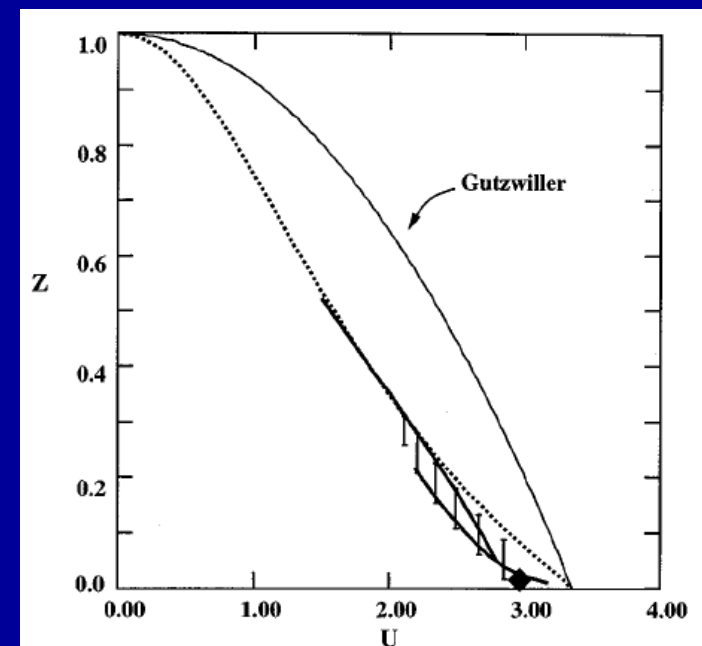
- Fermi surface is unchanged by interactions w/in DMFT for single orbital model. But Drude weight $\sim Z$
- At U_{c2} transition: $Z \rightarrow 0$ (\sim Brinkman-Rice)
- Heavy quasiparticles:

$m^*/m = 1/Z$ diverges at U_{c2}

(divergence reflects large entropy of insulator with fluctuating local moments)

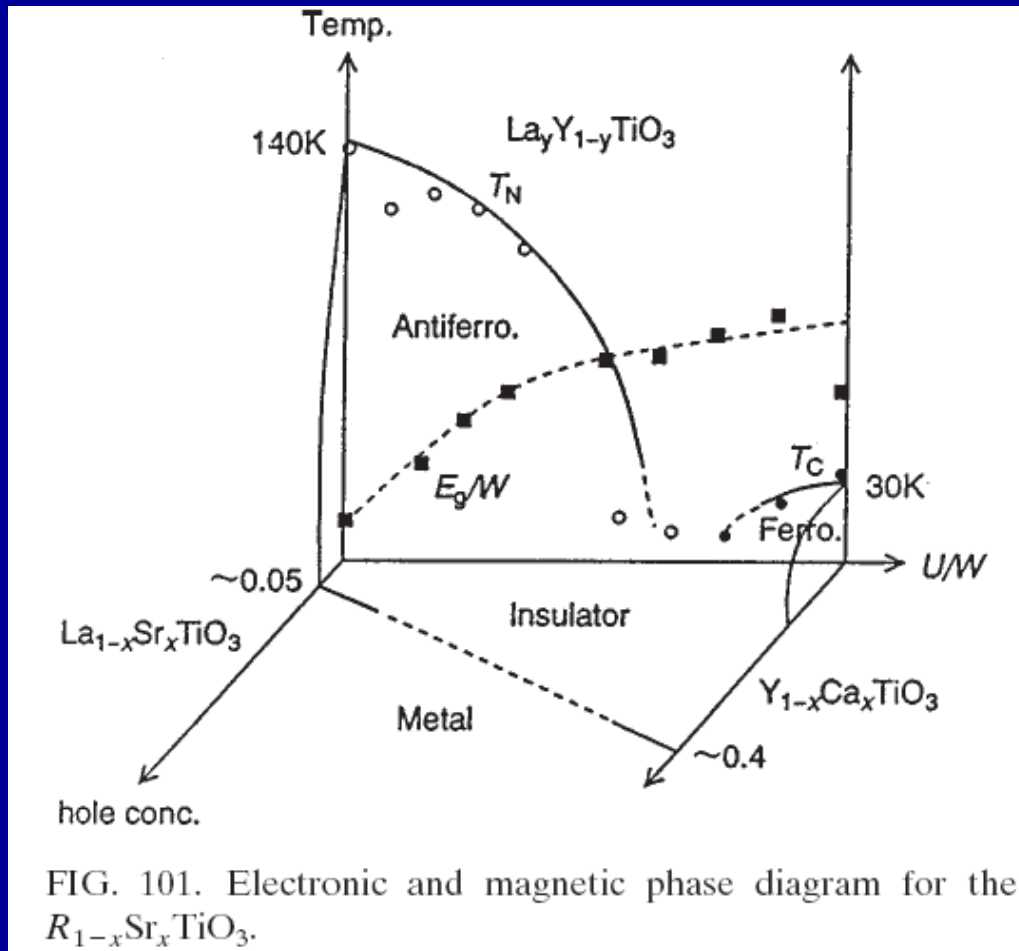
Near the transition:

$B \sim 1/Z^2$ (Kadowaki-Woods)

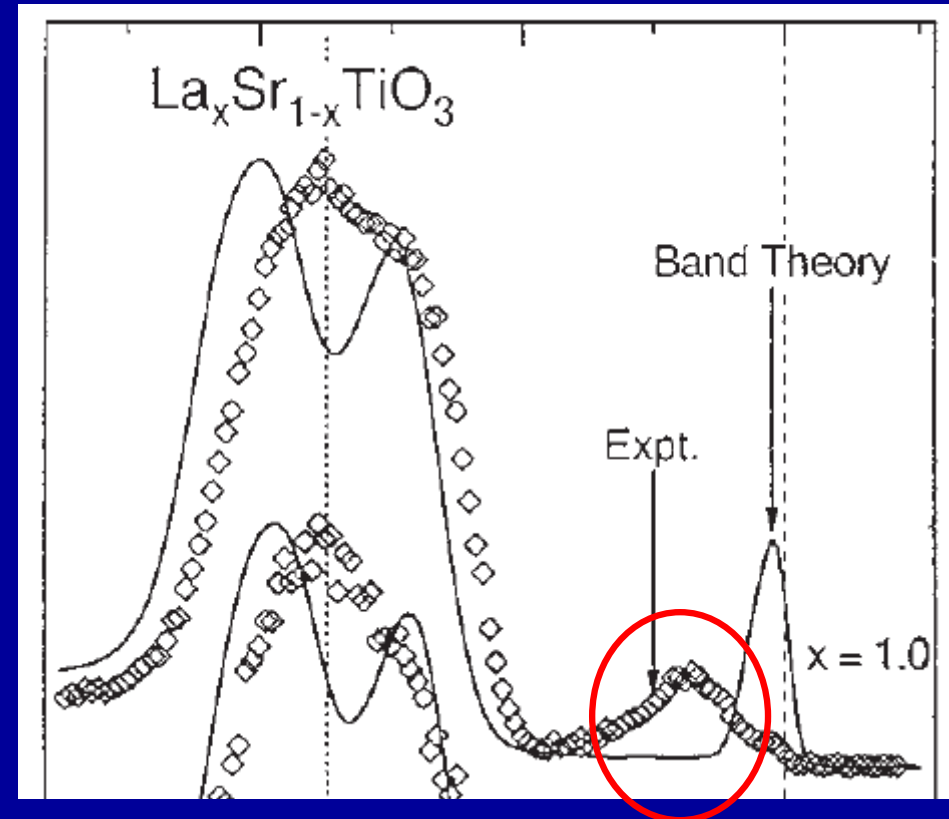


LaTiO₃: AF Mott insulator

AF persists up to ~ 5% hole-doping



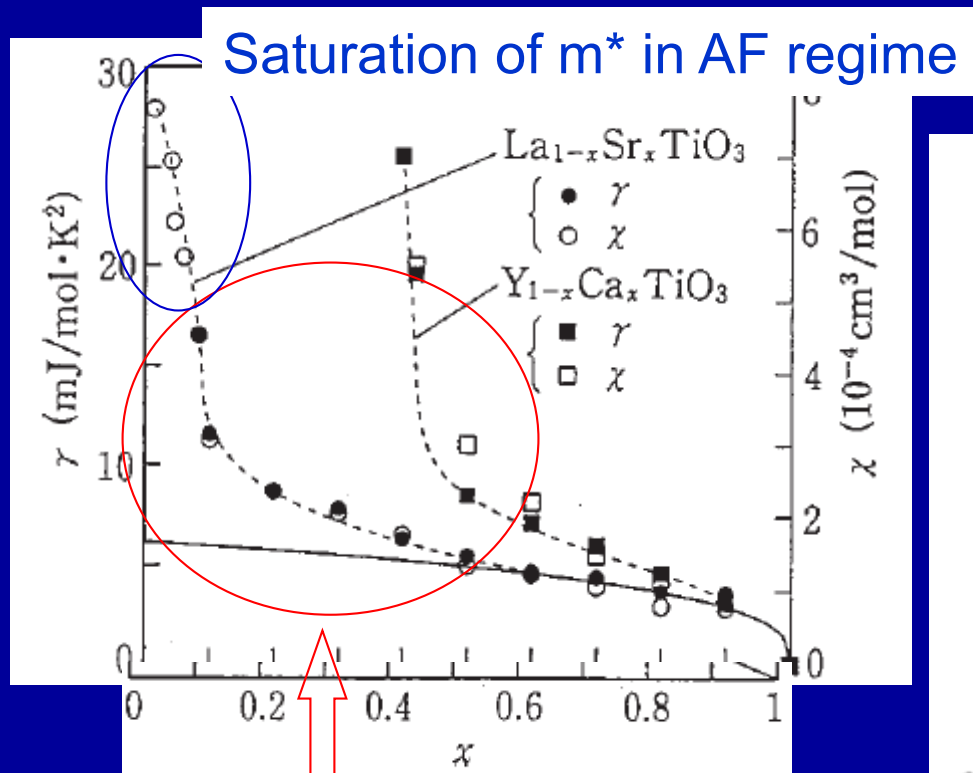
Photoemission spectrum: definitely a Mott insulator



Oxygen states

Lower Hubbard band $d1 \rightarrow d0$

Approach to the Mott state in titanates



Increase of effective mass

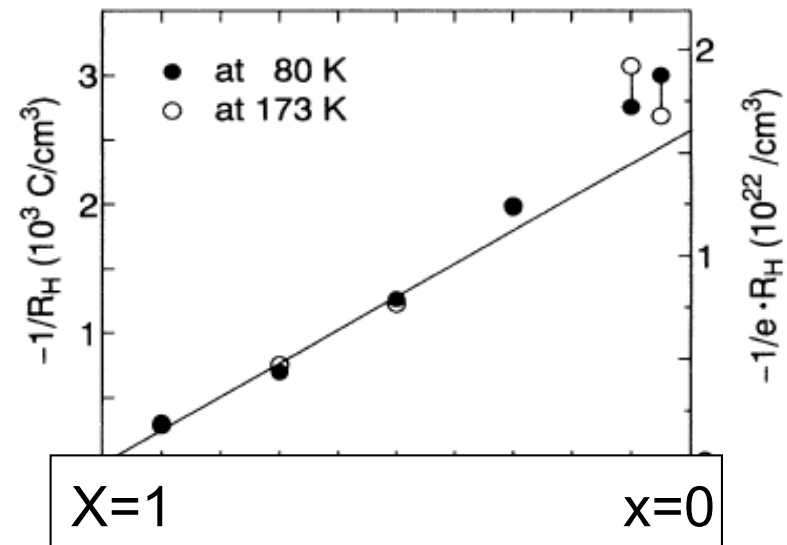
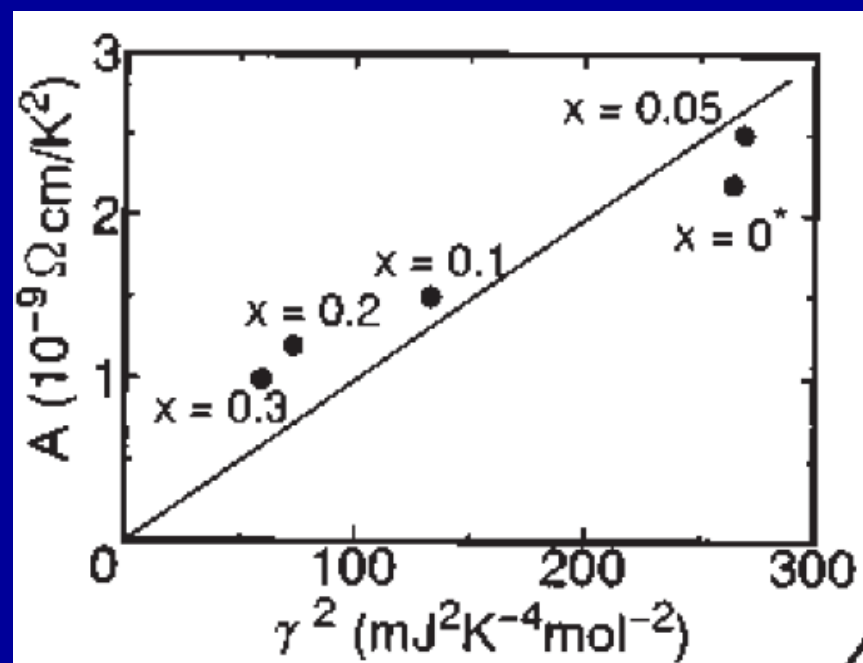
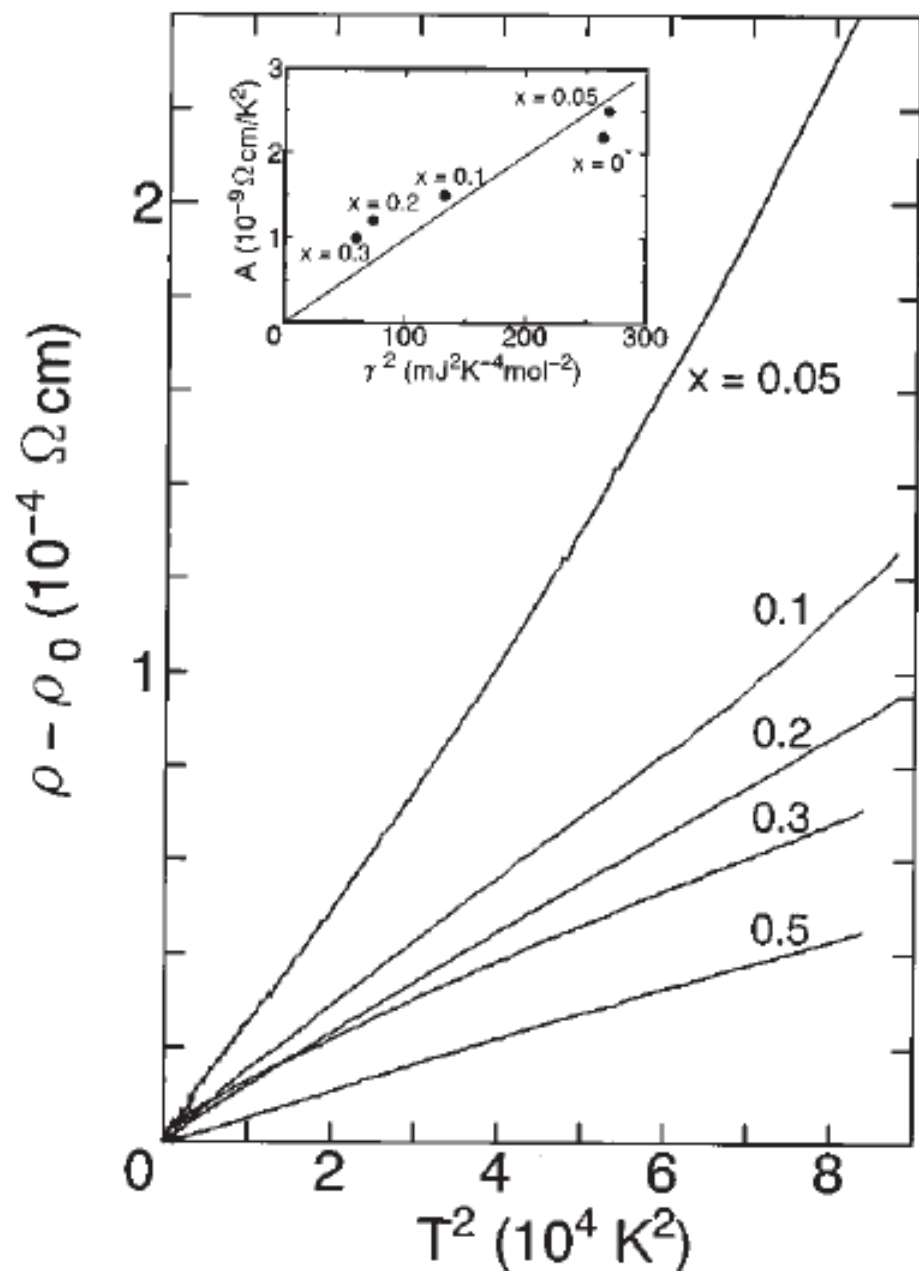


FIG. 2. The filling (x) dependence of the inverse of Hall coefficient (R_H^{-1}) in $\text{Sr}_{1-x}\text{La}_x\text{TiO}_3$. Open and closed circles represent the values measured at 80 K and 173 K, respectively. A solid line indicates the calculated one based on the assumption that each substitution of a Sr^{2+} site with La^{3+} supplies the compound with one electron-type carrier per Ti site.

R_H reported as $\sim T$ -independent
and consistent w/ large Fermi surface

Tokura et al.
PRL, 1993



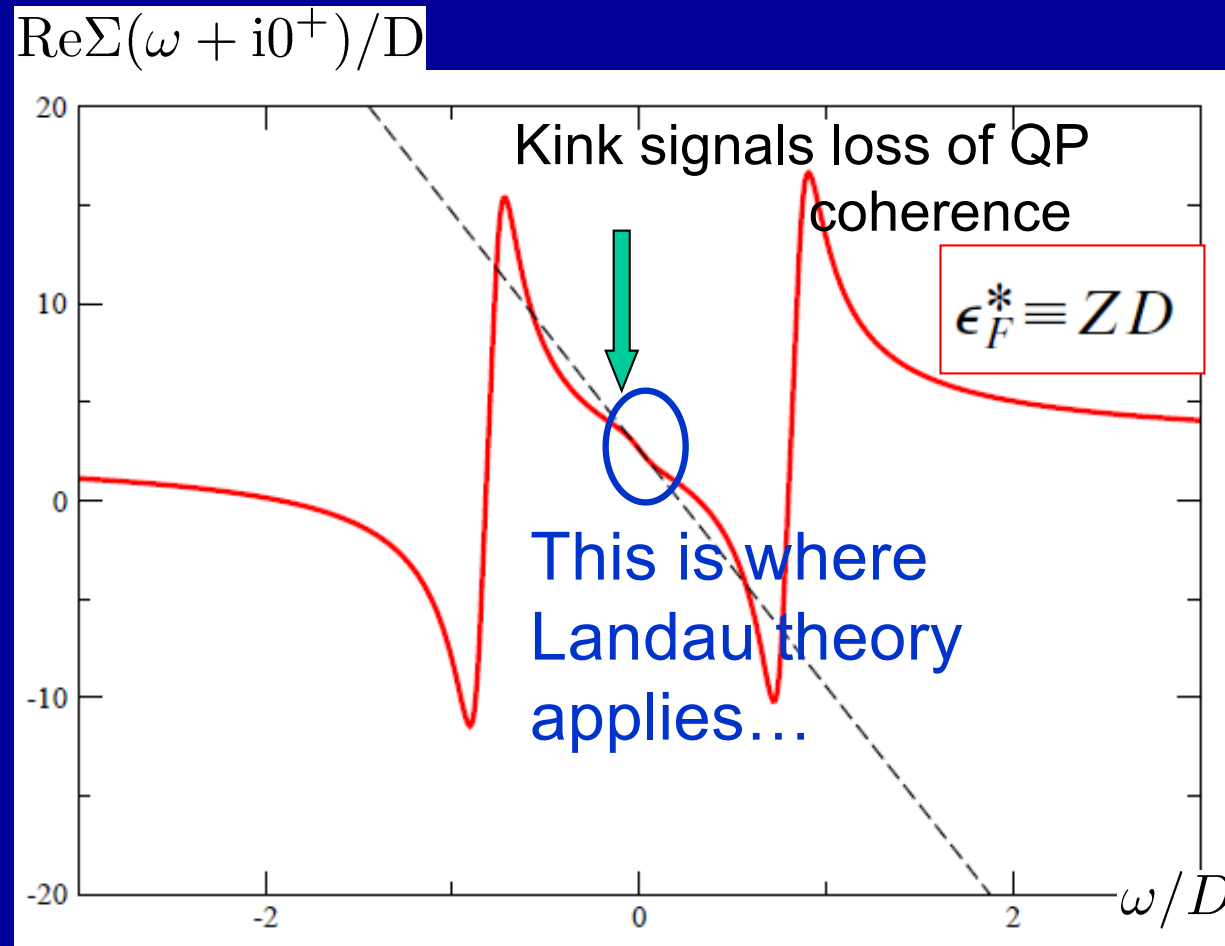
Titanates/transport:

$$\rho_{dc} = AT^2 + \dots$$

$$A/\gamma^2 \sim \text{const.}$$

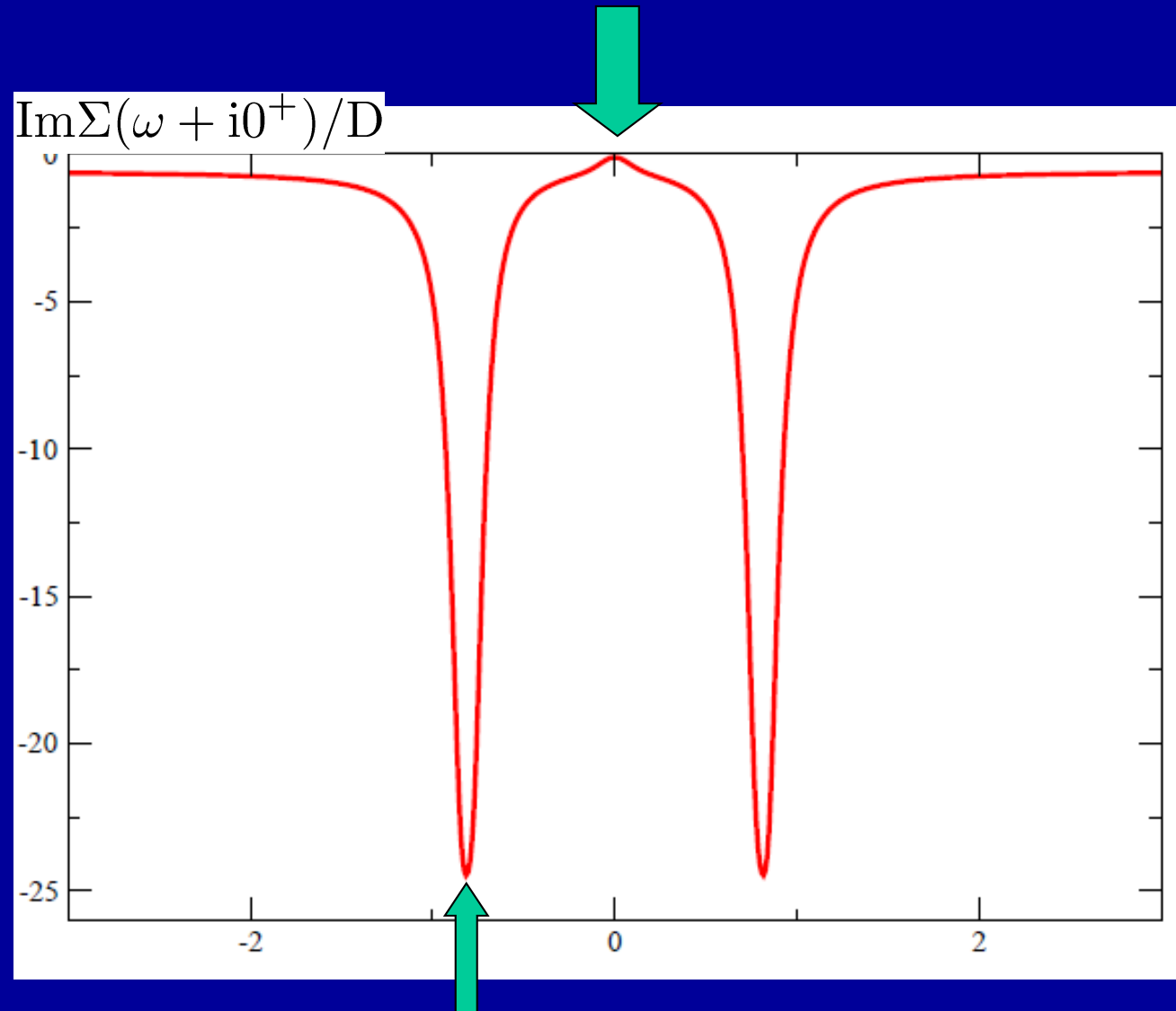
Fermi liquid behavior observed
 Below $\sim 100\text{K}$ @ 5% doping

But... there is (plenty of) life beyond the Fermi-liquid regime



CTQMC+Analytical continuation (Pade),
courtesy M.Ferrero, compares perfectly to NRG

$B\omega^2$ applies only below coherence scale
B-coefficient is enhanced $\sim 1/Z^2$



These 2 peaks will coalesce into a pole at $\omega=0$
as insulator is reached

'Kinks' of purely electronic origin in quasiparticle dispersion

LETTERS

Nature Physics 3 (2007) 168

Kinks in the dispersion of strongly correlated electrons

K. BYCZUK^{1,2*}, M. KOLLAR^{1*}, K. HELD³, Y.-F. YANG³, I. A. NEKRASOV⁴, TH. PRUSCHKE⁵ AND
D. VOLLHARDT¹

PRL 110, 246402 (2013)

PHYSICAL REVIEW LETTERS

week ending
14 JUNE 2013

Poor Man's Understanding of Kinks Originating from Strong Electronic Correlations

K. Held,¹ R. Peters,² and A. Toschi¹

¹*Institute of Solid State Physics, Vienna University of Technology, A-1040 Vienna, Austria*

²*Department of Physics, Kyoto University, Kyoto 606-8502, Japan*

(Received 25 February 2013; published 11 June 2013)

By means of dynamical mean field theory calculations, it was recently discovered that kinks generically arise in strongly correlated systems, even in the absence of external bosonic degrees of freedoms such as phonons. However, the physical mechanism behind these kinks remained unclear. On the basis of the perturbative and numerical renormalization group theory, we herewith identify these kinks as the effective Kondo energy scale of the interacting lattice system which is shown to be smaller than the width of the central peak.

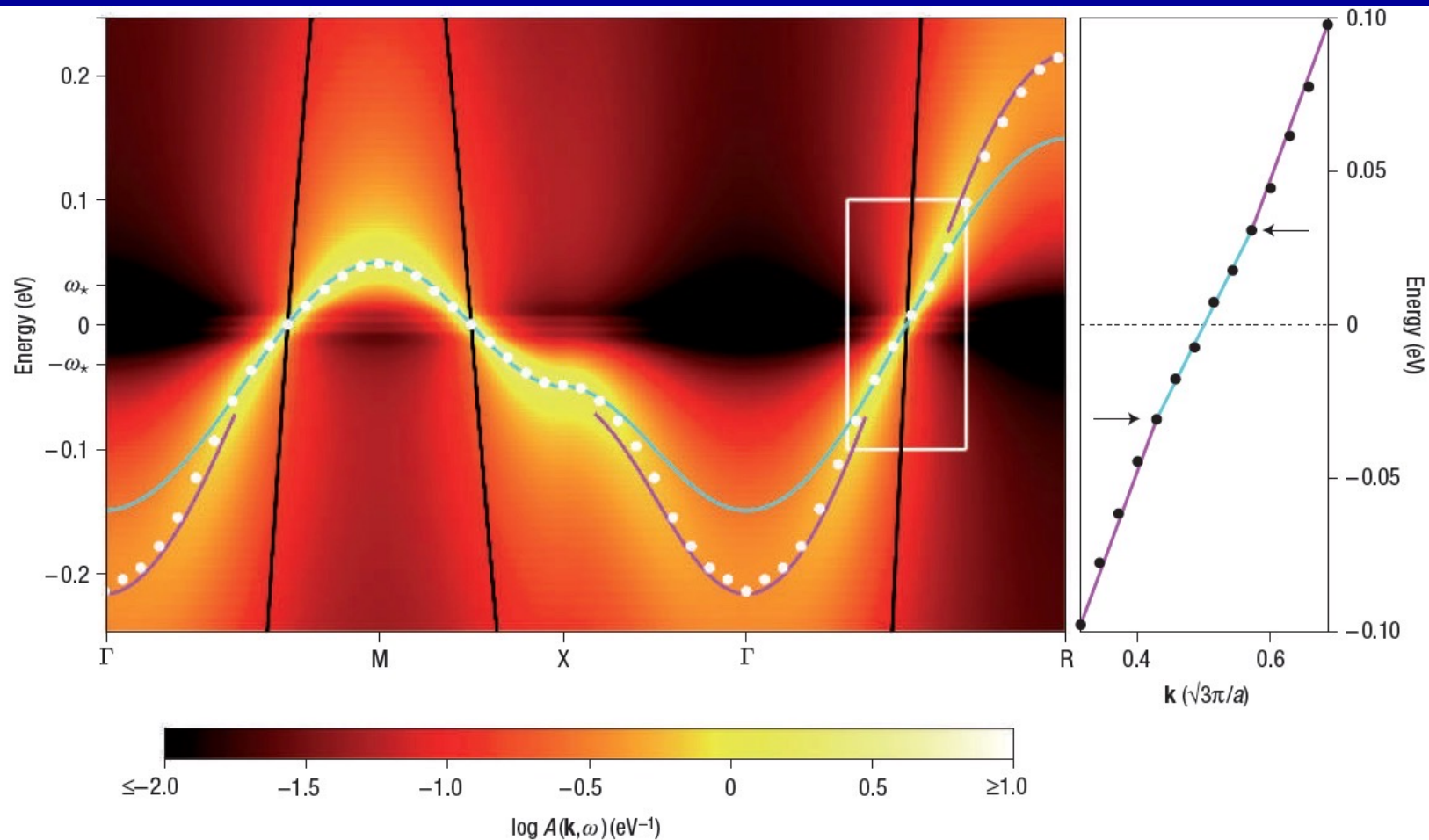


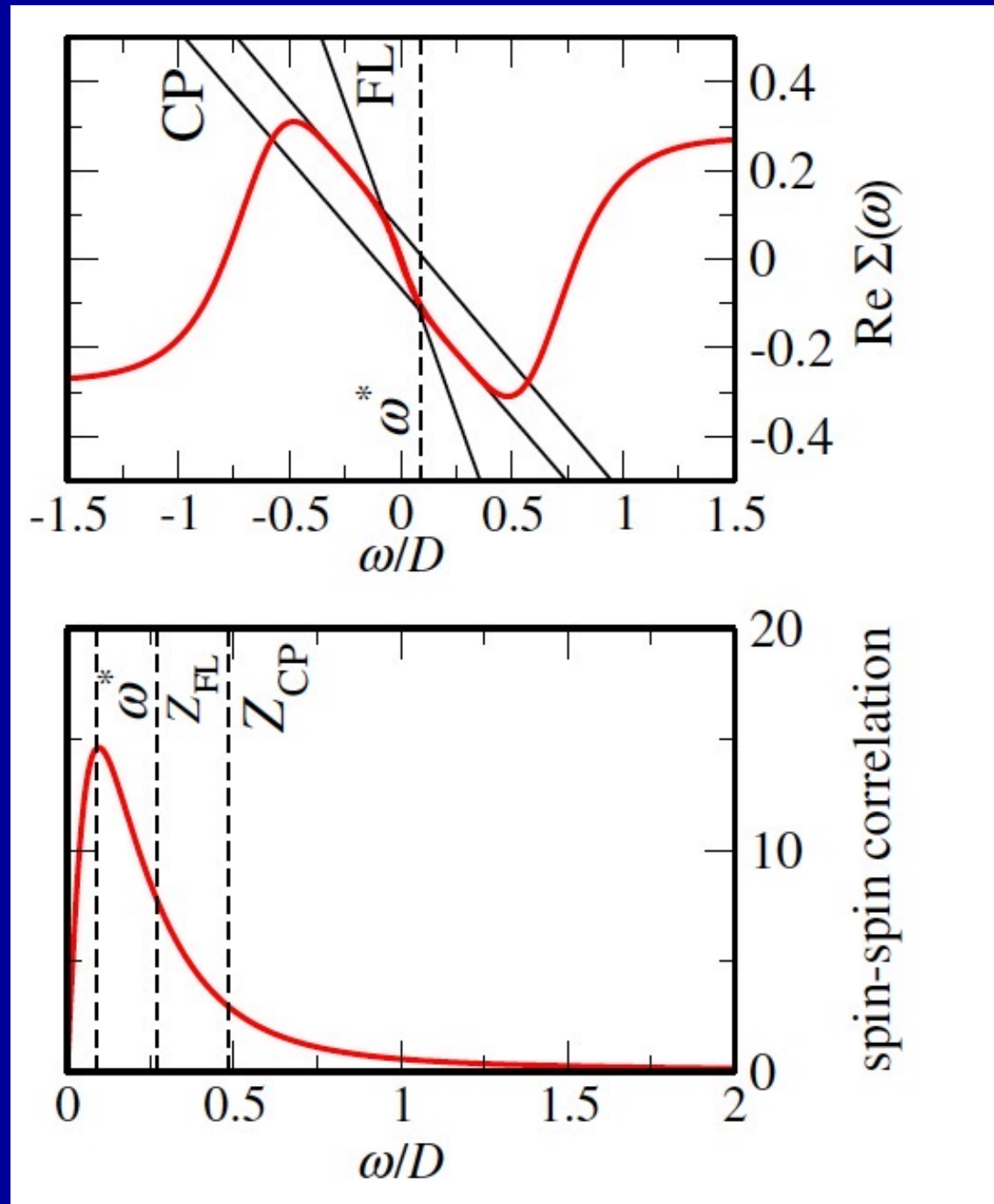
Figure 1 Kinks in the dispersion relation, $E_{\mathbf{k}}$, for a strongly correlated system. The intensity plot represents the spectral function $A(\mathbf{k}, \omega)$ (Hubbard model in DMFT, cubic lattice, interaction $U = 3.5$ eV, bandwidth $W = 3.46$ eV, $n = 1$, $Z_{\text{FL}} = 0.086$, $T = 5$ K). Close to the Fermi energy, the effective dispersion (white circles) follows the renormalized band structure, $E_{\mathbf{k}} = Z_{\text{FL}} \epsilon_{\mathbf{k}}$ (blue line). For $|\omega| > \omega_*$, the dispersion has the same shape but with a different renormalization, $E_{\mathbf{k}} = Z_{\text{CP}} \epsilon_{\mathbf{k}} - c \text{sgn}(E_{\mathbf{k}})$ (pink line). Here, $\omega_* = 0.03$ eV, $Z_{\text{CP}} = 0.135$ and $c = 0.018$ eV are all calculated (see the Supplementary Information) from Z_{FL} and $\epsilon_{\mathbf{k}}$ (black line). A subinterval of Γ -R (white frame) is plotted on the right, showing kinks at $\pm \omega_*$ (arrows).

Near U_{c2} :
Effective Kondo
problem
with FINITE
coupling.

(Fisher, Kotliar, Moeller
PRB 52 (1995) 17112; Moeller et
al. PRL 74 (1995) 2082)

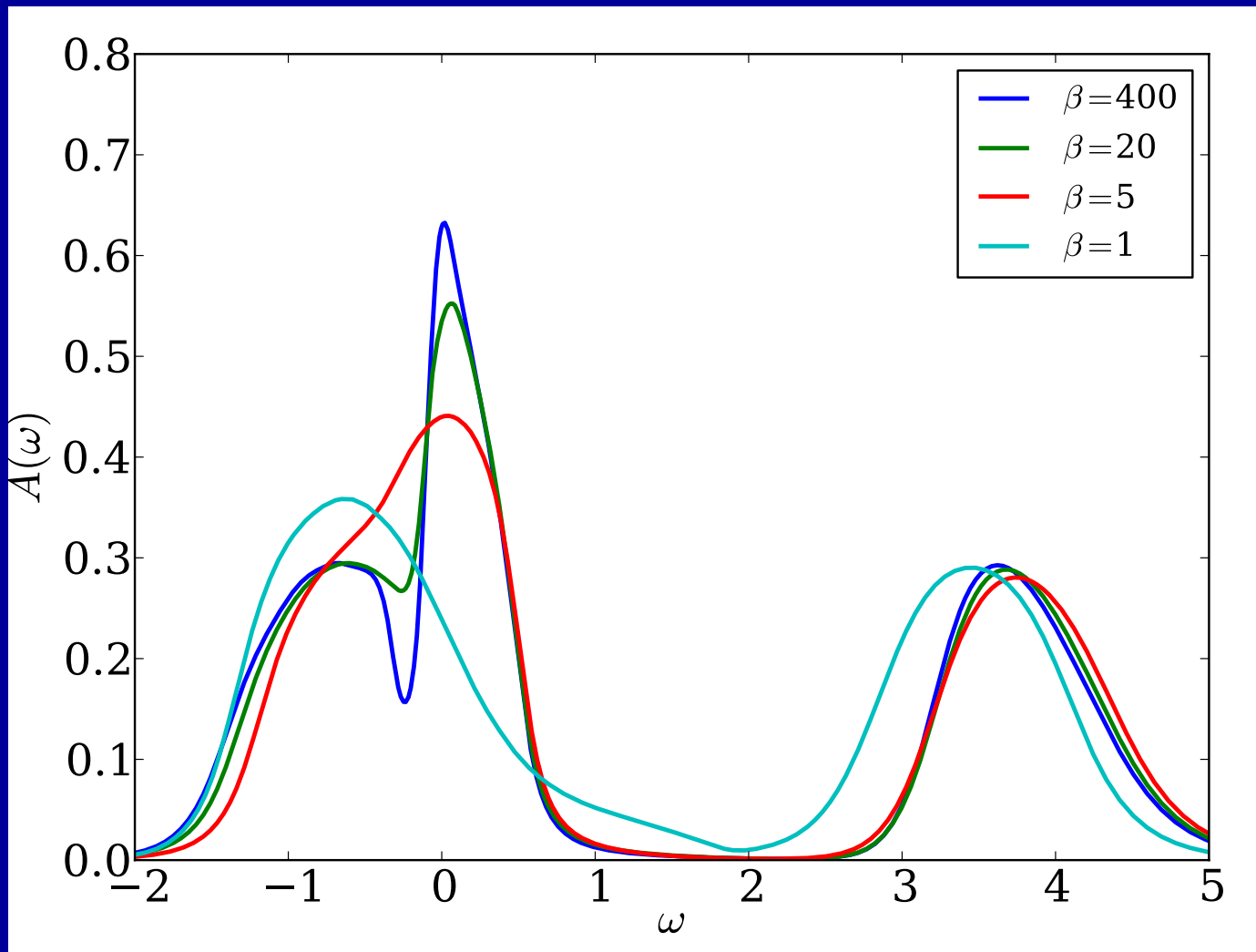
The kink is associated
with the effective Kondo
scale, which is smaller
than the width of the QP
peak

(Held et al., PRL 2013 →)

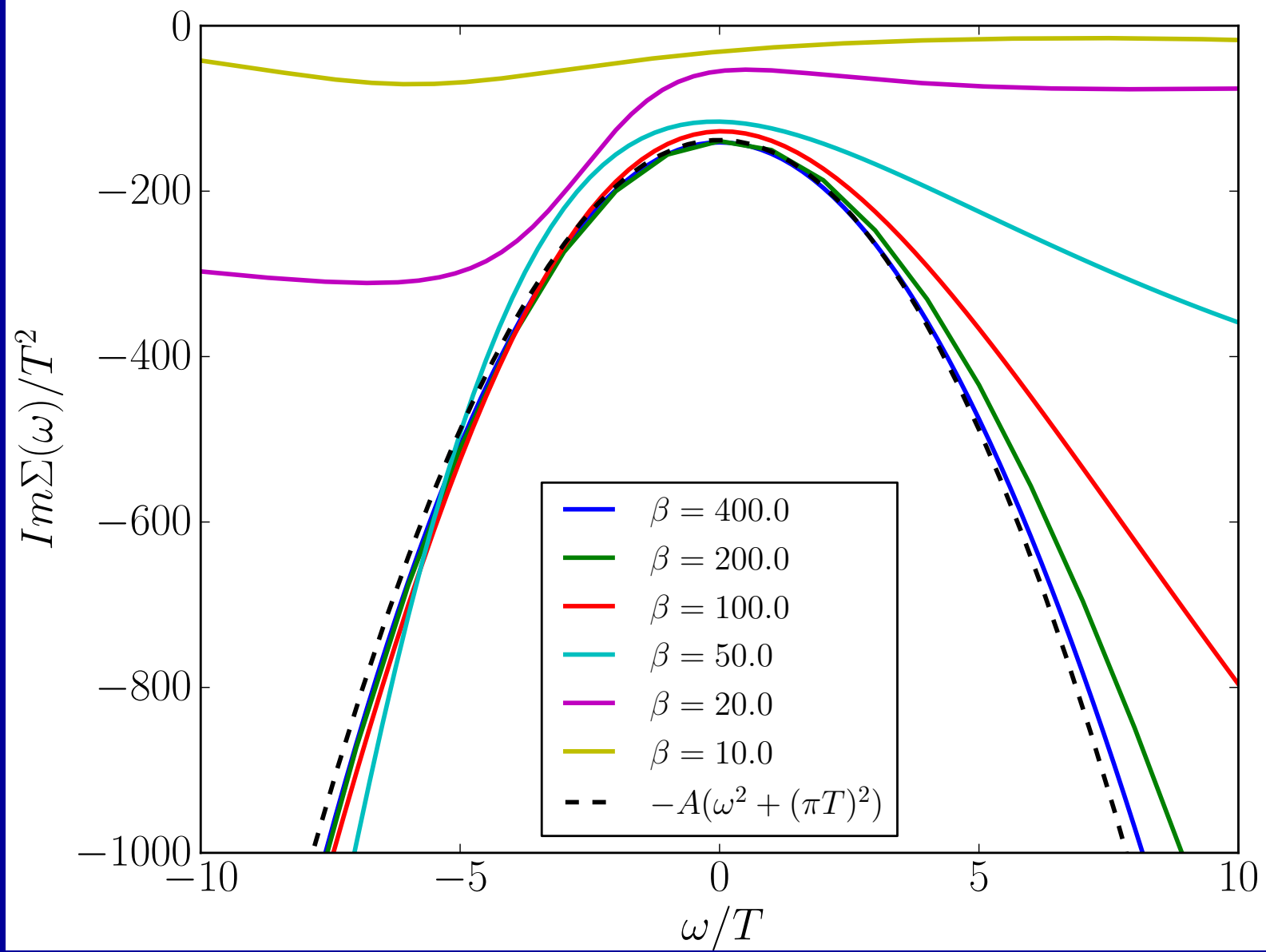


CT-HYB QMC and NRG allow for a high-accuracy exploration of the FL

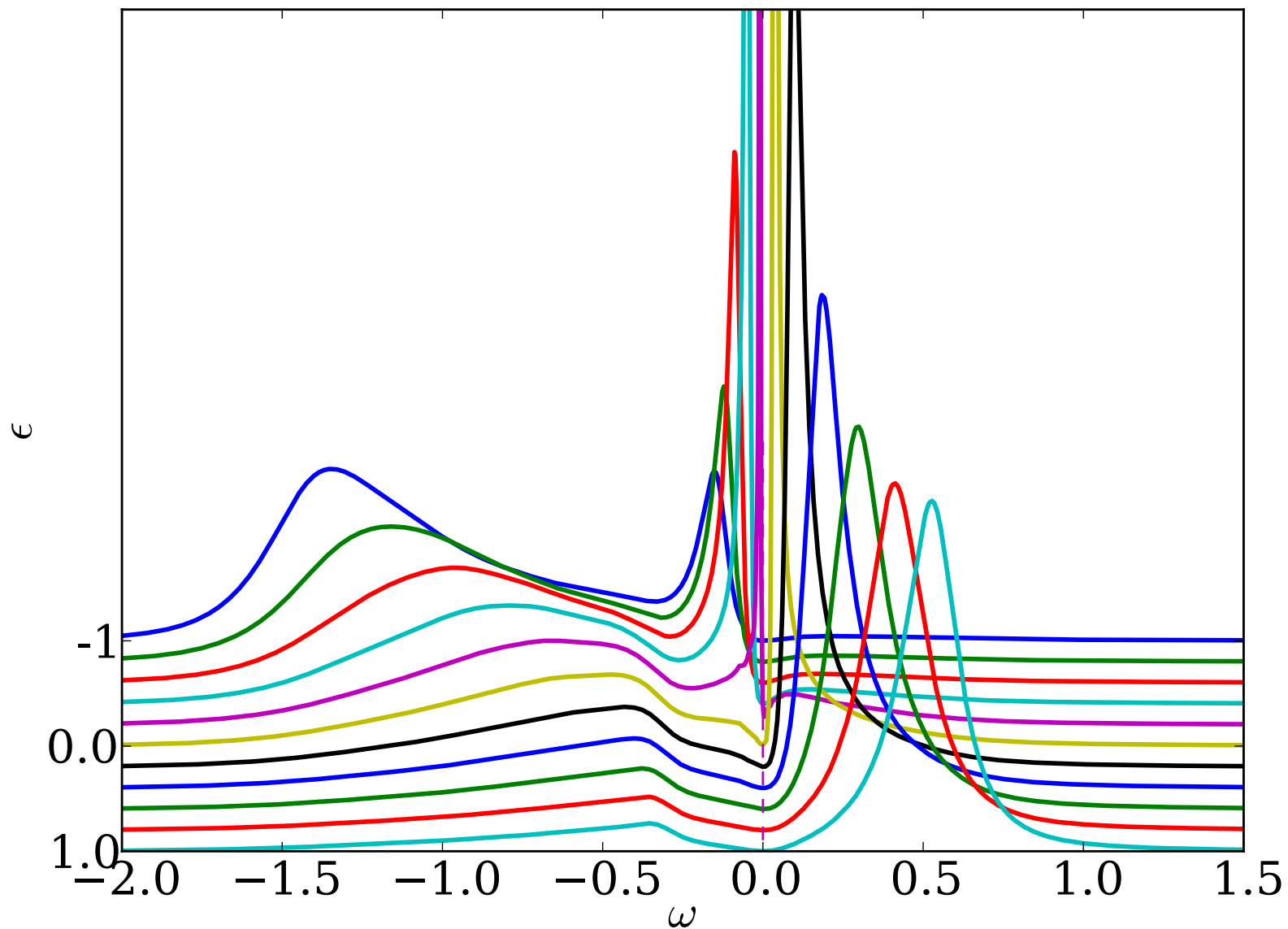
(M.Ferrero, J.Mravlje, R.Zitko, X.Deng, AG)

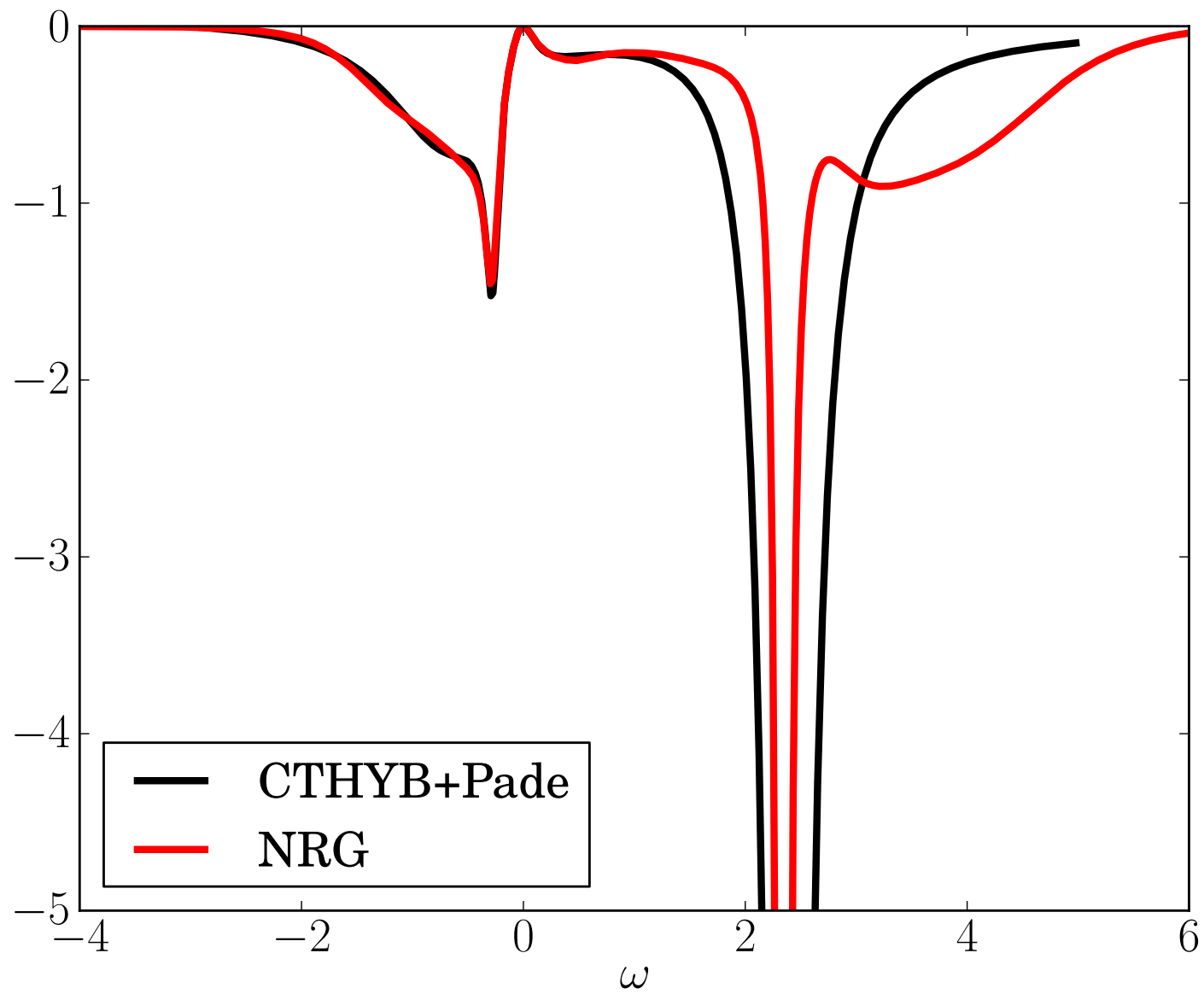


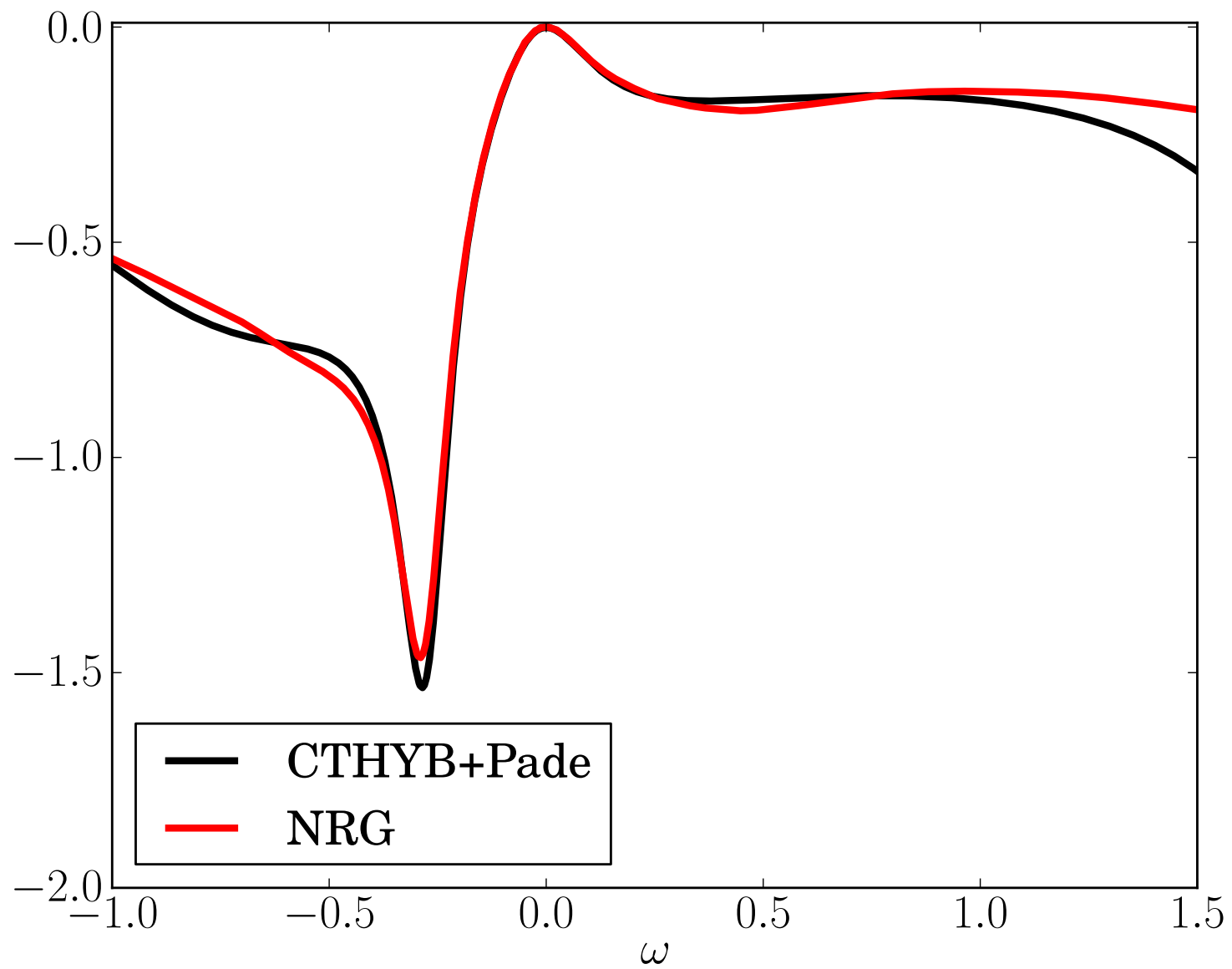
Bethe Lattice; $U/D=4$, 20%doping; NRG

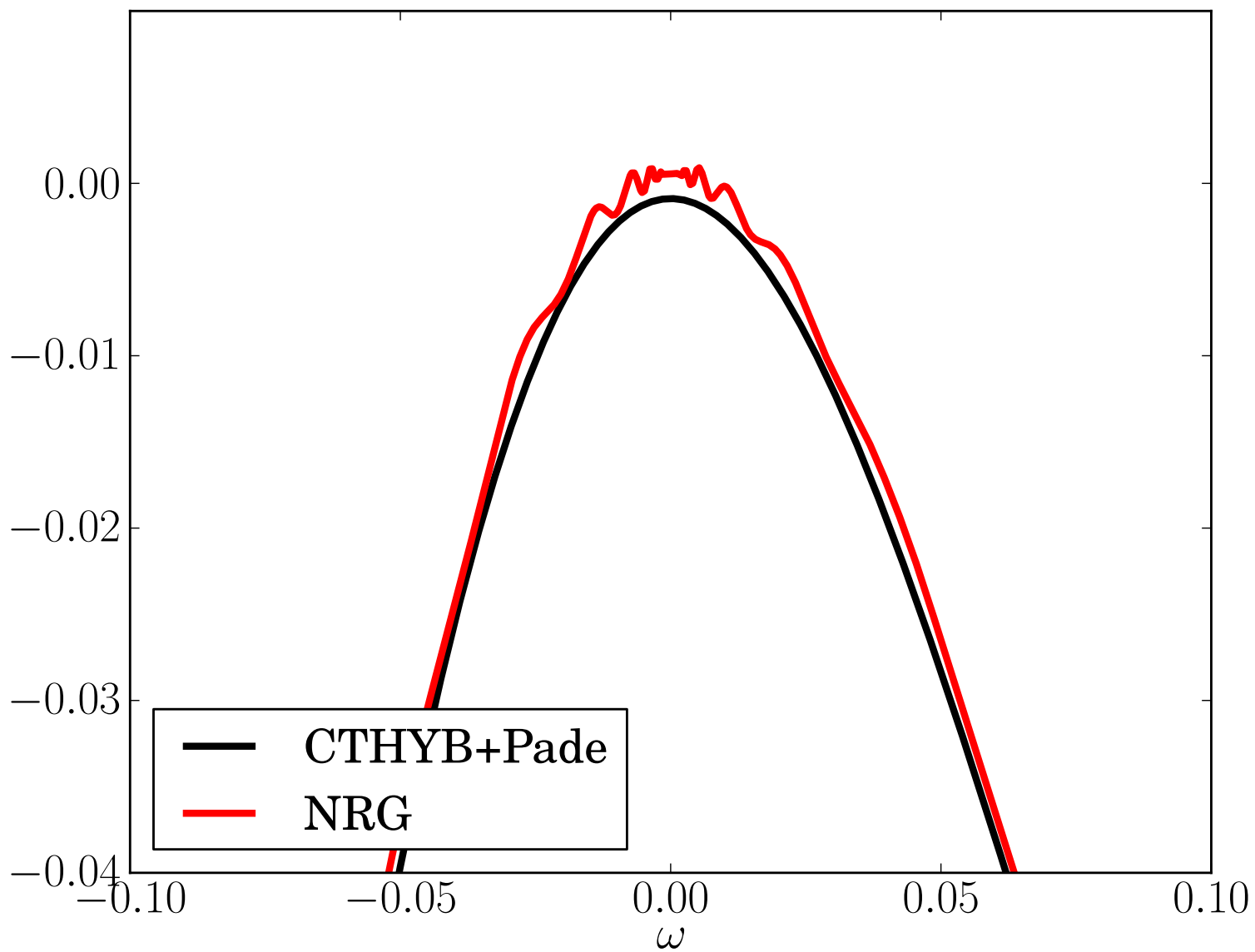


Momentum (energy) resolved spectral function









End of Section on Mott Transition

Atom in a bath:
Introduction to the single-impurity
Anderson model
with a DMFT perspective

`Anderson – Friedel- Wolff' model

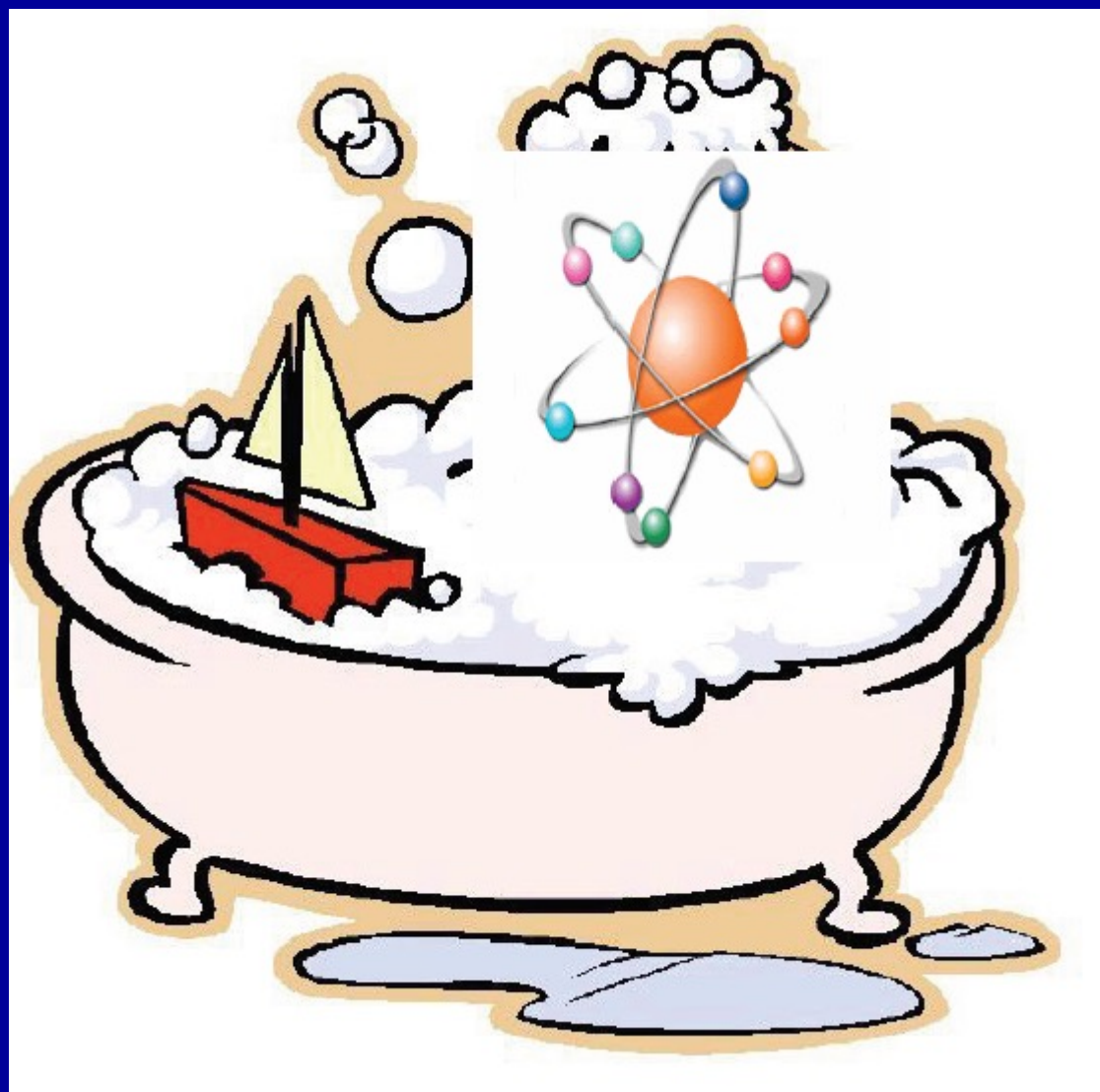
J.Friedel, Can.J.Phys 34, 1190 (1956)

P.W.Anderson, Phys Rev 124, 41 (1961)

P.A.Wolff, Phys. Rev. 124, 1030 (1961)

See also lectures at Collège de France, 2009-2010 cycle

“Atom in a bath”



Hamiltonian formulation: Anderson impurity model

$$H_c = \sum_{l\sigma} E_l a_{l\sigma}^+ a_{l\sigma}$$

$$H = H_c + H_{\text{at}} + H_{\text{hyb}}$$

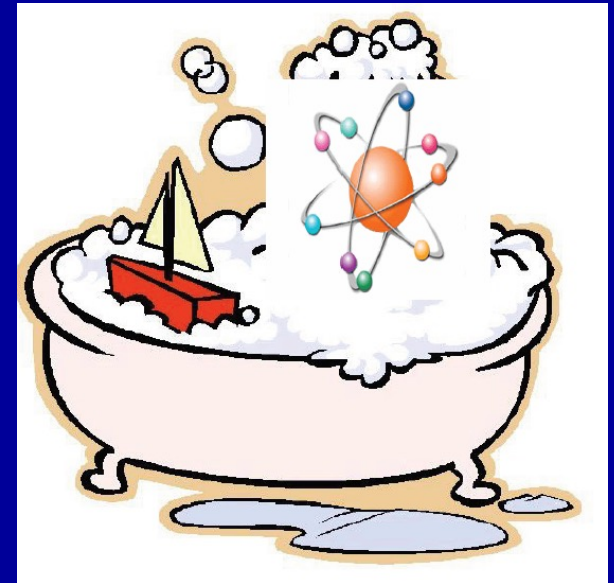
Conduction electron host (“bath”, environment)

$$H_{\text{at}} = \varepsilon_d \sum_{\sigma} d_{\sigma}^{\dagger} d_{\sigma} + U n_{\uparrow}^d n_{\downarrow}^d$$

Single-level “atom”

$$H_{\text{hyb}} = \sum_{l\sigma} [V_l a_{l\sigma}^+ d_{\sigma} + \text{h.c.}]$$

Transfers electrons between bath and atom – Hybridization, tunneling



Integrate out the bath: Effective action

$$S = S_{at} + S_{hyb}$$

$$S_{at} = \int_0^\beta d\tau \sum_{\sigma} d_{\sigma}^{\dagger}(\tau) \left(\frac{\partial}{\partial \tau} + \varepsilon_d \right) d_{\sigma}(\tau) + U \int_0^\beta d\tau n_{\uparrow}(\tau) n_{\downarrow}(\tau)$$

$$S_{hyb} = \int_0^\beta d\tau \int_0^\beta d\tau' \sum_{\sigma} d_{\sigma}^{\dagger}(\tau) \Delta(\tau - \tau') d_{\sigma}(\tau')$$

$$\Delta(i\omega_n) = \sum_l \frac{|V_l|^2}{i\omega_n - E_l}$$

$$\mathcal{G}_0^{-1}(i\omega_n) = i\omega_n - \varepsilon_d - \Delta(i\omega_n)$$

Effective 'bare propagator'.

“No Hamiltonian so incredibly simple has ever previously done such violence to the literature and to national science budgets”

Attributed to Harry Suhl by P.W. Anderson
in his 1978 Nobel lecture
[Rev Mod Phys 50 (1978) 191 p. 195]

[Although the Ising model is surely a serious competitor...]

Isolated 'atom'

$$H_{\text{at}} = \varepsilon_d \sum_{\sigma} d_{\sigma}^{\dagger} d_{\sigma} + U n_{\uparrow}^d n_{\downarrow}^d$$

Eigenstates:

- $|0\rangle$, $E = 0$
- $|\uparrow\rangle$ and $|\downarrow\rangle$, $E = \varepsilon_d$, *doubly degenerate* (in zero-field).
- $|\uparrow\downarrow\rangle$, $E = 2\varepsilon_d + U$

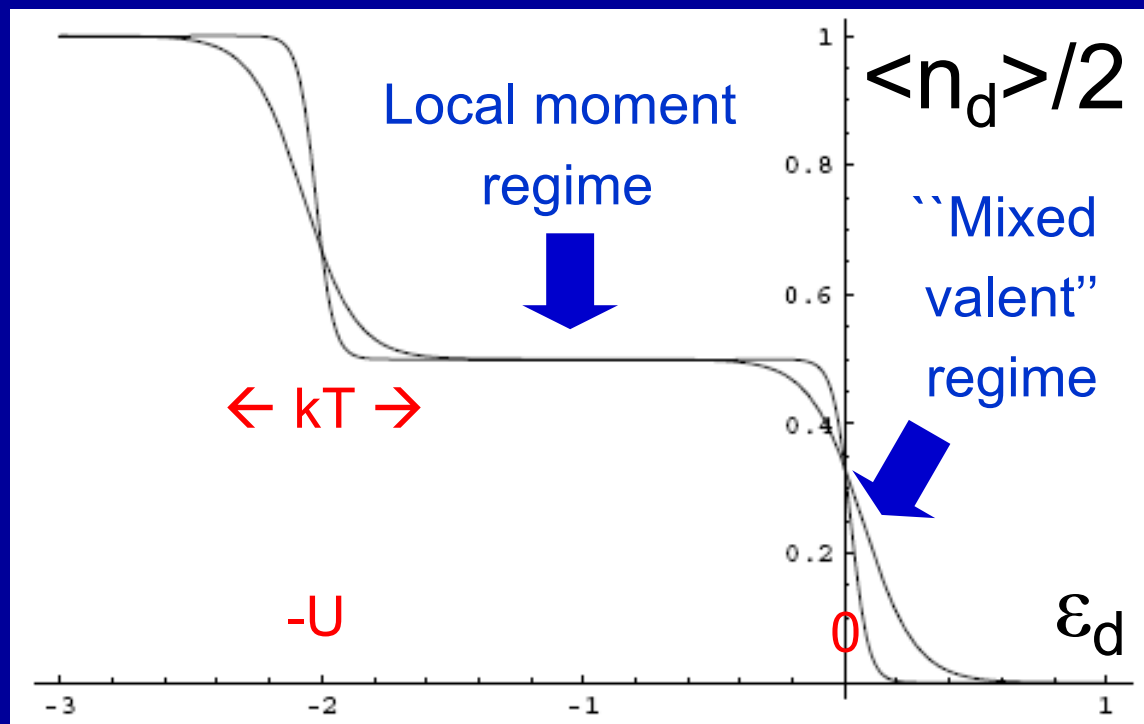
Level crossings:

- Between $|n=0\rangle$ and $|n=1\rangle$ at $\varepsilon = 0$
- Between $|n=1\rangle$ and $|n=2\rangle$ at $\varepsilon = -U$

Occupancy of the isolated atom :

$$n_{d\sigma} \equiv \langle d_{\sigma}^{\dagger} d_{\sigma} \rangle = \frac{n_d}{2} = \frac{1}{Z} (1 \times e^{-\beta \epsilon_d} + 1 \times e^{-\beta(2\epsilon_d+U)})$$

$$Z = 1 + 2e^{-\beta \epsilon_d} + e^{-\beta(2\epsilon_d+U)}$$



“Coulomb staircase”:
Blocking of charge by repulsive interactions, Except at points of level-crossing (charge degeneracy)

Plot of $n_d/2$ vs. ϵ_d for $U = 2$ at $\beta = 30$ and $\beta = 10$.

Spectroscopy of the isolated atom

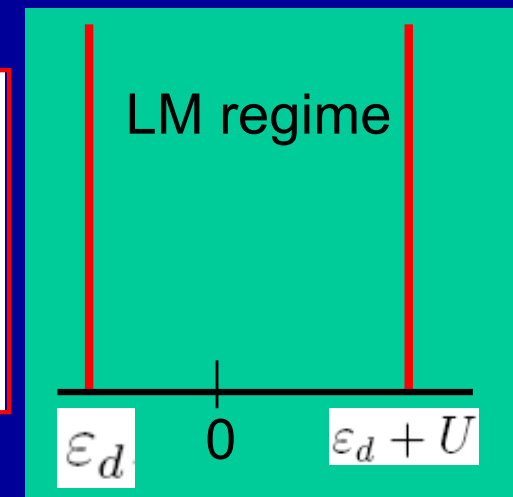
One-particle spectral function, at $T=0$:

$$\begin{aligned}
 A_d(\omega) &\equiv \sum_A |\langle \Psi_A | d_\sigma^\dagger | \Psi_0 \rangle|^2 \delta(\omega + E_0 - E_A) \quad (\omega > 0) \\
 &\equiv \sum_B |\langle \Psi_B | d_\sigma | \Psi_0 \rangle|^2 \delta(\omega + E_B - E_0) \quad (\omega < 0)
 \end{aligned}$$

and, at finite temperature:

$$A_d(\omega) \equiv \frac{1}{Z} \sum_{A,B} |\langle \Psi_A | d_\sigma^\dagger | \Psi_B \rangle|^2 (e^{-\beta E_A} + e^{-\beta E_B}) \delta(\omega + E_B - E_A)$$

$$\begin{aligned}
 A_d(\omega) &= \frac{e^{-\beta \varepsilon_d} + e^{-\beta(2\varepsilon_d + U)}}{Z} \delta(\omega - \varepsilon_d - U) + \frac{1 + e^{-\beta \varepsilon_d}}{Z} \delta(\omega - \varepsilon_d) \\
 &= \frac{n_d}{2} \delta(\omega - \varepsilon_d - U) + \left(1 - \frac{n_d}{2}\right) \delta(\omega - \varepsilon_d) \\
 &\quad [|\sigma\rangle \leftrightarrow |\uparrow\downarrow\rangle \text{ transition}] + [|\sigma\rangle \leftrightarrow |0\rangle \text{ transition}]
 \end{aligned}$$



Exact solution for a single site in the bath:

$$H = H_{\text{at}} + V \sum_{\sigma} (c_{\sigma}^{\dagger} d_{\sigma} + d_{\sigma}^{\dagger} c_{\sigma})$$

Conserved quantum numbers:

N, S, S^z

$1+4+6+4+1=16$ states

- $N = 0$: one state $|0\rangle$ ($S = S^z = 0$)
- $N = 1$: 4 states, $S = 1/2, S^z = \pm 1/2$
- $N = 2$: $S = 1$ a triplet of states
- $N = 2$: $S = 0$ three singlet states
- $N = 3$: 4 states
- $N = 4$: one states: $|\uparrow\downarrow, \uparrow\downarrow\rangle$

Focus on $N=2$ (ground-state) sector in LM regime:

- The $N = 2, S = 1$ triplet sector has eigenstates: $|\uparrow, \uparrow\rangle, |\downarrow, \downarrow\rangle$ and $\frac{1}{\sqrt{2}}[|\uparrow, \downarrow\rangle + |\downarrow, \uparrow\rangle]$. These states are insensitive to the hybridization V because the Pauli principle does not allow for hopping an electron through. Hence their energy is ε_d .

The $N = 2, S = 0$ sector is more interesting.

Basis set: $|\uparrow\downarrow, 0\rangle, \frac{1}{\sqrt{2}}[|\uparrow, \downarrow\rangle - |\downarrow, \uparrow\rangle], |0, \uparrow\downarrow\rangle$.

The matrix reads:
$$\begin{pmatrix} 2\varepsilon_d + U & \sqrt{2}V & 0 \\ \sqrt{2}V & \varepsilon_d & \sqrt{2}V \\ 0 & \sqrt{2}V & 0 \end{pmatrix}$$

Symmetric case $\varepsilon_d = -U/2$

$$E = 0, E_{\pm} = -\frac{U}{4} \pm \frac{1}{2}\sqrt{\frac{U^2}{4} + 16V^2}$$

The *ground-state* has energy E_- . For $V \ll U$, this reads:

$$E_0 = E_- \simeq -\frac{U}{2} - \frac{8V^2}{U} + \dots$$

Energy in SINGLET SECTOR is lowered by virtual hops

Double occupancy in intermediate state \rightarrow energy denominator $\sim U$

Ground-state wave-function:

with $\eta \sim \frac{V}{U} \ll 1$.

$$|\Psi_0\rangle = \sqrt{1 - \eta^2} |\mathcal{S}\rangle + \eta |\mathcal{D}\rangle$$

$$|\mathcal{S}\rangle \equiv \frac{1}{\sqrt{2}} [|\uparrow, \downarrow\rangle - |\downarrow, \uparrow\rangle]$$

$$|\mathcal{D}\rangle \equiv \frac{1}{\sqrt{2}} [|\uparrow\downarrow, 0\rangle + |0, \uparrow\downarrow\rangle]$$

Key points:

- Because of virtual hopping and the Pauli principle, a spin-singlet ground-state has been stabilized, in which the impurity spin is screened out by a conduction electron.
- Virtual hopping has induced a (small) admixture of states with $n_d = 0$ and $n_d = 2$ in the wave-function, hence allowing for charge fluctuations on the atom.

- The atomic limit $V=0$ is SINGULAR in the LM regime
 - A non-zero V lifts the ground-state degeneracy
- The ground-state becomes a singlet: the impurity moment is “screened” by binding w/ a conduction electron

$$G(z) = \sum_{j=1}^2 \left(\frac{a_j}{z - \epsilon_j} + \frac{a_j}{z + \epsilon_j} \right),$$

$$\epsilon_1 = \frac{1}{4} \left(\sqrt{U^2 + 64V^2} - \sqrt{U^2 + 16V^2} \right),$$

$$\epsilon_2 = \frac{1}{4} \left(\sqrt{U^2 + 64V^2} + \sqrt{U^2 + 16V^2} \right),$$

$$a_1 = \frac{1}{4} \left(1 - \frac{U^2 - 32V^2}{\sqrt{(U^2 + 64V^2)(U^2 + 16V^2)}} \right),$$

E.Lange

Mod Phys Lett B 12, 915 (1998)

arXiv:9810208

See also Appendix in
Alex Hewson's book

Spectral function for
1 site in the bath,
 $\frac{1}{2}$ filling

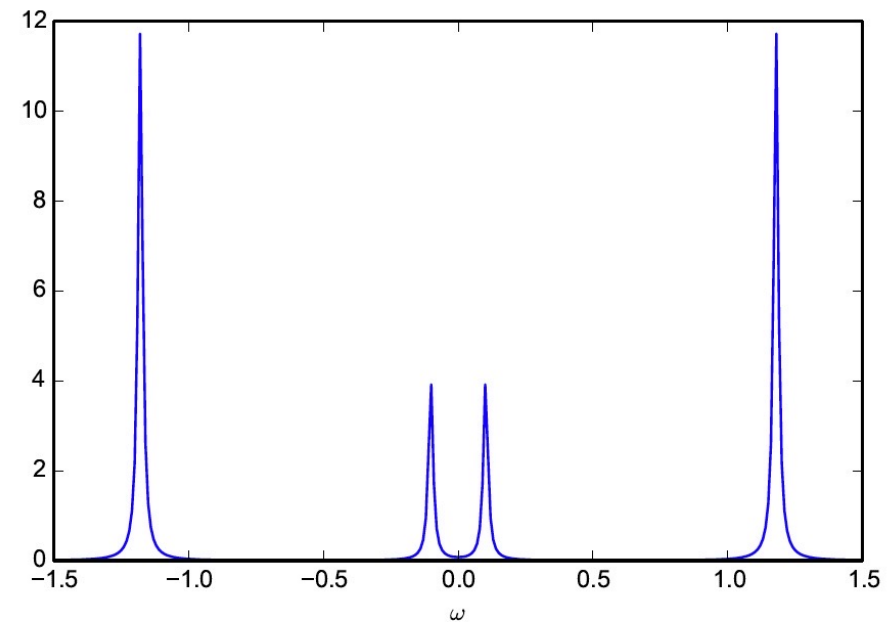


Figure 3: Spectral function for $U = 2.0$, $V = 0.2$

The simplest ED solver for DMFT: 1-bath site approximation ~ Gutzwiller/BR Focuses on quasiparticles only

M.Potthoff PRB 64, 165114 (2001)

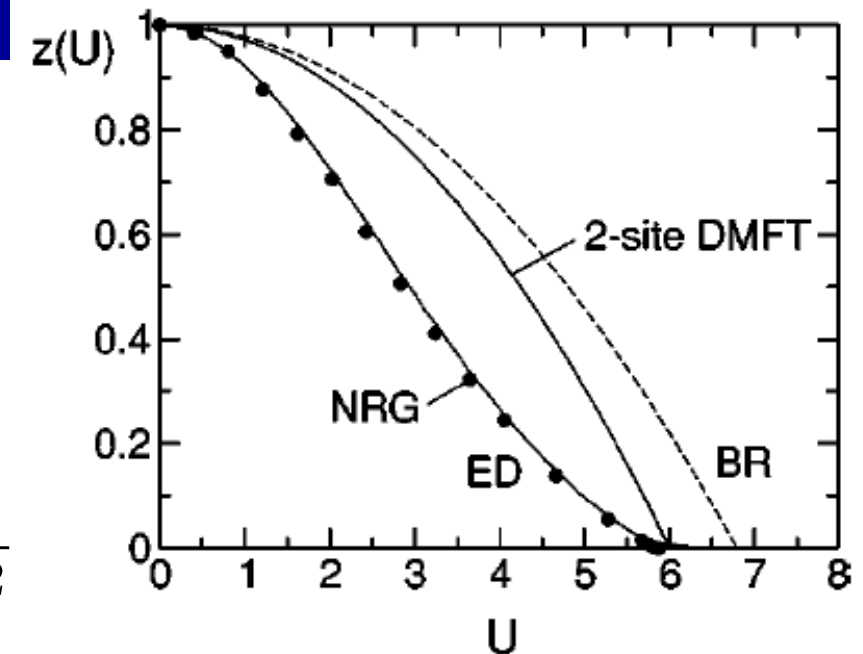
$$\Delta(\omega) = \frac{V^2}{\omega}$$

$$\Rightarrow \Sigma = \frac{U^2}{8} \left[\frac{1}{\omega - 3V} + \frac{1}{\omega + 3V} \right]$$

$$\Rightarrow Z^{-1} \equiv 1 - \left. \frac{\partial \Sigma}{\partial \omega} \right|_{\omega=0} = 1 + \frac{U^2}{36V^2}$$

$$V^2 = \frac{U^2}{36} \frac{Z}{1 - Z}$$

$$\Delta = \frac{D^2}{4} G \Rightarrow \frac{U^2}{36} \frac{Z}{1 - Z} = \frac{D^2}{4} Z$$



$$Z = 1 - \left(\frac{U}{3D} \right)^2$$

$$G(\omega) \simeq \frac{1}{2} \left[\frac{1}{\omega - \Delta(\omega) - U/2} + \frac{1}{\omega - \Delta(\omega) + U/2} \right]$$

$$\Delta = \frac{D^2}{4} G$$

$$\Rightarrow D^4 G^3 - 8D^2 \omega G^2 + 4(4\omega^2 + D^2 - U^2)G - 16\omega = 0$$

Gap at large- U
approximation:
Hubbard-like
ignore Kondo-like
processes/
quasiparticles

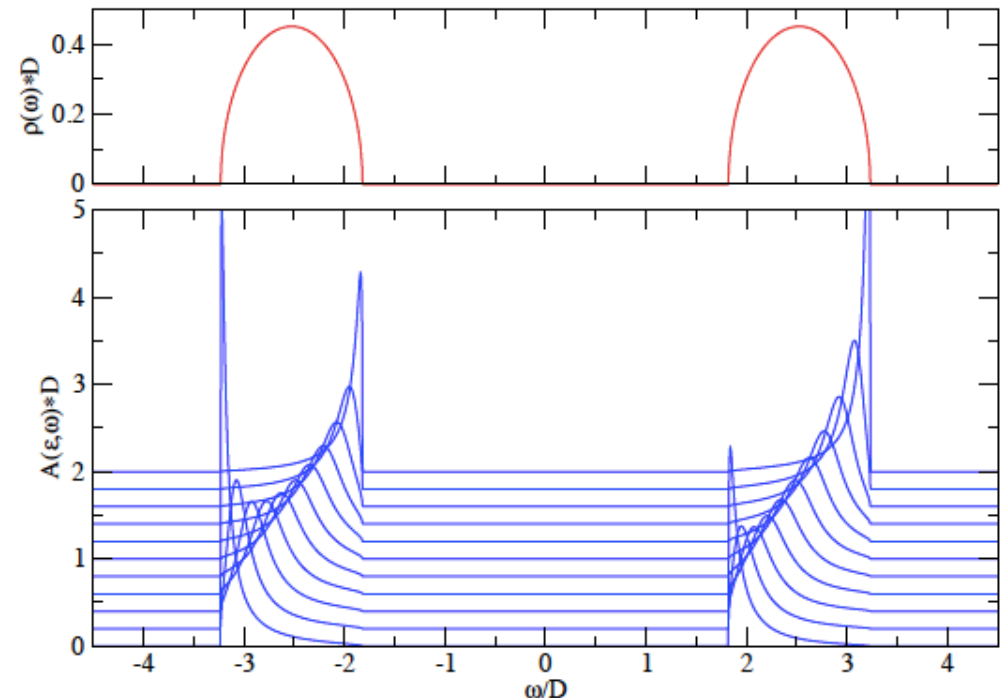
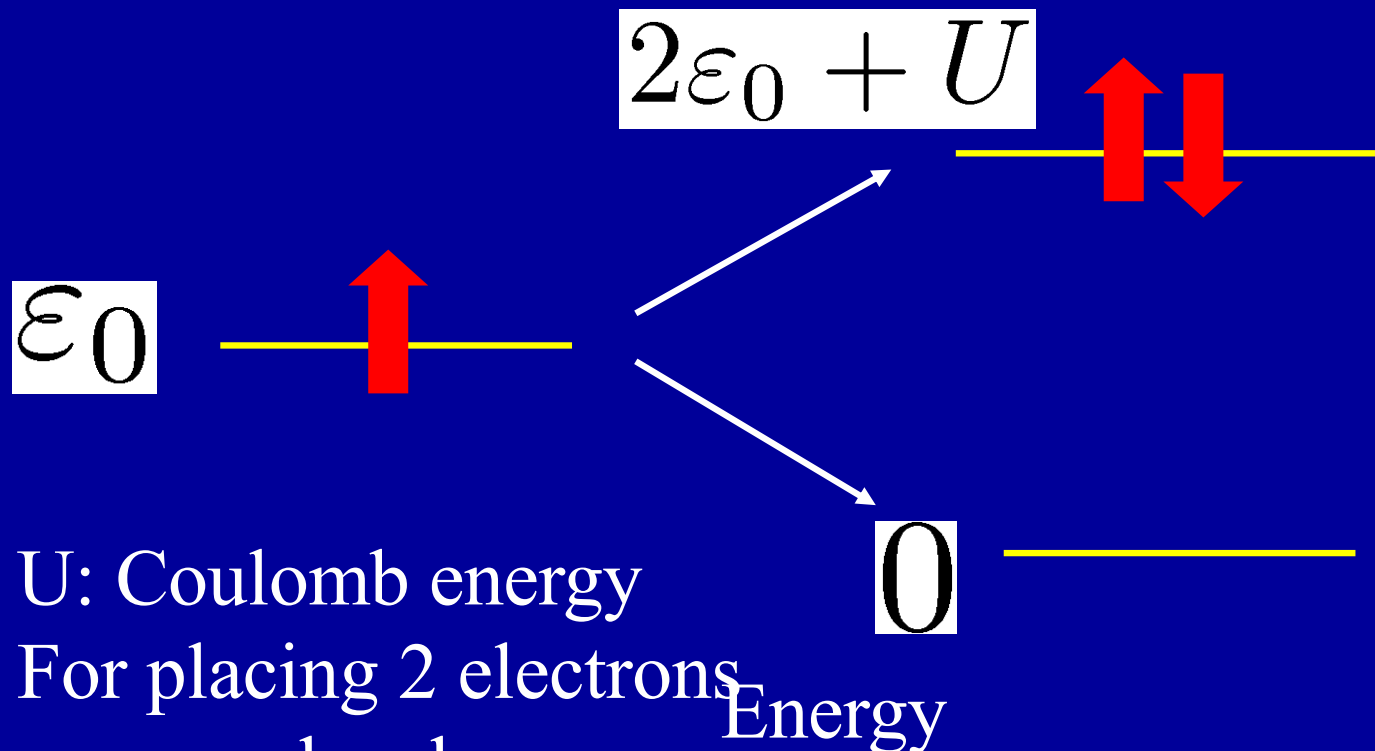


FIG. 10: Spectral density $\rho(\omega)$ (a) and ϵ -resolved spectral function $A(\epsilon, \omega)$ for several ϵ (from bottom to the top, $\epsilon = -D, \dots, D$ with a step 0.2) (b), with $U/D = 4.0$ and $T = 0$. The results are from Hubbard III approximation.

A "Hubbard satellite" is nothing but an *atomic transition*

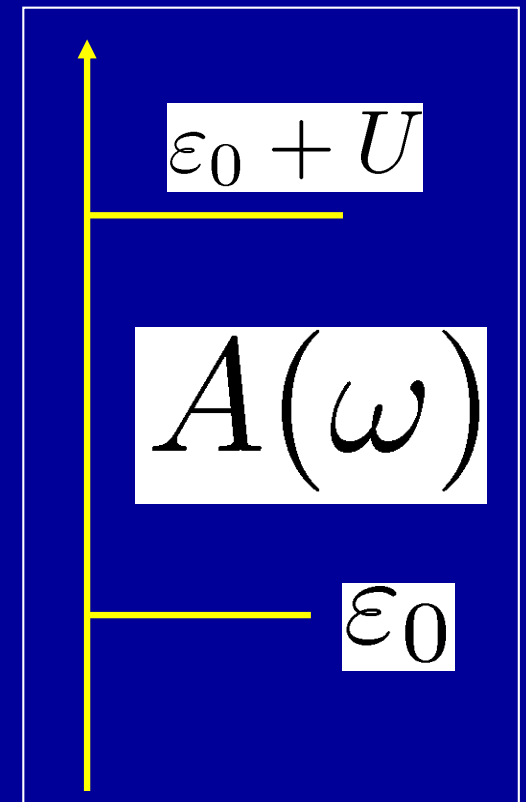
(broadened by the solid-state environment)

Imagine a simplified atom with a single atomic level



U: Coulomb energy

For placing 2 electrons
on same level



General many-body theory and (local) Fermi-liquid considerations

Focus on dynamics of impurity orbital: integrate out conduction electrons

→ Effective action for impurity orbital:

$$S = - \int_0^\beta d\tau \int_0^\beta d\tau' \sum_\sigma d_\sigma^\dagger(\tau') G_{d0}^{-1}(\tau - \tau') d_\sigma(\tau) + U \int_0^\beta d\tau n_\uparrow n_\downarrow$$

also reads:

$$S = S_{at} + S_{hyb}$$

$$S_{at} = \int_0^\beta d\tau \sum_\sigma d_\sigma^\dagger(\tau) \left(\frac{\partial}{\partial \tau} + \varepsilon_d \right) d_\sigma(\tau) + U \int_0^\beta d\tau n_\uparrow(\tau) n_\downarrow(\tau)$$

$$S_{hyb} = \int_0^\beta d\tau \int_0^\beta d\tau' \sum_\sigma d_\sigma^\dagger(\tau) \Delta(\tau - \tau') d_\sigma(\tau')$$

Feynman rules associated with this action (involving only time):

- A vertex U (local in time)

- A 'bare' propagator (retarded): $G_{d0}(\tau - \tau') \sim \rho_c / (\tau - \tau') + \dots$

The interaction leads to a self-energy for the d-orbital:

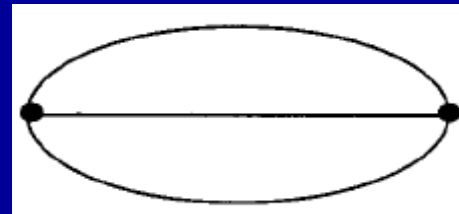
$$G_d(i\omega_n)^{-1} = G_{d0}(i\omega_n)^{-1} - \Sigma(i\omega_n)$$

(Local) Fermi-liquid form of self-energy, at $T=0$:

$$\Sigma'(\omega) = \Sigma(0) + \left(1 - \frac{1}{Z}\right) \omega + \dots$$

$$\Sigma''(\omega) = -A\omega^2 + \dots$$

First non-trivial diagram $O(U^2)$:



$$\sim U^2 \frac{1}{\tau^3} \rightarrow \Sigma'' \propto \omega^2$$

d-level spectral function, wide bandwidth limit, Fermi-liquid considerations:

$$A_d(\omega) = \frac{1}{\pi} \frac{\Gamma - \Sigma''(\omega)}{[\omega - \varepsilon_d - \Sigma'(\omega)]^2 + [\Gamma - \Sigma''(\omega)]^2}$$

Hence, at low-frequency:

$$A_d(\omega \simeq 0) = \frac{Z}{\pi} \frac{\tilde{\Gamma}}{(\omega - \tilde{\varepsilon}_d)^2 + \tilde{\Gamma}^2}$$

$$\begin{aligned} \Sigma'(\omega) &= \Sigma(0) + \left(1 - \frac{1}{Z}\right) \omega + \dots \\ \Sigma''(\omega) &= -A\omega^2 + \dots \end{aligned}$$

Resonance with renormalized level position and width, overall spectral weight Z:

$$\tilde{\varepsilon}_d = Z [\varepsilon_d + \Sigma(0)] \quad , \quad \tilde{\Gamma} = Z \Gamma$$

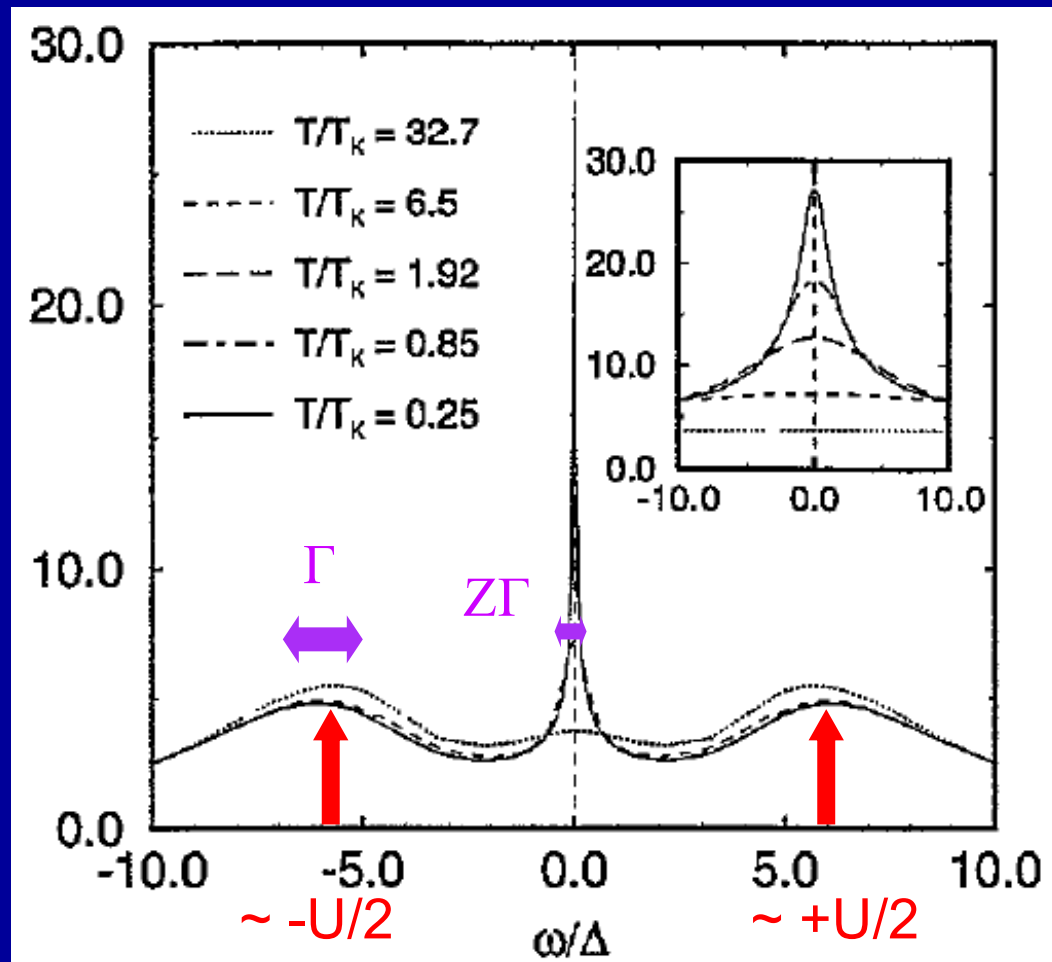
In particular, in particle-hole symmetric case (LM regime) $\varepsilon_d = -\frac{U}{2}$

$$A_d(\omega \simeq 0) = \frac{Z}{\pi} \frac{Z\Gamma}{\omega^2 + (Z\Gamma)^2} \quad A_d(\omega = 0) = \frac{1}{\pi\Gamma}$$

Width, Weight $\sim Z$
Height unchanged !

Numerical Renormalization Group (NRG) calculation

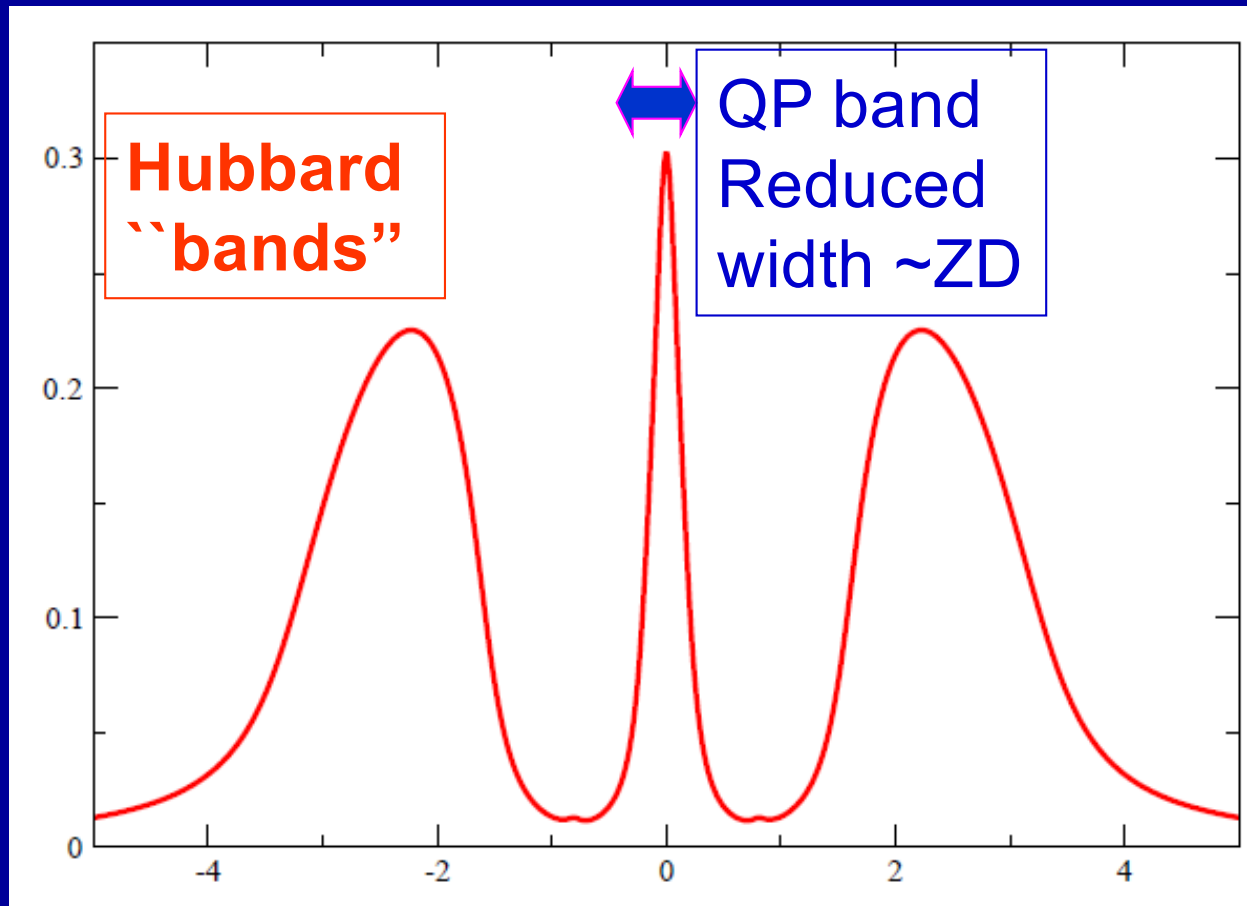
T.Costi and A.Hewson, J. Phys Cond Mat 6 (1994) 2519



Low energy associated with the resonance and quasiparticle excitations:

$$Z \sim T_K/\Gamma \sim \exp -\frac{8\Gamma}{\pi U}$$

The actual k-integrated spectral function has both Hubbard bands and low-energy quasiparticles



Value of $A(\omega=0)$ is pinned at $U=0$ value due to Luttinger theorem

→ Low-energy quasiparticles and incoherent Hubbard bands Coexist in one-particle spectrum of correlated metal

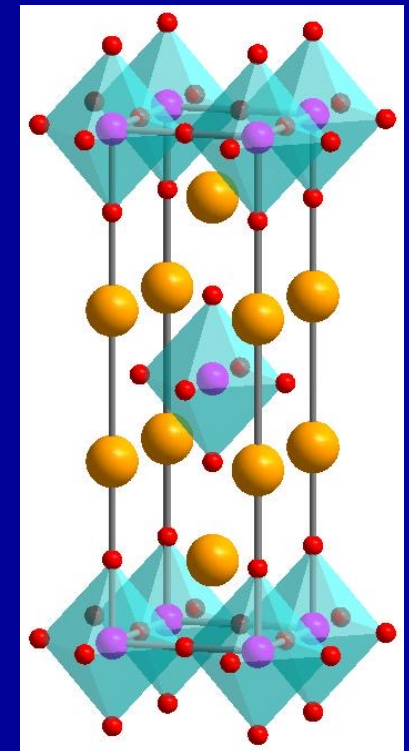
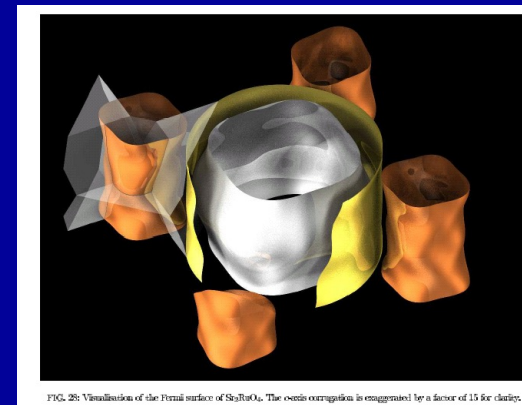
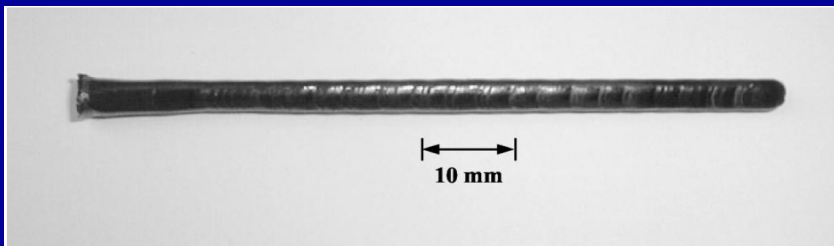
End of slides on AIM

Putting the DMFT *ansatz* directly to the test from high-resolution ARPES: Sr_2RuO_4

A.Tamai et al. Phys Rev X 9, 021048 (2019)



The 'fruit-fly' of Transition-Metal Oxides!



Large clean single-crystals

→ Investigated with basically all techniques in the experimentalist's toolbox

A.Mackenzie, Y.Maeno Rev Mod Phys 75, 657 (2003)

Simple Structure

Self-Energy: The DMFT *ansatz*

For a multi-band/multi-orbital material

$|\chi_m^{\mathbf{k}}\rangle$: A set of localized orbitals with many-body interactions $U_{m_1 m_2 m_3 m_4}$ are added: correlated Hilbert space

$|\psi_\nu^{\mathbf{k}}\rangle$: The (usually larger) set of Bloch bands (e.g. Kohn-Sham states) describing the material (larger Hilbert space)

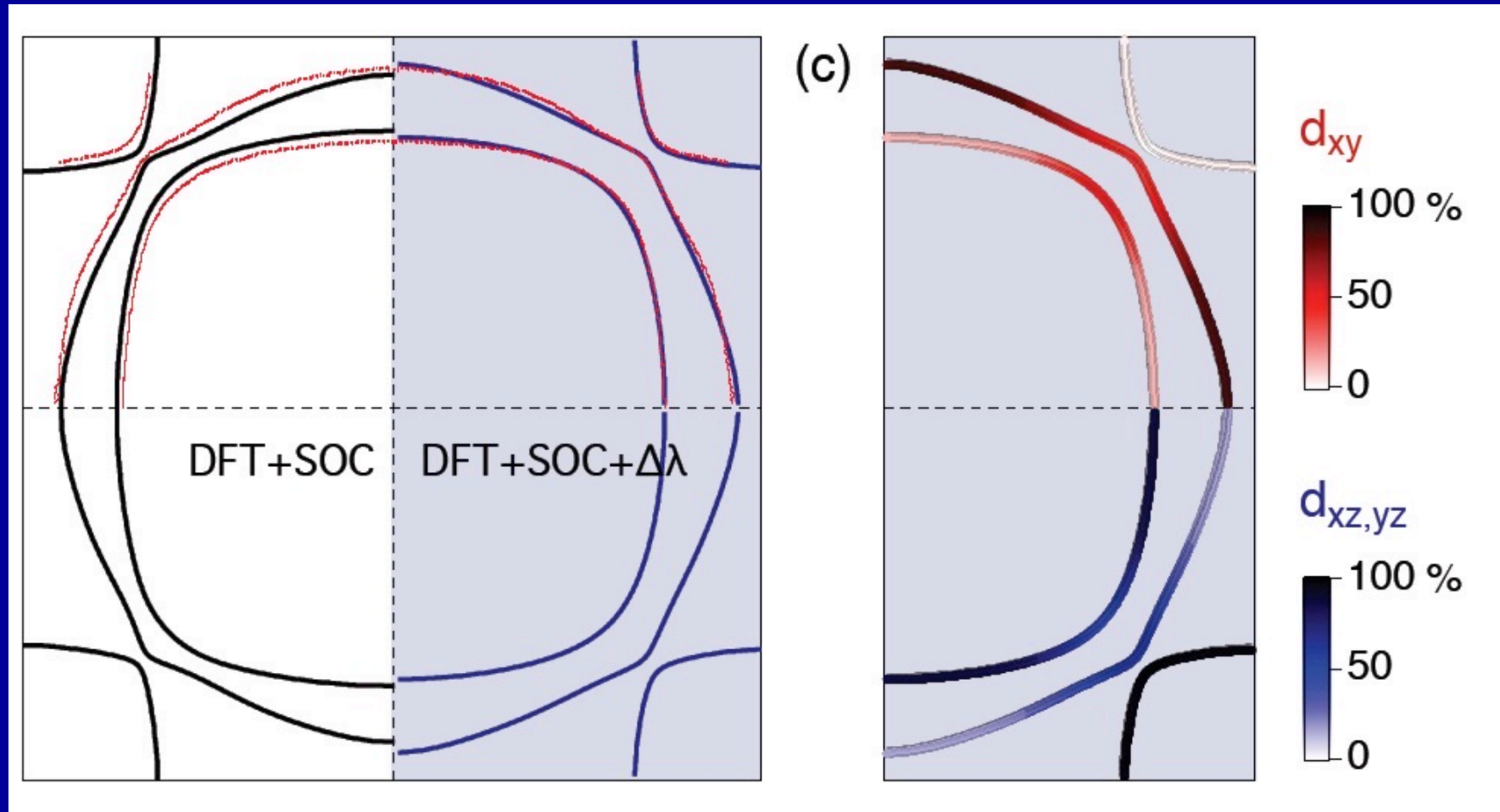
$$\Sigma_{\nu\nu'}(\omega, \mathbf{k}) = \sum_{mm'} \langle \psi_\nu^{\mathbf{k}} | \chi_m^{\mathbf{k}} \rangle \Sigma_{mm'}(\omega) \langle \chi_{m'}^{\mathbf{k}} | \psi_{\nu'}^{\mathbf{k}} \rangle$$

↑
Self-energy
`unfolded' to
the whole system
(k-dependent)

↑
Orbital content
of Bloch states
(k-dep)

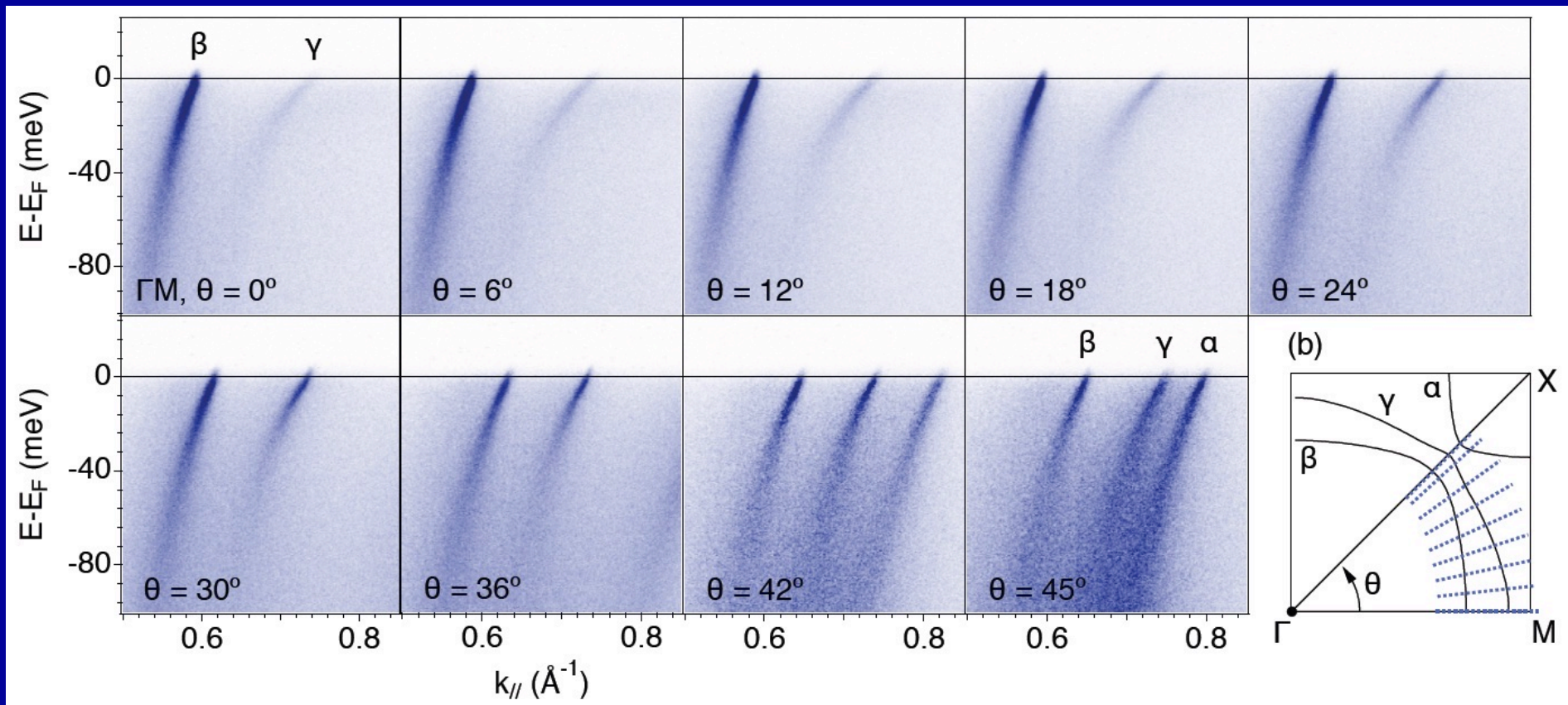
↑
Local self-energy
`unfolded' to
the whole system
(k-independent)

Orbital Content of Quasiparticle States is strongly angular dependent due to spin-orbit



DMFT prediction (Pavarini et al PRL 2016; Kim et al. PRL 2018):
Effective enhancement $\Delta\lambda$ of SOC \rightarrow Confirmed by experiments!

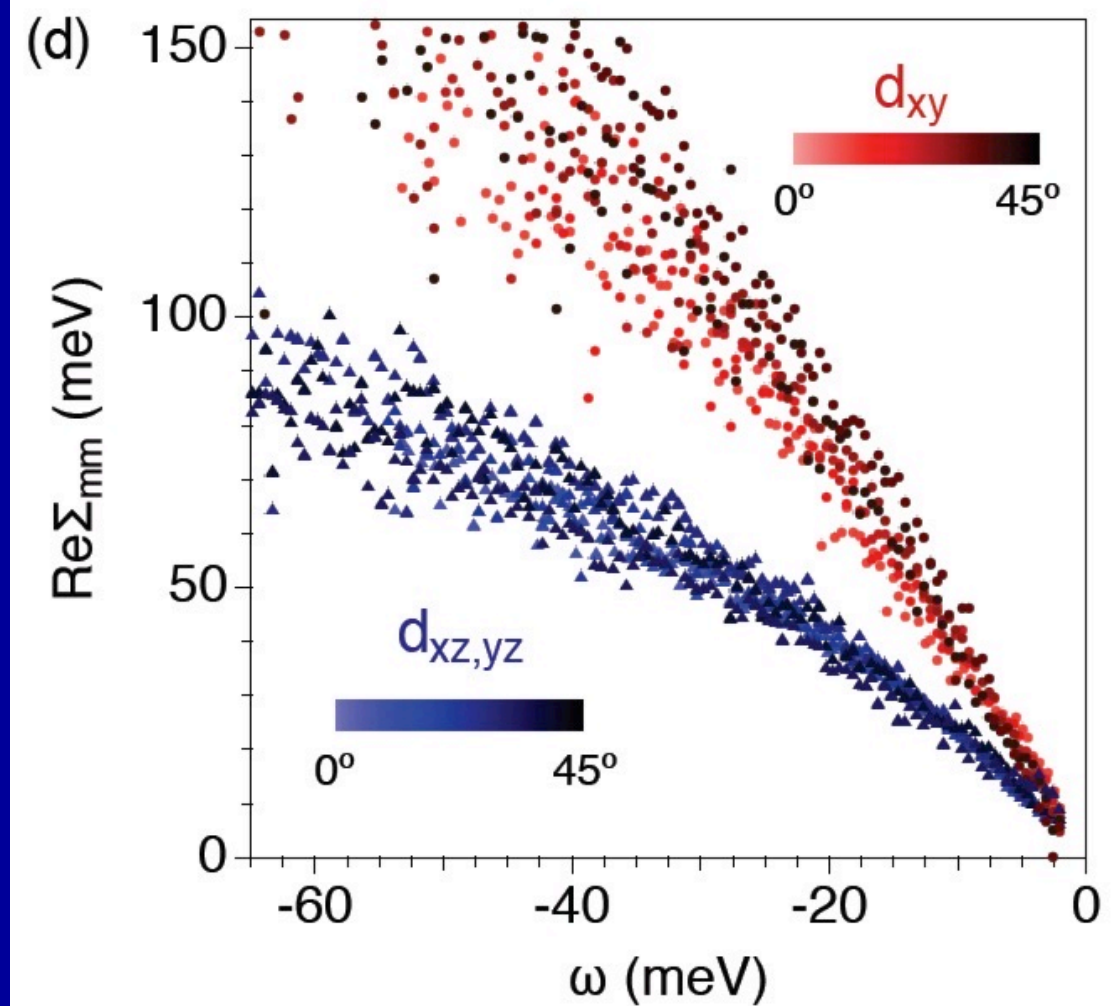
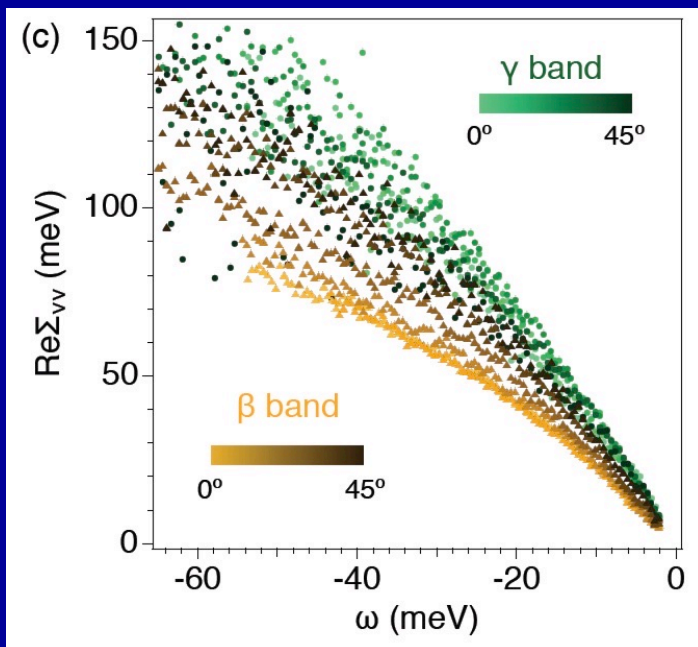
From ARPES MDC data: Extract self-energy for each angle θ



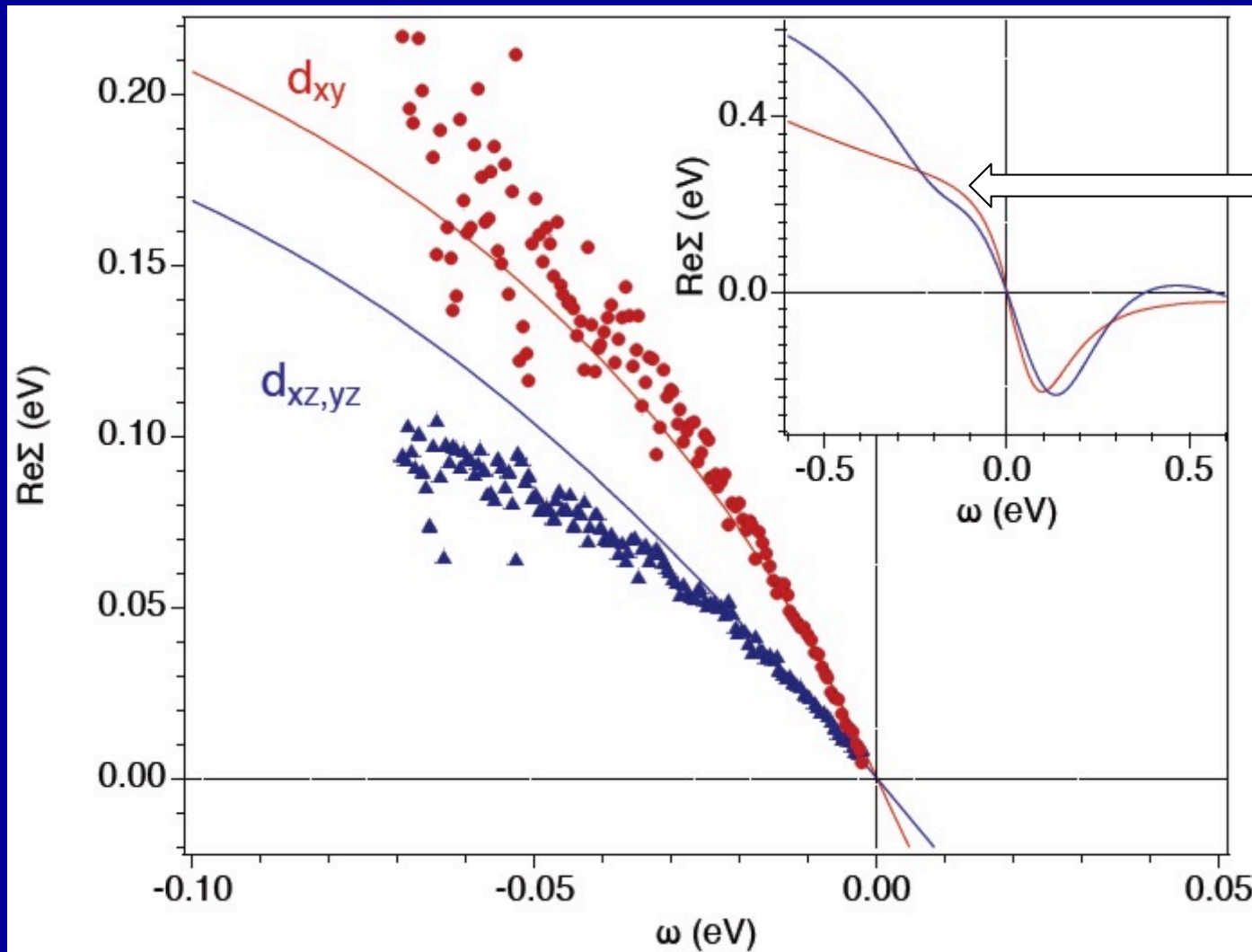
~ In orbital basis: Collapse of data corresponding to different angles !

→ DMFT 'Locality ansatz' is a good approximation

In contrast: strong angular dependence in band basis!



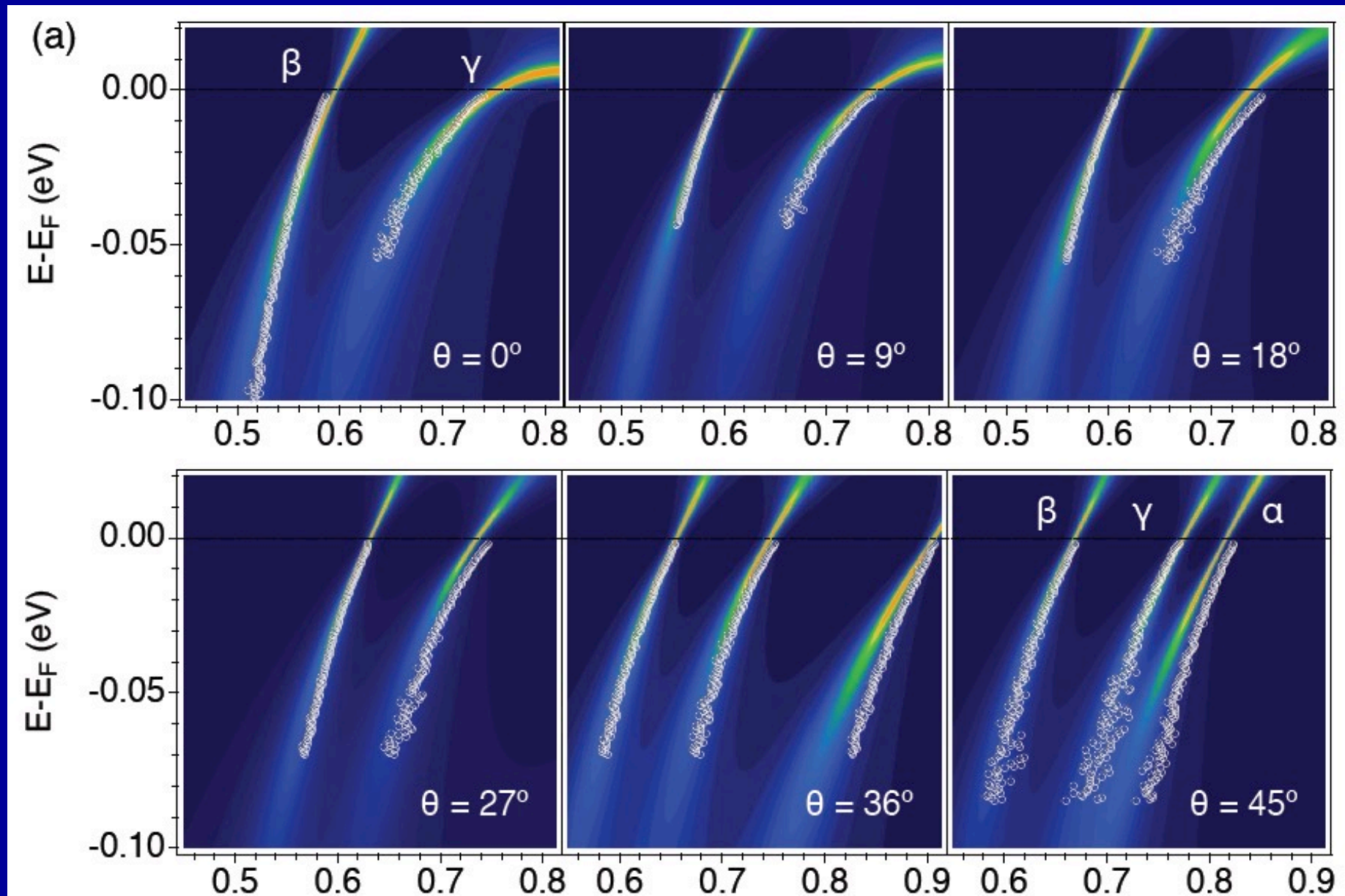
Comparison to LDA+DMFT self-energies



Kink
(electronic
origin
at $\sim 100\text{meV}$)

Comparing DMFT to ARPES

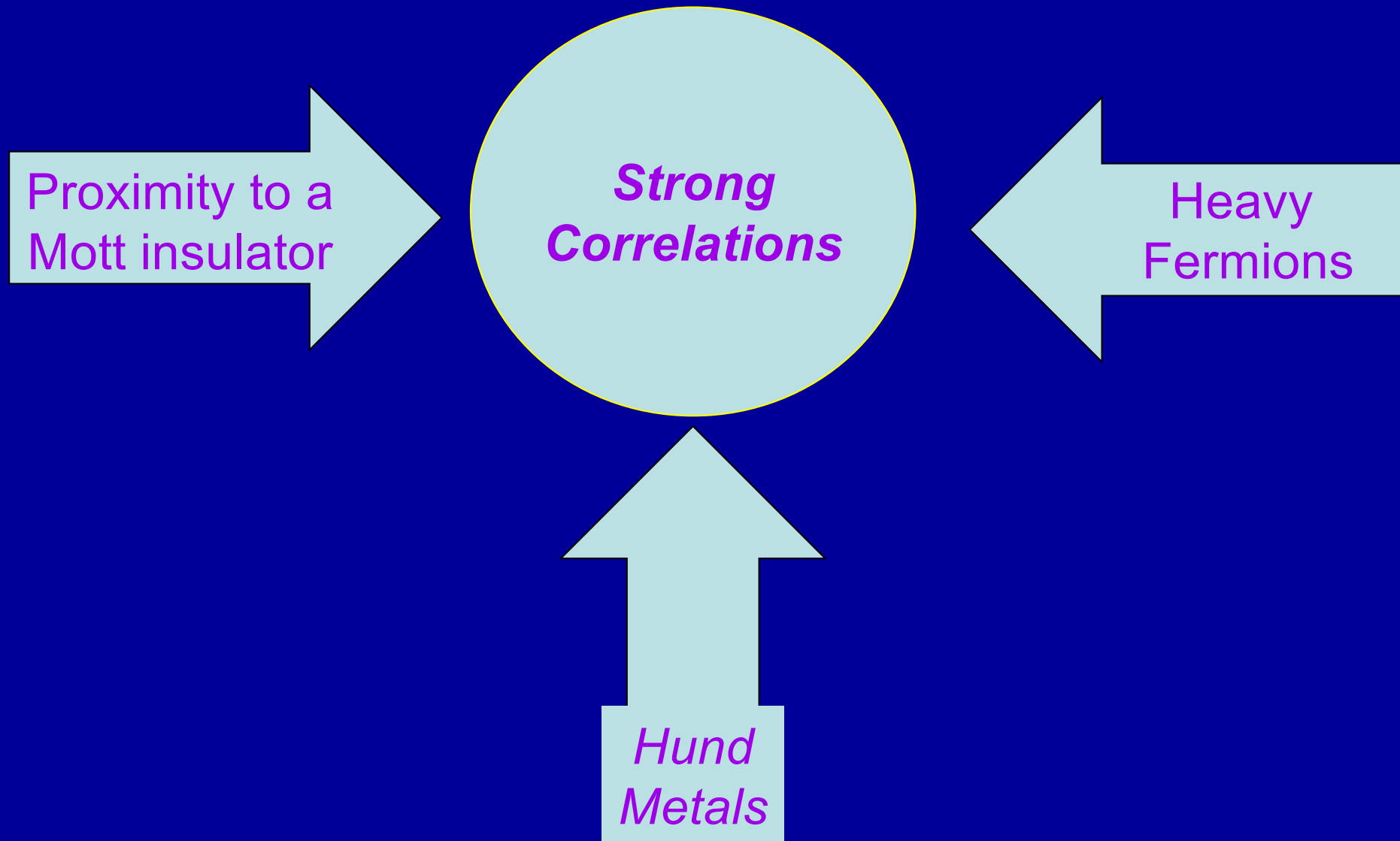
(Dots: ARPES MDCs. Colors: DMFT spectral intensity)



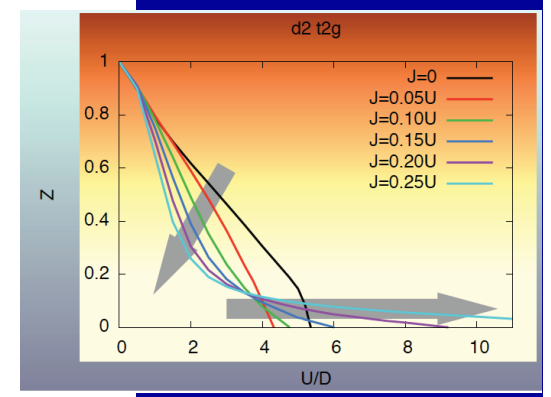
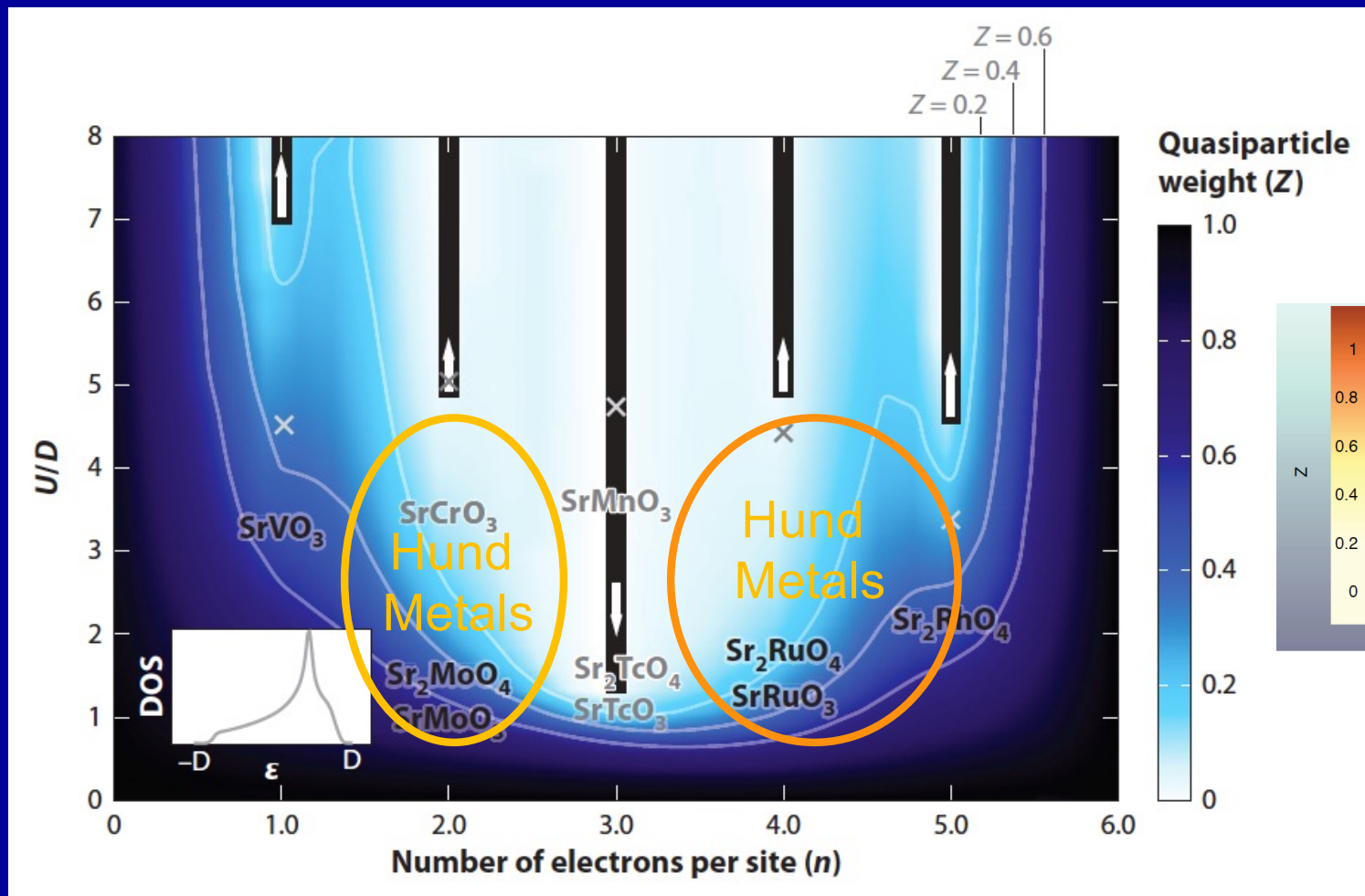
Sr_2RuO_4 is a member of the big and happy family of 'Hund Metals'

- Iron-Based Superconductors
- Oxides of 4d Transition Metals
- In the case of Sr_2RuO_4 , proximity to van Hove singularity also plays an important role, cf. comparison to Sr_2MoO_4
Karp et al. 125, 166401 (2020)
- **Hund Metals:** Haule and Kotliar New J. Phys. 11, 025021 (2009); Werner, Gull, Troyer and Millis, PRL 101, 166405 (2008); Mravlje et al. PRL106, 096401 (2011); Yin, Haule and Kotliar Nat Mat 10, 932 (2011); de'Medici et al. PRL 107, 256401 (2011); AG, de'Medici and Mravlje, Ann Rev Cond. Mat. Phys Vol 4 (2013), and many more...

Hund Metals: A distinct route to strong electronic correlations

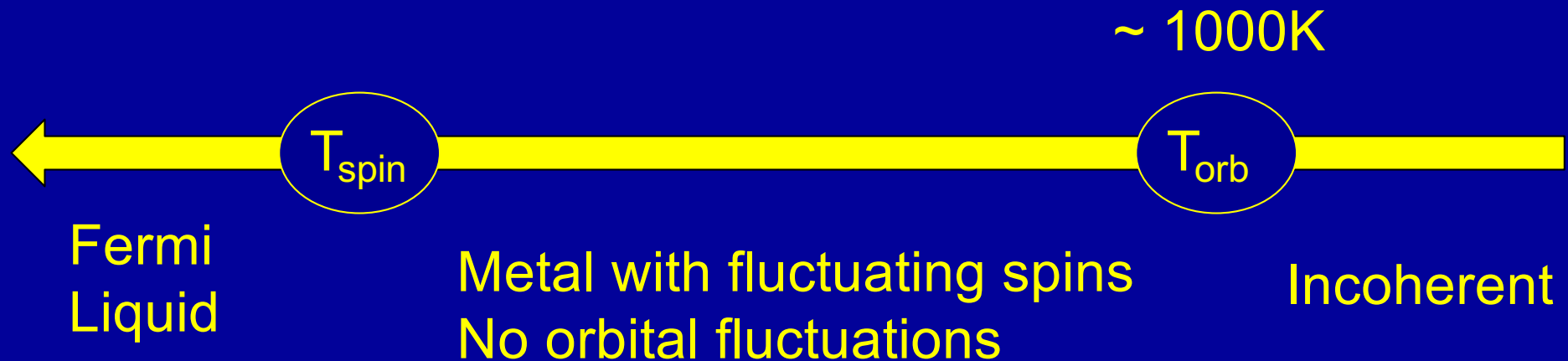


4d Transition-Metal Oxides: Strong Correlations Far From The Mott Transition

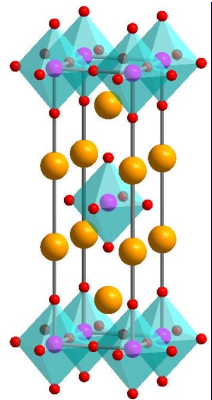


3d oxides: $U/D \sim 4$; 4d oxides: $U/D \sim 2$; D : $\frac{1}{2}$ bandwidth

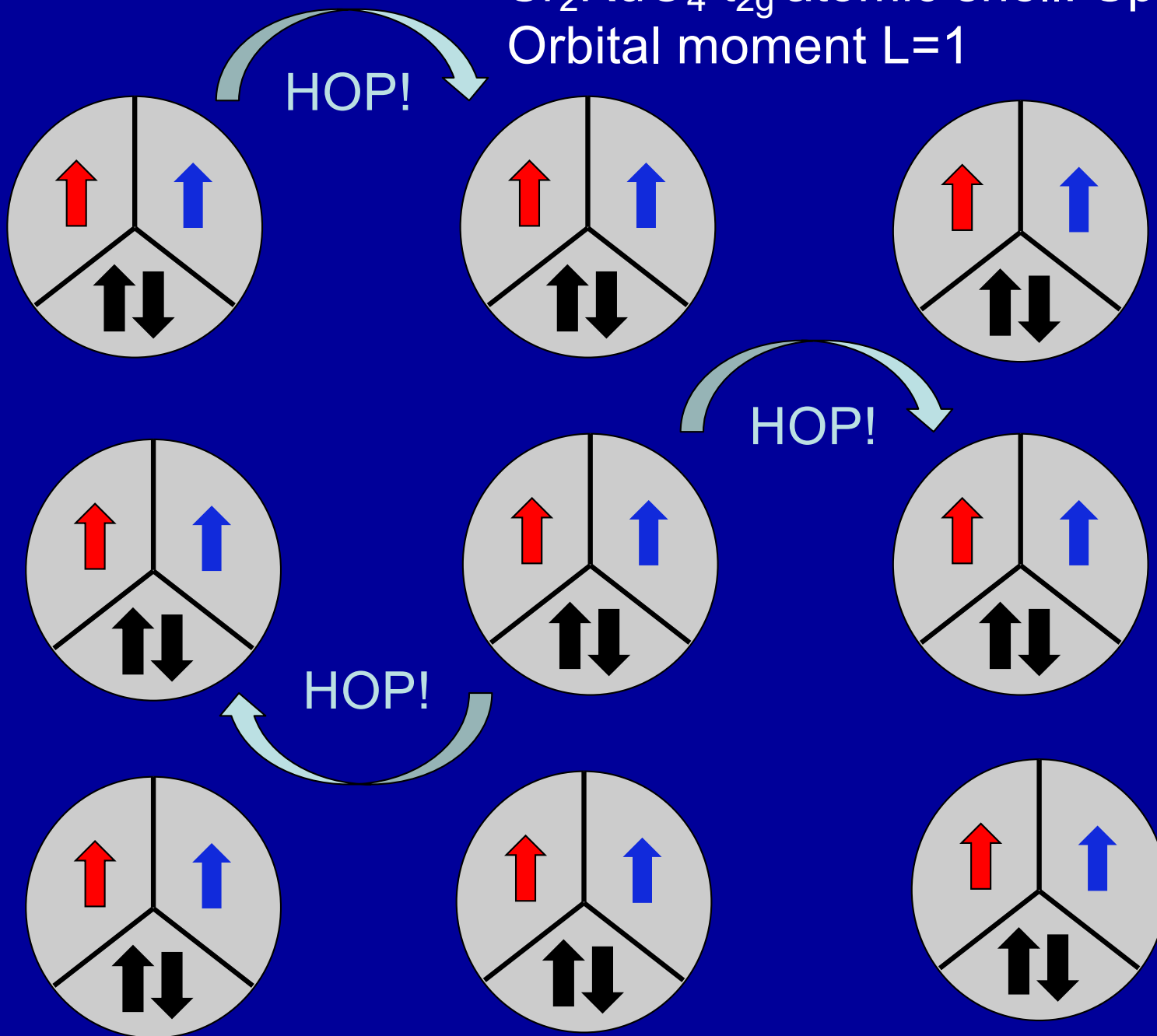
Hallmark of Hundness: Coherence of Spin and Orbital Degrees of Freedom Occurs at Distinct Scales



Now beautifully understood from a Renormalization Group perspective, cf. recent work by von Delft, Lee, Weichselbaum et al., Aron, Kotliar et al., Horvat, Žitko, Mravlje, Kugler et al.,
→ See Gabi's talk



Sr₂RuO₄ t_{2g} atomic shell: Spin S=1
Orbital moment L=1



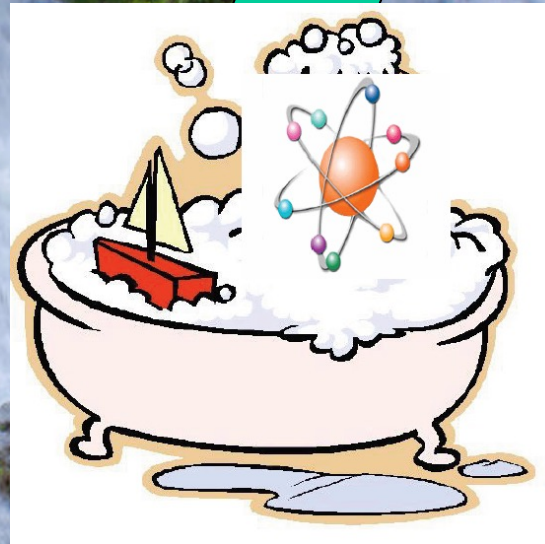
This is very much how we think about materials

In DMFT:

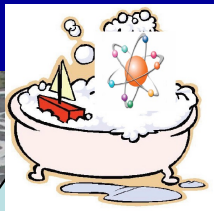
Start from local atomic configurations and follow the flow down into collective behaviour
Initially, spatial correlations are short-range

At lower energy, spatial correlations build up
→ Need to go beyond single-site DMFT

Atomic configurations/Multiplets
Intra-shell interactions+crystal fields



Including Spatial Fluctuations: Beyond Single-Site DMFT



EDMFT,
GW+DMFT...

Including
Long-wavelength fluctuations
w/ vertex: $D\Gamma A$, TRILEX,
Dual Fermions/Bosons,...

Cluster
Extensions
of DMFT:
CDMFT, DCA,...

Embedding Methods Are Controlled

Cluster extensions of single-site DMFT

→ 'Molecular' mean-field
(cf. Bethe-Peierls, Kikuchi)

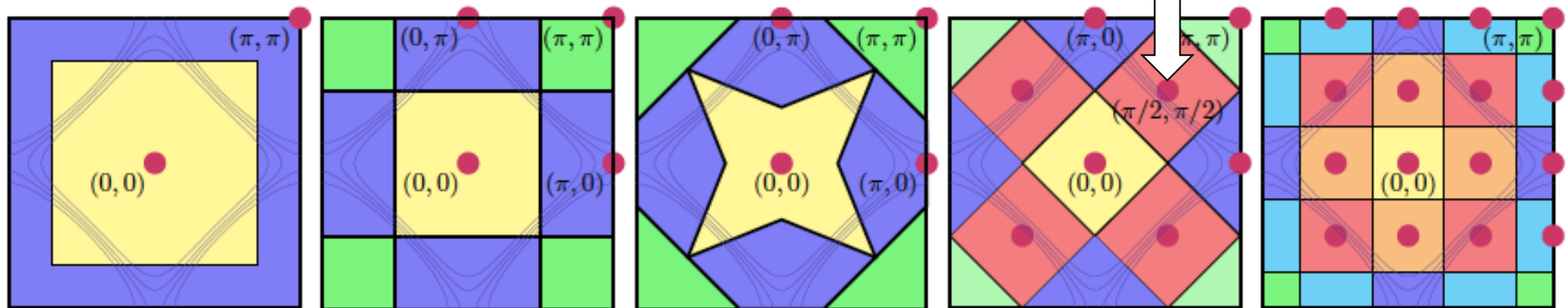
Several flavors, e.g. DCA: Patching momentum-space, cluster used to calculate self-energy at cluster momenta.

Self-energy approximated as piecewise constant in momentum space:

$$\Sigma(k, \omega) \simeq \Sigma(K, \omega) \quad (k \in P_K)$$

Antinode

Node



Numerous works by several groups in the last ~ 20 years

For reviews see:

- ²⁷ T. Maier, M. Jarrell, T. Pruschke, and M. H. Hettler, *Rev. Mod. Phys.* **77**, 1027 (2005).
- ²⁸ G. Kotliar, S. Y. Savrasov, K. Haule, V. S. Oudovenko, O. Parcollet, and C. A. Marianett, *Rev. Mod. Phys.* **78**, 865 (2006).
- ²⁹ A. M. S. Tremblay, B. Kyung, and D. Senechal, *Low Temp. Phys.* **32**, 424 (2006).

Cincinatti/Baton Rouge (Jarrell et al.), Rutgers (Kotliar, Haule et al.), Sherbrooke (Tremblay, Senechal et al., Kyung, Sordi), Columbia (Millis et al.), Michigan (Gull et al.) Oak Ridge (Maier et al.), Tokyo (Imada, Sakai et al.) Hamburg (Lichtenstein et al.), Rome (Capone et al.) Paris/Saclay/Orsay (Parcollet, Ferrero, AG, Civelli et al.), Stuttgart (Gunnarsson) etc...

To quote only one achievement:
These approaches have established
that the Pseudogap
in the doped 2D Hubbard model
is caused by spin correlations
(not pair or CDW fluctuations)

Many groups and authors 2005 → 2020
See e.g. PRX 8, 021048 for references

Recent 'handshake':

- With Tensor Network Methods (MEETS)
Wietek et al. PRX 11, 031007 (2021)
- With diagrammatic Mont Carlo (CDET)

Wu et al. PRB 96, 041105R, 2017; Simkovic et al. arXiv:2209.09237

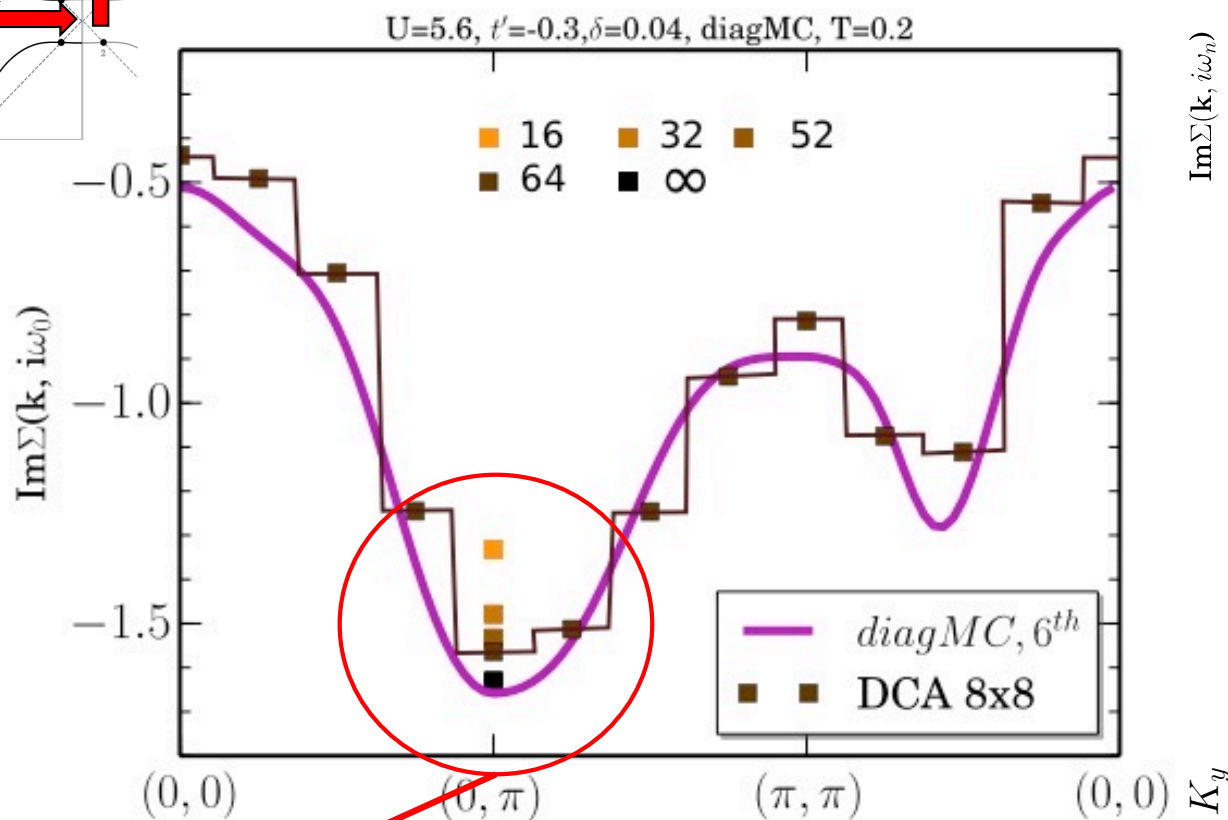
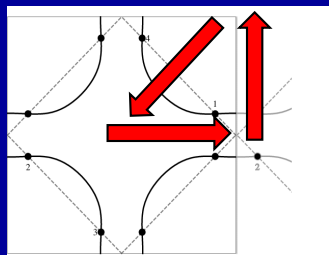
Controlled results, converged to infinite cluster size, are possible in part of the PG regime

Wei Wu, Ferrero, AG, Kozik PRB 96, 041105R (2017)

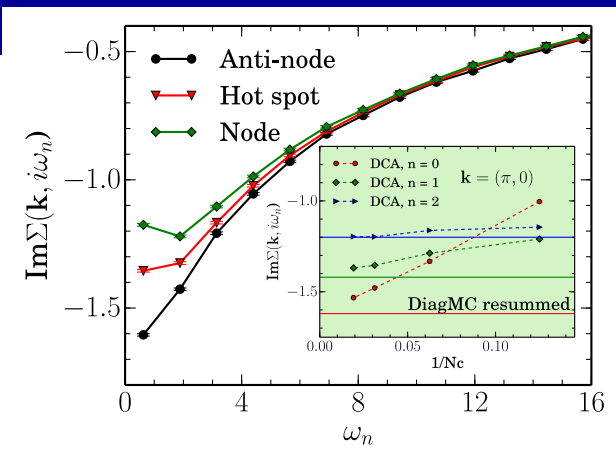
- For $U/t=5.6$, $t'/t=-0.3$ and doping $p=0.04$
(reference `Wei point' 😊)
- **CONVERGE** the self energy at $T=0.2t$ with two independent methods:
- DCA w/ convergence in cluster size
- Diagrammatic Monte Carlo on the Infinite Lattice
- Recently significant improvements to the DiagMC method (RDET) have allowed to reach $T/t=0.1$ Rossi, Simkovic, Ferrero EPL 132 (2020) 11001

DCA and DiagMC: quantitative agreement

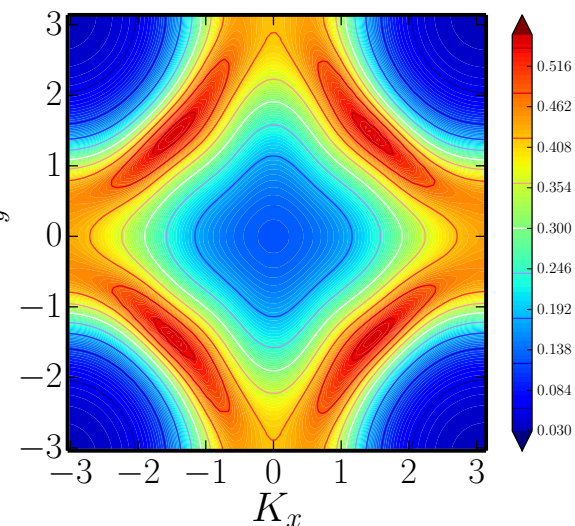
→ Computational solution of the 2D Hubbard model in this regime !



ImΣ becomes
LARGE
at antinode !



Nodal/Antinodal
Dichotomy



'Fluctuation Diagnostics'

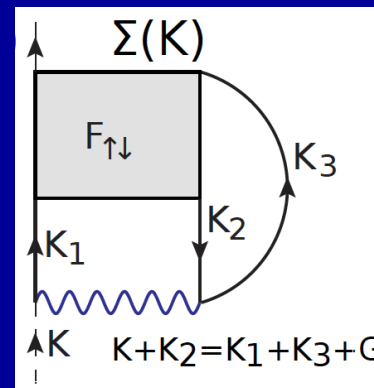
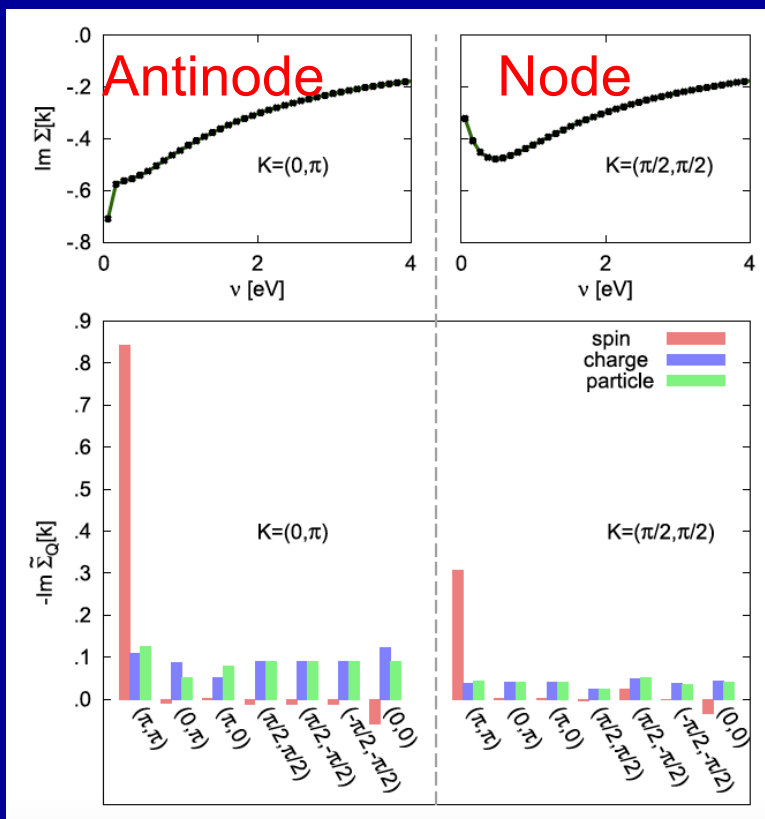
PRL 114, 236402 (2015)

PHYSICAL REVIEW LETTERS

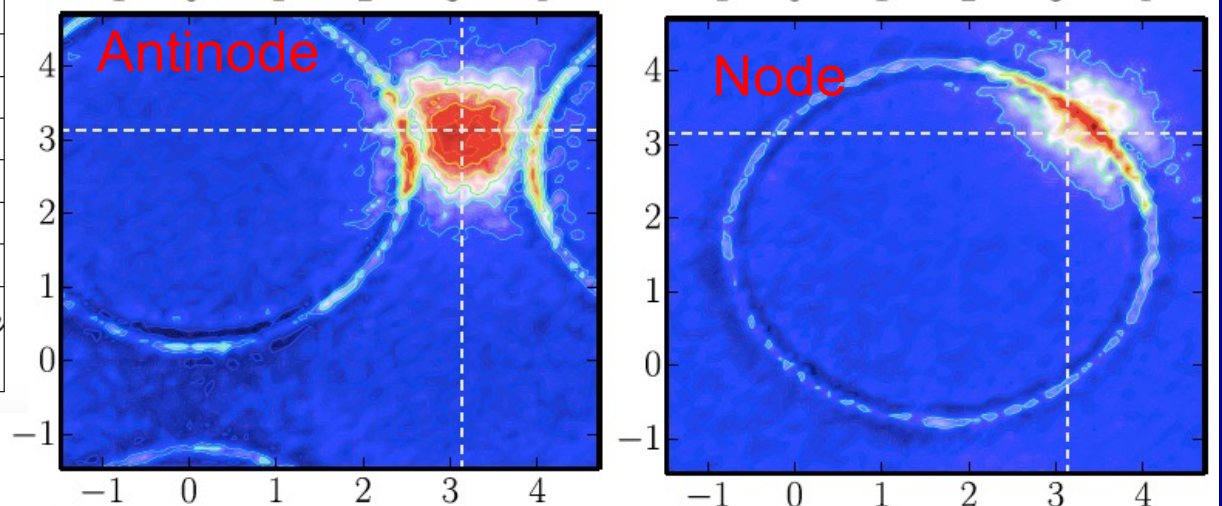
week ending
12 JUNE 2015

Fluctuation Diagnostics of the Electron Self-Energy: Origin of the Pseudogap Physics

O. Gunnarsson,¹ T. Schäfer,² J. P. F. LeBlanc,^{3,4} E. Gull,⁴ J. Merino,⁵ G. Sangiovanni,⁶ G. Rohringer,² and A. Toschi²



Wei et al. (2017) - DiagMC



DCA Gunnarsson et al

Conclusion
Outlook
Perspectives

...

*Shakespeare's anticipation of DMFT:
Correlation effects 'in a nutshell'*

*"O God! I could be bounded in a nutshell,
and count myself king of infinite space,
were it not that I have bad dreams !"*

William Shakespeare (in: Hamlet)



P.W. Anderson on DMFT:

In theory, the big news is the DMFT (dynamic mean-field theory) which gives us a systematic way to deal with the major effects of strong correlations.

After nearly 50 years, we are finally able to understand the Mott transition, for instance, at least in three dimensions, and to model the Kondo volume collapse in cerium.

*In: "The Future lies ahead" Proc. Intl. Conf on "Recent Progress in Many-Body Theories" Santa Fe, 2004 (World Scientific 2006)
Reprinted in "More and different. Notes from a thoughtful curmudgeon"*

Take-Home Message

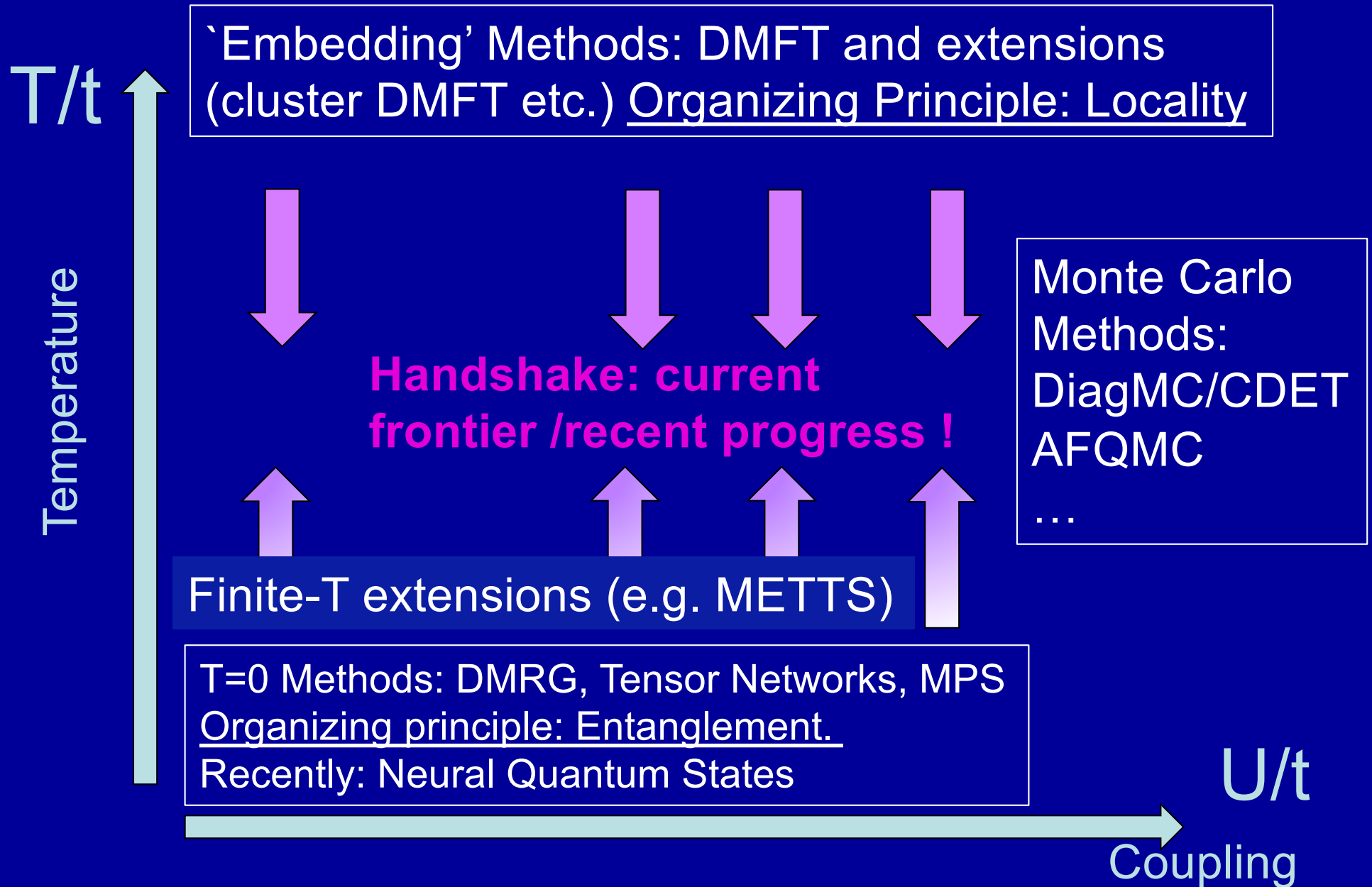
Dynamical Mean-Field Theory (DMFT),
combined with electronic structure methods,
has transformed our ability to
understand, calculate and predict
the properties of materials
with strong electronic correlations

Numerous opportunities for further developments...

Looking Ahead...

- **Looking forward to the next big advance on `impurity solvers`.** Promising candidates: Inchworm, Real-time (quasi)MC, Fork Tensor Product States, METTS,...
- **Long-range interactions and spatial correlations:** GW+DMFT, Making vertex-based extensions more efficient, Combinations with lattice DiagMC,...
- **Designing new embedding schemes:** `full-cell' embedding, SEET,...

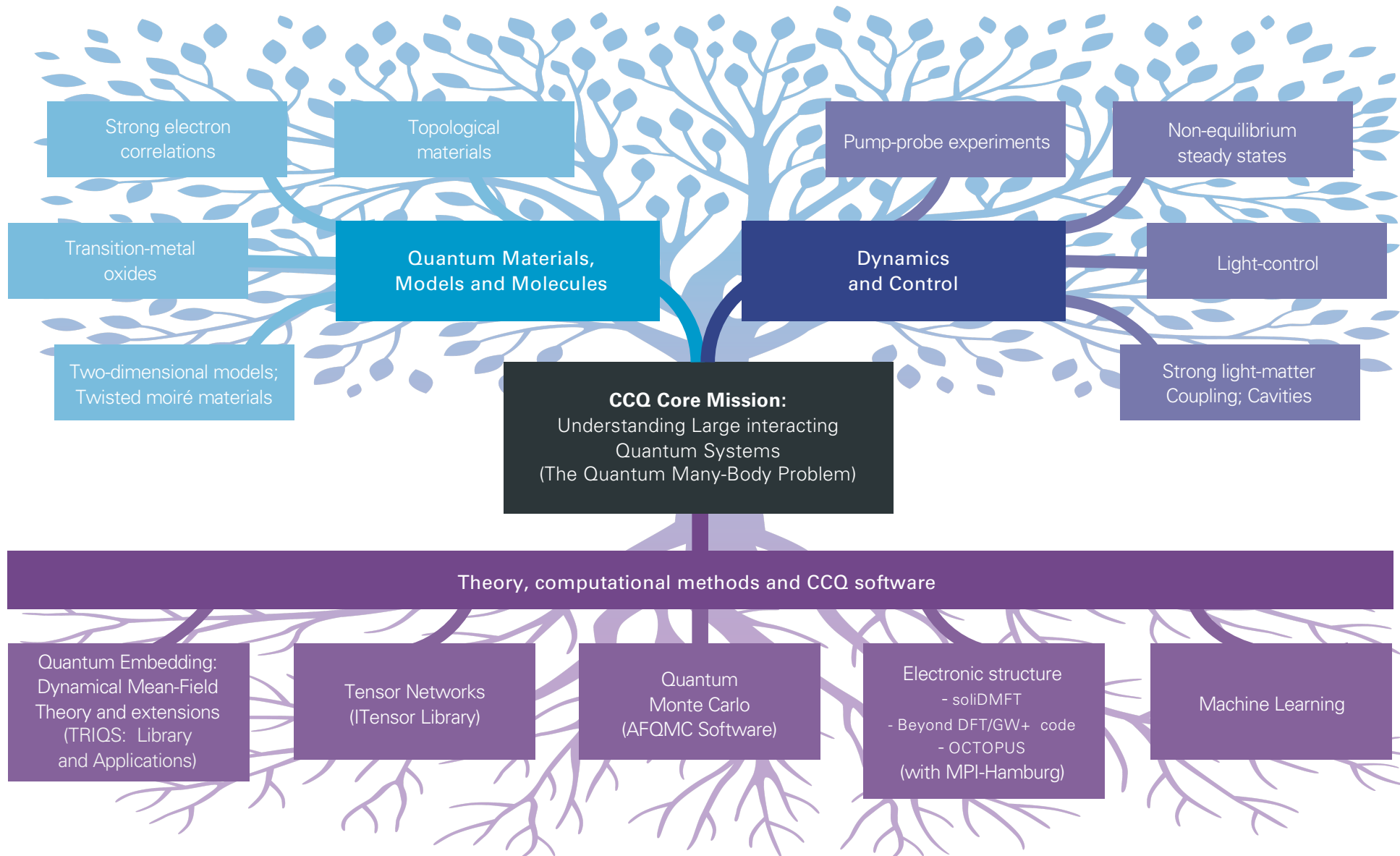
Computational Methods: Handshake!



A heartfelt 'THANK YOU!' to collaborators and friends over the years, and especially to:

Igor Abrikosov, Markus Aichhorn, Oscar Akerlund, Bernard Amadon, Ole K. Andersen, Ryotaro Arita, Ferdi Aryasetiawan, Dmitri Basov, Felix Baumberger, Sophie Beck, Jean-Sebastien Bernier, Christophe Berthod, Silke Biermann, Jean-Philippe Brantut, Stuart Brown, Sebastien Burdin, Massimo Capone, Iacopo Carusotto, Sara Catalano, Andrea Cavalleri, Maximilien Cazayous, Peter Cha, Johan Chang, Shubhayu Chatterjee, Marcello Civelli, Dorothee Colson, Pablo Cornaglia, Theo Costi, Luca de' Medici, Tung-Lam Dao, Jean Dalibard, Lorenzo De Leo, Xiaoyu Deng, Claribel Dominguez, Philipp Dumitrescu, Martin Eckstein, Claude Ederer, Olle Eriksson, Michel Ferrero, Matthew Fishman, Serge Florens, Jennifer Fowlie, Atsushi Fujimori, Yann Gallais, Alexandru Georgescu, Thierry Giamarchi, Marta Gibert, Daniel Gempel, Marco Gioni, Charles Grenier, Paco Guinea, Emanuel Gull, Alexander Hampel, Philipp Hansmann, Syed Hassan, Kristjan Haule, Karsten Held, Masatoshi Imada, Didier Jaccard, Dieter Jaksch, Denis Jerome, Mikhail Katsnelson, Eun-Ah Kim, Minjae Kim, Michael Köhl, Corinna Kollath, Gabriel Kotliar, Evgeny Kozik, Werner Krauth, Hulikal Krishnamurthy, Fabian Kugler, Mathieu Le Tacon, Giacomo Mazza, Andy Millis, Jernej Mravlje, Laurent Laloux, Frank Lechermann, Ivan Leonov, Sasha Lichtenstein, Peter Lunts, Andy Mackenzie, Roman Mankowsky, Yigal Meir, Takashi Miyake, Jocienne Nelson, Yusuke Nomura, Olivier Parcollet, Indranil Paul, Eva Pavarini, Oleg Peil, Luca Perfetti, Lode Pollet, Dario Poletti, Sasha Poteryaev, Leonid Pourovskii, Cyril Proust, Malte Rösner, Javier Robledo-Moreno, Marcelo Rozenberg, Angel Rubio, Alexander Rubtsov, Subir Sachdev, Alain Sacuto, Tanusri Saha-Dasgupta, Shiro Sakai, Christophe Salomon, Vito Scarola, Thomas Schäfer, Mathias Scheurer, Darrell Schlom, Anirvan Sengupta, Michael Sentef, Sriram Shastry, Kyle Shen, Qimiao Si, Nicola Spaldin, Tudor Stanescu, Miles Stoudenmire, Hugo Strand, Damien Stricker, Alaska Subedi, Louis Taillefer, Anna Tamai, Ciro Taranto, Jeremie Teyssier, Jan Tomczak, Yoshi Tokura, Alessandro Toschi, André-Marie Tremblay, Jean-Marc Triscone, Alexei Tselik, Veronica Vildosola, Dirk van der Marel, Jan von Delft, Cedric Weber, Tim Wehling, Nils Wentzell, Felix Werner, Philipp Werner, Alexander Wietek, Steve White, Wei Wu, Pavel Wzietek, Manuel Zingl, Rok Žitko **Apologies to those I didn't mention for lack of space or by mistake...!**

The Research Ecosystem of the Center for Computational Quantum Physics of the Flatiron Institute, Simons Foundation, New York



16 Faculty Members, 22 Postdocs

Job Opportunities at CCQ

Intern program

- 10 weeks during summer
- undergrad - to 1st year graduate
- application in December - February

PreDoc program

- 4 months, twice annually
- 1st - 3rd year graduate
- application in September (now) for start in mid to late January 2023

PostDoc

- 2+1 years, start in September
- application starting in September (one year before)

<https://www.simonsfoundation.org/flatiron/careers/?tab=job-openings¢er=ccq>
(bit.ly/3L3wJC1)

Also note: We offer some graduate student fellowships for students applying to the Columbia, NYU, CUNY/CCNY graduates schools (also soon: SISSA, Trieste)